National Aeronautics and Space Administration

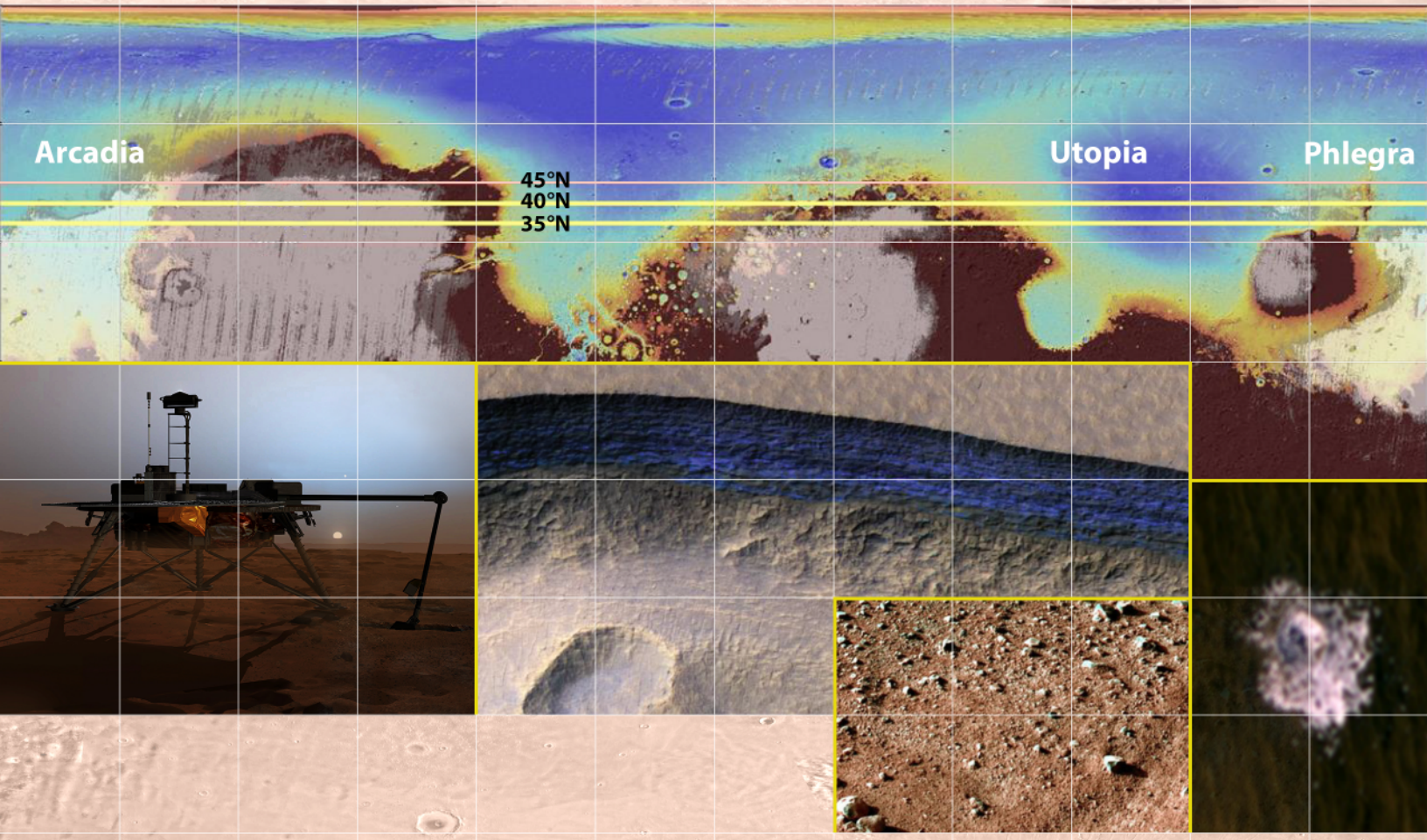

Mars **Life** Explorer

June 9, 2021
Mission Concept Study
Planetary Science and Astrobiology
Decadal Survey

www.nasa.gov

Science Champion
Amy Williams
amywilliams1@ufl.edu
University of Florida

JPL Point of Contact
Brian Muirhead
brian.k.muirhead@jpl.nasa.gov
Jet Propulsion Laboratory,
California Institute of Technology

Disclaimers/Acknowledgements

Pre-Decisional Information – For Planning and Discussion Purposes Only

The research was carried out at the Jet Propulsion Laboratory, California Institute of Technology, under a contract with the National Aeronautics and Space Administration (80NM0018D0004).

The cost information contained in this document is of a budgetary and planning nature and is intended for informational purposes only. It does not constitute a commitment on the part of JPL and/or Caltech.

Cover images from top clockwise:

- General regions with ice in mid-northern latitudes (graphic adapted from Golombek, M., et al. 2021. "SpaceX Starship Landing Sites on Mars." 52nd Lunar and Planetary Science Conference, LPI Contrib. No. 2548)
- Impact excavated mid-latitude ice imaged from HiRISE
- Mars Phoenix mission image showing ice polygons at the landing site
- Near-surface slab ice (in blue, from Mars orbit) indicative of Mars Life Explorer accessible mid-latitude safe landing sites (Dundas, C. M., et al. 2018. "Exposed Subsurface Ice Sheets in the Martian Mid-Latitudes." *Science* 359 (6372): 199-201)
- Artist's concept of InSight simulating the Mars Life Explorer lander drilling subsurface

Study Participants

Science Representatives

Planetary Science and Astrobiology Decadal Survey 2023–2032

- Amy Williams, Lead Representative
- Will Brinckerhoff
- Bethany Ehlmann, Vice Chair, Panel on Mars
- Claire Newman
- Bruce Jakosky
- Vicky Hamilton, Chair, Panel on Mars

Jet Propulsion Laboratory

- Amy Hoffman
- Ying Lin
- Others

Study Team Members

- Study Lead: Brian Muirhead
- Deputy Study Lead: Steve Matousek
- Chief Engineer Consultant: Hoppy Price
- Lead Systems Engineer: Nathan Barba
- Systems Engineer: Robert Miller
- Systems Engineer/Team-X continuity: Jonathan Murphy
- Payload: Amy Hofmann
- Mission Design: Ryan Woolley
- Sampling System: Paul Backes
- Sampling System: Tyler Okamoto
- Costing: Jahning Woo
- Program Office: Chad Edwards; Tony Freeman; Greg Garner
- Lockheed Martin: Richard Warwick
- Honeybee Robotics: Kris Zacny

With significant additional participation from the members of JPL's A-Team and Team X

Table of Contents

For reader convenience, links for this study are provided for navigation purposes. After following a link, you can return to the previous page by pressing Command + Left Arrow (Mac) or Alt + Left Arrow (PC), or by using the Acrobat Page Navigation toolbar.

Appendices

Mars Life Explorer (MLE)

Search for signatures of life and understand habitability of near-surface ice

MLE is a life detection mission and more...

- Search for modern biosignatures
- Characterize down borehole thermophysical properties & habitability of ice/ice-cemented regolith
- Quantify near-surface water vapor flux associated with ice and minerology over 1 Martian year

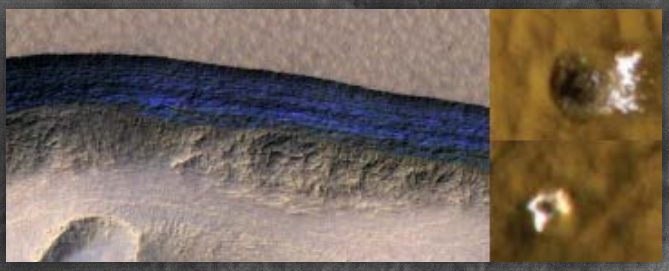

Near-surface slab ice indicative of MLE accessible mid-latitude safe landing sites (in blue, from Mars orbit (Dundas et al. 2018)

Impacts excavate mid-latitude ice (Byrne et al. 2009)

Science Objectives and Decadal Questions

A) **Search for organic molecules, non-equilibrium gases, and isotopes** associated with ice and regolith and evaluate their possible biological origin.
MEPAG Goal I, Objective A, Sub-objective A1

B) **Assess the habitability** of the near-subsurface environment with respect to required elements to support microbial life, microbial energy sources, and compounds toxic to microbes.
MEPAG Goal I, Objective A, Sub-objective A2

C) **Quantify the down borehole thermophysical properties** of the **ice/ice-cemented regolith** and any role for liquid water in its creation or modification.
MEPAG Goal II, Objective B, Sub-objective B1

D) **Determine the processes that preserve/ modify/ destroy** these ice deposits in the modern climate.
MEPAG Goal II, Objective A

#11 **Search for life elsewhere:** Is there evidence of past or present life in our Solar System beyond Earth and how do we detect it?

#10 **Dynamic habitability:** Where in our Solar System do potentially habitable environments exist, what processes led to their formation, and how do planetary environments and habitable conditions co-evolve over time?

#6 **Atmosphere and climate evolution on solid bodies:** What establishes the properties and dynamics of solid body atmospheres and exospheres, and what governs material loss to and gain from space and exchange between the atmosphere and the surface and interior?

Why did planetary climates evolve to their current varied states?

Objective		Measurement Description (B=Baseline, T=Threshold)	B	T
Organics & modern life	A1	Extract organics from sample	X	X
	A2	Detect and characterize organics (e.g. amino acids, fatty acids)	X	X
	A3	Quantify the relative abundances of amino acids & fatty acids	X	X
	A4	Quantify enantiomeric excess of amino acids	X	X
	A5	CO_2, CH_4, and other trace gasses	X	X
	A6	H, C, O, N, S isotopic measurements	X	X
Habitability	B1	Evolved volatile gasses from pyrolysis; combustion of TOC	X	X
	B2	Analysis of both inorganic and small organic cations and anions	X	Par.
	B3	Silicate, oxide, salt, amorphous phase characterization	X	Par.
	B4	Major and minor element chemistry	X	X
Borehole science	C1	Temperature profile of the borehole	X	X
	C2	Downhole imaging	X	X
	C3	Conductivity profile of borehole resistivity	X	X
Meteorology & water flux	D1a	Temperature, pressure	X	X
	D1b	Water vapor flux (abundance) between surface & atmosphere	X	X
	D1c	3D & surface wind stress	X	X
	D2	LW and SW radiative fluxes at surface	X	X

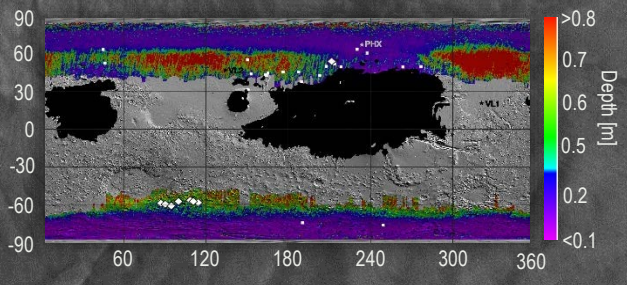

Ice depths modeled via THEMIS, compared to HiRISE ice observations (Piqueux et al., 2019). Much of 45°N (e.g. Arcadia Planitia) contains ice within <1 m depth. White symbols are ice excavated by impacts.

Data and analysis show water ice is accessible within 1m of the surface at multiple accessible landing sites

Study Shows Multiple Instrument Options to Meet Measurement Needs Within Engineering and Programmatic Constraints

Payload

	Baseline Mission Example Payload			
Measurement objective	**Objective A** 1) Organics [Pyrolysis-GC-MS, Laser Desorption Evolved Gas Analysis (EGA)] 2) Trace gases [EGA, Tunable Laser Spectrometer (TLS)] 3) Isotopes [TLS] 4) Evolved volatile gases [EGA]	**Objective B** 1) Mineralogy & amorphous phases 2) Elemental chemistry 3) Inorganic and small organic ions [Conductivity analysis] 4) Evolved volatile gases [EGA]	**Objective C** 1) Temp. and conductivity profiles in borehole 2) Downhole imaging	**Objective D** 1) Temp., pressure 2) Water vapor flux 3) 3D & surface wind stress 4) Radiative flux
Representative Payload	1,2,3,4) DraMS w/ EGA & Mini-TLS	1,2) CheMinX (XRD/ XRF) 3) MECA 4) EGA (part of Obj. A payload)	1) Honeybee drill temp. & conductivity 2) Honeybee drill imager	1) MEDA T & P sensors 2,3) Sonic anemometer & TLS 4) MEDA TIRS

MLE is payload-agnostic and has assumed representative payloads to meet mission objectives within engineering and cost constraints. (No contributions were considered)

Baseline Payload Mass	CBE (kg)
Engineering:	
Single-segment 2-m drill	20
3 DOF drill boom	7
Drill avionics box	7
Biobarrier	3
Gas sample transfer system	8
InSIght Context Camera	1
Science:	
Biosignature detection suite	35
Chemistry, mineral, conductivity suite	14
Wind, water, radiative flux suite	3
Downhole eng. sensor & imager	2
CBE subtotal	100
Total with 50% margin	150

Spacecraft

High heritage from InSight for cruise, EDL lander

2-m drill and sample transfer system: Honeybee Robotics TRIDENT system ('22 & '23 lunar science missions)

IV-b PP implementation based on past mission forward PP and new generation cleaning and assay techniques

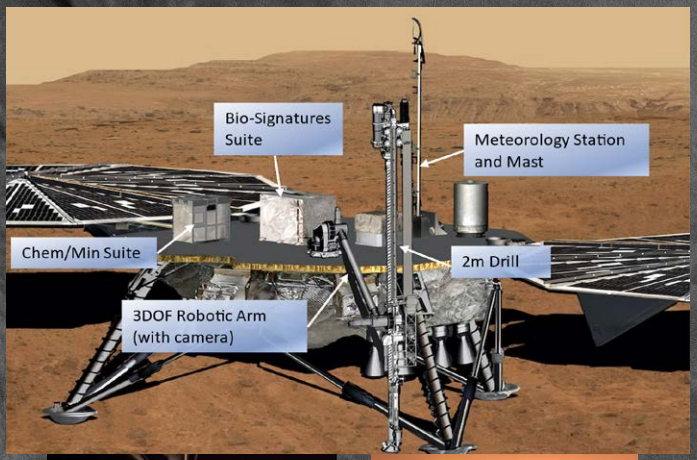

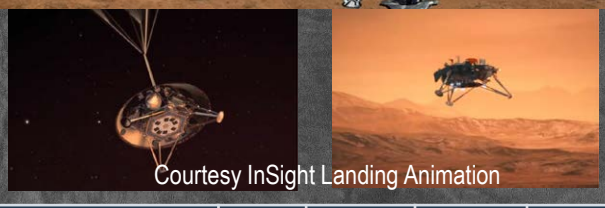

Courtesy InSight Landing Animation

Cost and Schedule

MLE baseline cost (FY25$)	Estimate	Reserves		Total
Development A-D	$807M	50%	$404M	$1,211M
Launch vehicle	$275M	N/A	N/A	$275M
Operations E/F	$96M	25%	$24M	$120M
Full lifecycle cost	$1,178M	36%	$428M	$1,606M

MLE Mass w/ InSight Comparison	CBE (kg)	MPV (kg)	Tol Mgn %	InSight (as built)
Launch Flight System	852	1039	22%	572
Payload	100	150	50%	52
Launch Dry	952	1189	25%	624
Lander Fuel	116	116	N/A	66
Launch Wet Total	1068	1305	22%	690
Entry Dry Total	872	1087	25%	544
Dry Lander Total	452	565	25%	354

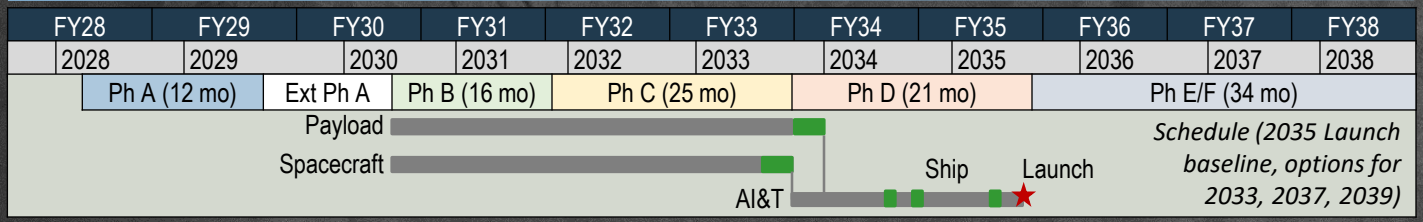

Schedule (2035 Launch baseline, options for 2033, 2037, 2039)

EXECUTIVE SUMMARY

MLE has the potential to be the first mission to sample and analyze ice in the mid-latitudes in the search for life below the surface of Mars.

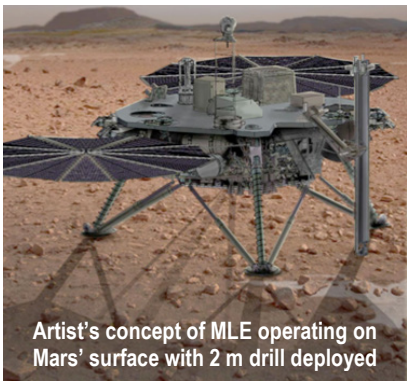
Artist's concept of MLE operating on Mars' surface with 2 m drill deployed

Mars Life Explorer (MLE) is a mission capable of discovering, if they exist, the signatures of life in ice formations close to the Martian surface—close enough to drill into, extract from, and analyze on board a robotic lander of New Frontiers (NF) class. MLE could launch in the early-to late 2030s, land within a vertical meter of Martian mid-latitude ice, drill for samples to a 2-meter depth, and study those samples on site.

MLE would address some of the Planetary Decadal Survey's most compelling science questions, including: (1) Is there evidence of past or present life in our Solar System beyond Earth and how do we detect it? (2) Where in our Solar System do potentially habitable environments exist, what processes led to their formation, and how do planetary environments and habitable conditions co-evolve over time? (3) Why did planetary climates evolve to their current varied states?

MLE searches for modern biosignatures—including organics, gases, and isotopes—that could indicate biological activity within these geologically recent materials. The mission could also characterize the habitability of the ices including availability of nutrients and energy sources, and evaluate thermophysical properties to assess whether liquid water played a role in deposit formation or modification. MLE has strong relationships in its implementation approach to a 2019 Mars Exploration Program Analysis Group (MEPAG) Ice and Climate Evolution Science Analysis group (ICE-SAG) polar lander drill concept and the Vision & Voyages Polar mission, with the main difference being biosignature objectives at lower, warmer latitudes with near-surface ice.

Because this mission would interrogate materials of high interest to future human landed missions, there is clear Human Exploration and Operations Mission Directorate (HEOMD) synergy. While we do not presently include HEO-specific objectives, there is strong overlap with science objectives B, C, and D and HEO Strategic Knowledge Gaps (SKGs).

This study provides a "proof of concept" that a static solar-powered lander moderately larger than the currently operating InSight lander, with a redeployable 2-meter drill and capable payload addressing well defined science objectives, fits within envisioned NF-class resources ($1.1B FY25, Phases A–D) in the next decade. A baseline point design is fully described with science and technical parameters including a model payload and with a range of possible implementations that are capable of making the needed measurements. The mission could support launches in 2033, 2035, 2037, or 2039 and operate for at least 120 sols, with large margins allowing further weather station operations for a full Martian year. Drilling happens relatively quickly, leaving the bulk of the mission operations timeline available for sample analysis and other science. The flexibility provided by this concept allows future Principal Investigators (PIs) to propose specific, optimized payloads within the NF mission constraints and give high confidence of answering the question of whether Mars has or recently had life in the mid-latitude near-surface ice.

MLE Science Objectives
A. Search for organic molecules and non-equilibrium gases associated with ice and regolith and evaluate their possible biological origin (e.g., MEPAG Goal I, Objective A, Sub-objective A1)
B. Assess the habitability of the near-subsurface environment with respect to required elements to support life, energy sources, and possible toxic elements (e.g., MEPAG Goal I, Objective A, Sub-objective A2)
C. Determine the thermophysical properties of the ice/ice-cemented regolith and any role for liquid water in its creation or modification (e.g., MEPAG Goal II, Objective B, Sub-objective B1)
D. Determine the processes that preserve/modify/ destroy these ice deposits in the modern climate (e.g., MEPAG Goal II, Objective A)

1 SCIENTIFIC OBJECTIVES

Search for signatures of life and understand habitability of near-surface ice.

Whether there is life beyond Earth is one of humanity's most compelling questions. Mars is among the few planetary bodies in our solar system where evidence of extant life could be found by a robotic mission in the near-term and awareness of the potential for current habitats on Mars has drastically increased in recent years (e.g., (Cabrol 2021), and references therein). As our understanding of the Martian environment evolves, we have been able to 'follow the water' and 'follow the carbon' to now search for life on Mars. We are currently in the nascent stages of searching for ancient life on Mars with the Mars 2020 rover, Perseverance, and the first step in Mars Sample Return (Muirhead et al. 2020). However, the profound question remains of whether there is extant life on Mars, sequestered away in some protected ecological niche. Here, we baseline a mission concept for the Mars Life Explorer (MLE), a search for extant life through modern biosignatures, using one of the suggested potential habitats as the target: mid-latitude terrain with ice within 2 m of the surface.

MLE would build on NASA's goal to seek signs of life with a sophisticated and high heritage payload that can characterize organic compounds, trace gases, and isotopes within brines, ice, and ice-cemented regolith in the near-subsurface down to 2 meters. In the event extant life is not detected, the MLE lander would also accomplish novel science with a broad payload to address organic geochemistry, habitability, stability, and thermophysical properties of ice, and the Martian climate and water cycle in the unexplored Martian subsurface. Potential contamination concerns mean that the time to search for modern life on Mars is in the 2030s, prior to the possible arrival of human astronauts (Conley and Rummel 2010).

1.1 SCIENCE QUESTIONS AND OBJECTIVES

Scientific Objectives

The MLE mission seeks to answer the question "Does modern life exist associated with mid-latitude Martian sub-surface ice deposits, and what is the habitability of these deposits now and over recent Martian history?" In pursuit of answers to these profound questions, the MLE mission would address some of the **2023–2032 Decadal Survey's** most compelling science questions, including:

Q11: Search for life elsewhere. Is there evidence of past or present life in our Solar System beyond Earth and how do we detect it?

Q10: Dynamic habitability. Where in our Solar System do potentially habitable environments exist, what processes led to their formation, and how do planetary environments and habitable conditions co-evolve over time?

Q6: Atmosphere and climate evolution on solid bodies. Why did planetary climates evolve to their current varied states?

These questions are cross-cutting areas of study with relevance beyond Mars. The four objectives of the MLE mission address these compelling questions:

A. Search for organic molecules, non-equilibrium gases, and isotopes associated with ice and regolith and evaluate their possible biological origin (e.g., MEPAG [Mars Exploration Program Analysis Group] Goal I, Objective A, Sub-objective A1 and A3). This maps to Decadal Survey Q11.
B. Assess the habitability of the near-subsurface environment with respect to required elements to support microbial life, including microbial energy sources (e.g., MEPAG Goal I, Objective A, Sub-objective A2). This maps to Decadal Survey Q11 and Q10.
C. Determine the thermophysical properties of the ice/ice-cemented regolith down borehole and any role for liquid water in its creation or modification (e.g., MEPAG Goal I, Objective A, Sub-objective A2 and Goal II, Objective B, Sub-objective B1). This maps to Decadal Survey Q10 and Q6.
D. Determine the processes that preserve, modify, and destroy these ice deposits in the modern climate (e.g., MEPAG Goal II, Objective A, Sub-objective A2). This maps to Decadal Survey Q10 and Q6.

The search for modern life on Mars must select a single promising location to begin. MLE is designed to determine the variety and cycling of organics, salts, and water vapor in this key environment even if life is not present, expanding our fundamental knowledge of terrestrial planet habitability.

Why Mid-Latitude Ice?

Many types of habitats have been proposed in the search for modern life (e.g., (Cabrol 2021)), including deep aquifers, higher latitude sites (e.g., the Phoenix landing site), or lower latitude sites with signs of recent water (e.g. Cerberus Fossae). We do not preclude a future MLE to these locales but for the purposes of the New Frontiers-class mission concept study point design chose mid-latitude ice.

Mid-latitude (i.e., ~45°N) ice-rich terrain represents one of the modern habitable environments on Mars. Models of ice stability distribution within the current Martian climate indicate that water ice should be stable in the mid-latitudes (~40–50°) within a meter of the surface and stable closer to the surface near the poles (Bramson et al. 2015). The modern mid-latitude climate controls the unstable nature of the subsurface ice in this mid-latitude region (Bramson et al. 2015; Bramson et al. 2017). This instability is a boon, as the putative episodic melting (Butcher et al. 2017) can potentially generate a modern habitable environment. The ice in these regions is modeled to be a mix of 'pore-filling' ice in shallow regolith pore spaces and relatively pure excess ice (Bramson et al. 2015) as revealed by several investigations, including ice-exposing impacts (Dundas et al. 2018) and radar detection of massive ice in debris-covered glaciers (Holt et al. 2008). Another habitability criterion is the presence of a radiation-protected environment. Much research has been invested in understanding how life on Mars may protect itself from radiation without the standard terrestrial model that utilizes the magnetic field to attenuate ultraviolet (UV) radiation and solar energetic particles (SEPs) (Hallsworth 2021). MLE will sample down to 2 meters to access a depth at which UV irradiation (at <20 mm) and SEPs (cm to m scale) will be attenuated (Pavlov et al. 2012; Fornaro et al. 2018). As discussed below, samples are immediately delivered to the internal science instruments, such that radiation exposure is not an issue for the retrieved samples.

Mars Life Explorer Synergies

Synergies with Robotic Exploration Activities

Mars Life Explorer complements the arc of robotic Mars missions conducted through the Mars Exploration Program (Figure 1-1). Mission objectives built upon each other in a grand architecture such that we have been enabled to 'follow the water', 'explore habitability', and finally to "seek signs of (ancient) life'. The MLE mission takes the next step in Mars exploration by addressing the bold question of whether life exists <u>today</u> in Martian mid-latitude ice. This modern life and habitability explorer mission may operate in parallel with or following Mars Sample Return but would provide the greatest insight by operating prior to the arrival of humans on Mars.

Figure 1-1. Evolving science strategies for Mars exploration. As of this writing, Mars 2020 has landed at Jezero crater, ExoMars launch is delayed until 2022 and Mars Sample Return has started Phase A. MLE complements this arc of robotic Mars missions.

Synergies with Human Exploration Activities

The presence and nature of shallow ground ice is of interest for in situ resource utilization (ISRU) by future human explorers and addresses aspects of MEPAG Goal IV (prepare for human exploration) (MEPAG NEX-SAG 2015; MEPAG 2020). Although this study does not include Human Exploration and Operations (HEO) specific objectives explicitly, future proposers are encouraged to consider HEO collaborations as there is strong overlap with MLE Science Objectives B, C, and D and HEO Strategic Knowledge Gaps (P-SAG 2012). Additionally, there is great interest from the scientific community in seeking extant life prior to the arrival of human astronauts (and their inevitably accompanying microbiomes). The extent to which human microbiota may forward contaminate Mars is under study (Fairén et al. (2017) and references therein). To be confident in the identification of modern Martian life, we must know that the life detected did not originate from terrestrial forward contamination. Therefore, in a most conservative approach, we must search for modern life prior to the arrival of humans on Mars. In addition, any detection of extant life may modify approaches to human exploration, including the choice to not send humans to Mars (Persson 2019).

Landing Site Requirements

A driving requirement of the MLE mission in the mid-latitudes is access to mid-latitude ice within 1 meter of the surface utilizing a 2-meter drill. SHARAD radar coupled with terrain analyses revealed shallow ice across the northern mid-latitudes of Mars (e.g., (Bramson et al. 2015)). Recent work by Piqueux et al. (2019) used data from Mars Climate Sounder (MCS) and Thermal Emission Imaging System (THEMIS) to derive the depth to the water ice table within 1 m of the surface (Figure 1-2). This new analysis and continued data collection (e.g., the Subsurface Water Ice Mapping on Mars study, Morgan et al. (2021)) increase the confidence that a lander can be safely delivered over a subsurface ice deposit within 1 meter of the surface. Additionally, although THEMIS data have confirmed the discontinuous presence of subsurface ice, these same data were used with great success to select the Phoenix landing site (Figure 1-3), albeit at a more northerly latitude (Bandfield 2007; Bandfield and Feldman 2008).

The MLE life science mission is designed to be accomplished in Mars spring and summer in the mid-latitudes (e.g., ~45°), with the planned sizing of the solar array and batteries operation for a full Mars year, consistent with the environment experienced by InSight is expected. However, MLE has looked at options to augment the solar arrays with actuators to mitigate dust accumulation to increase confidence the lander survives a full Mars year to complete the Objective D measurements. There is also flexibility in sizing the power system to enable the mission to move to slightly higher latitudes if this is required to help ensure the presence of ice within 2 m of the surface.

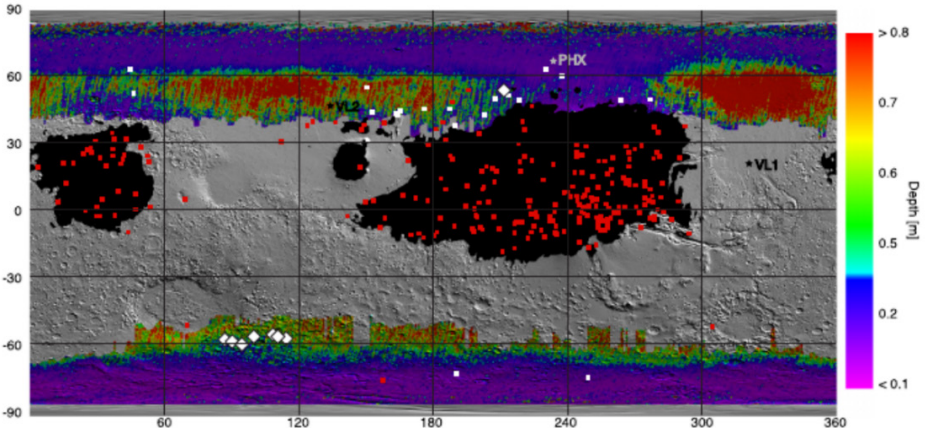

Figure 1-2. Ice depths modeled via THEMIS, compared to HiRISE ice observations (Piqueux et al. 2019). Much of 45°N (e.g., *Arcadia Planitia*) is modeled to contain ice water within <1 m depth. Ice depths (contours) + HiRISE images of ice excavated by impacts (white symbols), red = impacts with no ice; black = dusty regions unsuitable as landing sites.

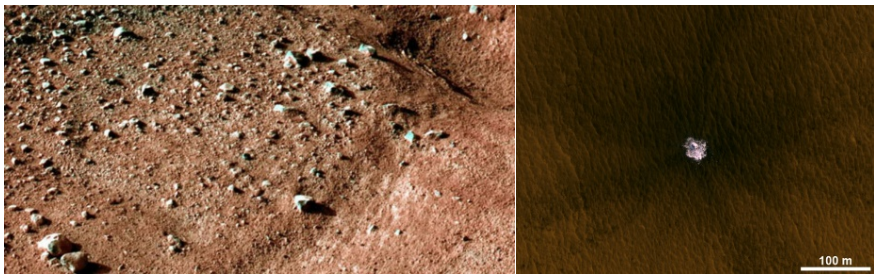

Figure 1-3. Ice polygons at the Phoenix landing site; recent impacts expose ice.

General landing site locales were proposed for MLE as a proof-of-concept. One highlighted region is *Arcadia Planitia*, at *ca.* 45°N. Potential safe landing sites for a static lander, in the mid-latitudes of *Arcadia Planitia*, with ice near the surface, have been identified (Golombek et al. 2021). Although this specific study was for a vehicle with precision landing capabilities, acceptable ellipses in the 10 km class are readily evident in regions of Arcadia and possibly other areas. To achieve the desired landing accuracy, MLE has baselined the use of guided entry, which had been proposed for Phoenix, but descoped as unneeded, but has been used very successfully on MSL and Mars 2020.

MLE Science Traceability and an Instrument-Agnostic Approach

To address the question "Does modern life exist associated with mid-latitude Martian ice deposits, and what is the habitability of these deposits now and over recent Martian history?" the MLE team has used the four objectives and the measurement and instrument information as shown in the Science Traceability Matrix (STM; Table 1-2) to develop the MLE concept based on a modular, instrument-agnostic approach, in which several difference instruments or instrument suites may be selectable to address the mission objectives.

Objective A: Search for organic molecules, non-equilibrium gases, and stable isotopic trends associated with ice, ice-cemented regolith, and regolith within incremental measurements of 20 cm down to 2 meters depth. MLE searches for evidence of extant life via the detection of organics, gases, and isotopes that may be consistent with recent life (e.g., amino acid chirality (Callahan et al. 2013), carbon number preference in fatty acids (Williams et al. 2019), significantly depleted isotopic ratios consistent with metabolic activity, presence of disequilibrium gases, etc., see Hays et al. (2017) and references therein) in the form of modern or moderately-degraded biosignatures. The baseline does not carry nanometer-scale microscopy or nucleobase-specific sequencing to further interrogate any life found, as these technologies are currently lower Technology Readiness Level (TRL), but a future proposer could consider such enhancements.

Objective B: Assess the habitability of the near-subsurface environment with respect to required elements to support microbial life, including microbial energy sources. An assessment of habitability is one of the three pillars required to search for evidence of life on Mars (MEPAG 2020). These assessments should include investigations of chemistry and mineralogy that reveal thermodynamic disequilibria (i.e., suitable energy sources); physicochemical environmental factors (e.g., temperature, pH, salinity, radiation) that bear on the stability of covalent and hydrogen bonds in biomolecules; and the presence of bioessential elements (i.e., C, H, N, O, P, S) and metals.

Objective C: Quantify the down borehole thermophysical properties of the ice and ice-cemented regolith and any role for liquid water in its creation or modification. This objective will constrain the availability of liquid water with respect to duration, extent, and chemical activity in recent or modern habitable environments. This includes assessment of freeze-thaw cycles in icy deposits that are sufficiently close to the surface to experience diurnal and seasonal temperature changes.

Objective D: Determine the processes that preserve, modify, and destroy mid-latitude ice deposits in the modern climate. MLE will quantify the exchange of water between reservoirs by recording the net flux of water vapor out of the surface over a full Mars year, via measuring simultaneous 3-D wind and water vapor abundances at 10–20 Hz frequency from a coupled Tunable

Laser Spectrometer (TLS) and sonic anemometer system. In addition, MLE will measure the drivers for this exchange, which include net radiative heating (via a radiometer), sensible heat flux, and surface wind stress (both obtained via the sonic anemometer + pressure and temperature sensors). A full year is needed to assess if net loss occurs in the modern climate, to estimate the loss rate, and to connect to drivers (e.g., solar heating, winds).

The approach taken in this study is to show representative instrument capabilities and characteristics (including mass, power, volume, and cost) that meet the respective science objectives that are based on past, current and future instruments, without declaring a specific "baseline" instrument(s) [Table 1-1]). Flight heritage from previous landers and NASA instrument maturation efforts in life detection, coupled with a composition by multiple teams enables the MLE concept to leverage many different instruments or instrument suites. Table 3-1 details the science measurements to be made as part of the costed baseline and threshold mission options. The characteristics of the representative instruments/suites are shown in Table 3-2, which are the basis for accommodation on the spacecraft (with margin) and for costing and reserves discussion provided in Section 5. The detailed information about different instrument capabilities and supporting detailed information on specific instruments used to define the representative payloads in Table 3-2, are included in Appendix B. This approach to payload definition has been used to provide constraints on the capabilities of the engineering payload, the drill and sample delivery system, and the spacecraft, including providing a basis for appropriate margins in engineering resources. MLE has taken advantage of the deep and current experience of industry to define high heritage engineering systems that can meet the challenges of landing and operating on Mars within a New Frontiers-class budget.

Table 1-1. Example of the instrument-agnostic approach of MLE using a subset of considered payload choices for Objectives A and B.

Objective	Measurements	Baseline (chosen for baseline costing)	Alternative Baseline	Alternative Baseline
A. Organics and modern life	Organics, Organics structure, Trapped gases, Light isotopes	DraMS + (EGA, TLS) (mass spectrometry + pyrolysis gas chromatography & laser desorption)	MOMA + (EGA, TLS) (mass spectrometry + pyrolysis gas chromatography & laser desorption)	SAM + (EGA, TLS) (mass spectrometry + pyrolysis gas chromatography)
B. Habitability	Major/minor element chemistry, mineralogy, redox, salts, total organic chemistry	CheMinX (XRD/XRF) MECA (conductivity via wet chemistry)	APXS, Mössbauer, MLPS (IR spectrometer)	MICA (wet chem, pH), APXS

APXS = Alpha-Particle X-ray Spectrometer; CheMin = Chemistry and Mineralogy; DraMS = Dragonfly Mass Spectrometer; EGA = Evolved Gas Analyzer; MICA = Microfluidic Icy-World Chemistry Analyzer or Minerals Identified through CRISM Analysis; MLPS = Mid- and Long-wave Infrared Point Spectrometer; MOMA = Mars Organic Molecule Analyzer; TLS = Tunable Laser Spectrometer; XRD = X-ray Diffraction; XRF = X-ray Fluorescence

Leveraging Drill Technology and Concept of Operations for Novel Science

Because the drill technology is instrumental to the mission, we discuss it in greater detail here and in Section 3 and Appendix D. The Honeybee TRIDENT (The Regolith and Ice Drill for Exploration of New Terrains) drill (Zacny et al. 2021) is presented as the nominal drilling system for MLE. A 2-meter rigid single-stem drill system was selected since it could fit across the proposed lander deck. Penetration into the surface can be accomplished with rotary-hammer drilling as has been demonstrated on Curiosity; therefore, rotary hammer drilling was selected for MLE. This drilling system is not comparable to the InSight mole approach, which relied on frictional interactions with the hole wall for downward motion, and its related in situ performance challenges (Good et al. 2021). Three degrees of freedom on the drill arm ensure that the drill can achieve at least three distinct drill solutions to avoid surface and subsurface drilling impediments. Margin in the concept of operations timeline and power permits up to three full-depth unique drill holes during the prime mission.

Sample transfer from the drill to the instruments is achieved by pneumatic delivery. After reaching the desired depth, the drill auger is pulled to the surface, and cuttings are brushed into a sample container and a puff gas carries the powdered sample to sample chambers in the science instruments on the lander. Pneumatic sample transfer uses a small volume of noble gas stored in a tank at the foot of the drill assembly.

1.2 SCIENCE TRACEABILITY

Table 1-2. Science Traceability Matrix. (* = many others possible)

Science Objective	Measurement Objective	Measurement Requirement	Baseline Notional Instruments*	Mission Requirements
A. Search for organic molecules and non-equilibrium gases associated with ice and regolith and evaluate their possible biological origin	Detect organic compounds in ice and non-ice phases at 20 cm depth intervals down to 2 m	Sample extraction and detection (at 10 parts per billion by weight [ppbw] sensitivity) of organics over a wide range of water solubility, volatility, and molecular weight to at least 1000 u	Organic Extractor and Separation Mass Spectrometer (e.g., DraMS GC-MS (gas chromatography mass spectrometry) with MSL SAM EGA (evolved gas analysis) and SAM mini-TLS (tunable laser spectrometer))	Landing payload where ice is within 1 m of surface
	Targeted organic structural characterization to determine biogenicity (via abundance patterns, diversity/ complexity of species, and chirality)	Detect and structurally characterize amino acids, fatty acids, carboxylic acids, alkanes, polycyclic aromatic hydrocarbon (PAHs), and any compounds of higher complexity, e.g., peptides, porphyrins, and polynucleotides, with a detection limit of 10^{-11} mole		Drill to 2 m for sample acquisition with precision of 20 cm or better
		Quantify the relative abundances of any amino acids to glycine (Gly) to an accuracy within 10%		
		Quantify enantiomeric excess (ee) of at least three chiral proteinogenic amino acids to an accuracy within 5%	Chiral Sensitive Separation Detector (e.g., chiral GC column on DraMS, SAM, or MOMA)	
	Determine the composition of ice-trapped gases	CO_2, CH_4, and other trace gases with sensitivity of 2 ppb direct	Tunable Laser Spectrometer (e.g., SAM TLS)	Transfer of volatiles to sealed capsule
	Determine sources of ice/gases, using light isotopes as tracers	H, C, O, N, S isotopic measurements within <10 per mil precision		Carousel of sample capsules to hold materials from different depth intervals
B. Assess the habitability of the near-subsurface environment with respect to required elements to support life, including energy sources	Determine volatile abundances, redox chemistry, and total organic and inorganic carbon	Evolved volatile gases from pyrolysis; combustion for total organic carbon (TOC)	Evolved Gas Analysis (e.g., SAM EGA)	Same as above
	Identify salts and potential for aqueous chemistry	Analysis of both inorganic and small organic cations (e.g., alkali metals, amines and alkanolamines) and anions (e.g., perchlorates, chloride, organic acids)	Conductivity Detector (e.g., Phoenix MECA [Microscopy, Electrochemistry, and Conductivity Analyzer] wet chemistry)	
	Determine bulk mineralogy	Silicate, oxide, salt, amorphous phase characterization	X-ray diffraction (e.g., CheMinX XRD)	
	Determine bulk chemistry	Major (e.g. Na, K, Ca, Mg, Al, Fe) and minor element chemistry	X-ray fluorescence (e.g., CheMinX XRF) (or Alpha Particle X-Ray Spectrometer [APXS])	
C. Determine the thermophysical properties of the ice/ ice-cemented regolith and any role for liquid water in its creation or modification	Determine the subsurface temperature profile	Temperature profile of the subsurface and monitoring of borehole temperature as a function of time	Thermal sensors on drill (e.g., drill engineering sensors)	Ring and column imaging of the drill hole and downhole measurement
	Assess changes in texture and physical properties downhole	Downhole imaging, mineralogy, texture and layering observations at the cm scale	Imaging (e.g., Honeybee Drill Imager)	
	Determine the subsurface electrical conductivity profile	Conductivity profile of the subsurface and monitoring of borehole resistivity as a function of time	Electrical conductivity sensors on drill (e.g., drill engineering sensors)	
D. Determine the processes that preserve/ modify/ destroy these ice deposits in the modern climate	Determine controls on the exchange of water vapor between reservoirs	Temperature, pressure, fluxes of water vapor between the surface and atmosphere, surface wind stress	Pressure and air temperature sensors (e.g., Mars 2020 Mars Environmental Dynamics Analyzer [MEDA] Pressure Sensor and Air Temperature Sensor)	Measurements over at least 1 Mars year
			TLS with channel for water vapor coupled with 3-D sonic anemometer (SA)	
	Surface energy balance and thermal environment, including sensible heat flux	Longwave (LW) and shortwave (SW) upward and downward radiative fluxes at surface	Radiometer (e.g., Mars 2020 MEDA Thermal Infrared Sensor (TIRS) with additional downward SW)	

2 MISSION CONCEPT DEVELOPMENT APPROACH

The Mars Life Explorer (MLE) concept will allow future Principal Investigators (PIs) to answer fundamental life science questions by sampling mid-latitude subsurface ice, using engineering heritage from Phoenix/InSight (lander/EDL) and lunar missions in 2022–2023 (drilling and sample delivery), within the constraints of a New Frontiers-class mission.

2.1 CONCEPT DEVELOPMENT CONSTRAINTS

The following are the primary constraints and key drivers that have been provided by the Mars Decadal Subcommittee and developed by the study team to guide the development of the overall concept:

From Mars Decadal Subcommittee:

- Mid-latitude landing sites identified as likely having ice within 1 m of the surface (specific landing site conditions and location options are to be identified). Other sites including higher latitude Phoenix-like or none-to-little ice Cerebus Fossae-like sites are also options.
- 2 m drill depth capability and sample delivery from discrete depths to science instrument(s)
- Accommodate instruments to meet the four objectives in the Science Traceability Matrix (STM; Table 1-2)
- New Frontiers(NF)-class scope and cost cap ($1.1B), but the cost cap is not a hard constraint

From study team (including knowledge and experience with past NF-class missions):

- Class B overall reliability
- Use 2035, 2037, and 2039 launch readiness dates (LRDs) for mission design and entry, descent, and landing (EDL) with a baseline LRD of 2035. 2033 is also an option.
- Design lander and EDL to be a contracted NASA mission, building on mission heritage including missions like Phoenix and InSight but with augmentations to the aeroshell, parachute, propulsion, power, and structure to accommodate larger science and engineering payload (150 kg vs. ~60 kg)
- Develop mission design and operations strategy consistent for an all-solar-powered mission for up to a full Mars year for the meteorology instrument
- Meet assumed planetary protection categorization of IVb for specific hardware to meet science objectives

2.1.1 STUDY STRATEGY

The MLE study strategy is based on meeting the science objectives and constraints while leaving flexibility for future mission PIs in proposing specific measurements and instruments ("instrument-agnostic approach"). The strategy will use the four science objectives as the basis for representative instrument capabilities without specifying specific instruments. Within each level, a wide list of past, present, and future instruments have been identified to meet the specific objectives and with specific engineering characteristics (see Appendix B for the detailed summary tables and fact sheet-level information used to prepare the tables). For each instrument level, there will be a bounding capability in terms of engineering resources, e.g., mass, power, energy, volume, interfaces, concept of operations, and cost to be used to size the flight system, with margin

The overall study strategy is to show an "existence-proof" of a mission(s) that meets the science objectives and constraints, including appropriate technical and programmatic margins. The study will use JPL's A-Team and Team X to develop and characterize a "minimum mission" that meets only the highest priority science objectives; this will be considered a "reference threshold" mission. Various key trades will be conducted to establish the engineering payload (drill and sample delivery

system) and spacecraft, including cruise stage, aero-entry system, and lander. The MLE study team is supported by Team X, Lockheed Martin (LM), and Honeybee Robotics.

Once a "reference threshold mission" is established within the NF-class constraints, alternatives in scope, based on adding in additional science instrument capabilities, will be evaluated for impacts on engineering resources (e.g., mass, power), concept of operations, reserves, and budget to determine whether an option beyond the threshold can fit within the NF constraints. If such an option exists, it will be established as the baseline. Alternate assumptions, including different reserves and overall budget constraints, will also be used to identify possible options for further science enhancement beyond the baseline.

2.2 KEY TRADES

The following is a summary of the key trades that were evaluated early in the study process:

1. Science objectives and STM (Table 1-2) – traded with payload options to establish a range of performance and costs.
2. Payload definition – representative payloads were identified (past, present, and future) that could meet specific measurements defined in the STM. Traded payload options including analysis systems performance and engineering characteristics.
3. Drill and sample transfer concepts – evaluated various studies, proposals, and developments (including international, e.g., ExoMars) focused on Honeybee Robotic concepts based on past experience with the TRIDENT (The Regolith and Ice Drill for Exploration of New Terrains) concept (to be flown to the Moon in '22 and '23 and pneumatic sample transfer. Alternate options for drill string configuration and sample acquisition/transfer were evaluated.
4. Sample processing and delivery to instruments concepts – worked with science representatives, Honeybee Robotics, and experienced JPL engineers to develop options including what the sampling system does vs. the instrument front-ends, e.g., should instruments or spacecraft provide a sample carousel? Included were approaches to maintain sample integrity.
5. Landing site options – initial options were provided by the Decadal Survey panel and were evaluated along with other options. A number of possible sites were used to evaluate the mission design and establish safe landing sites with a high likelihood of ice within 1 m based on a landing error ellipse of ~10 km.
6. Mission design – evaluated mission design space around LRDs of 2035, 2037, and 2039 that could deliver a representative lander mass range to mid-latitudes with acceptable margins. An earlier LRD of 2033 was also looked at as an alternative option.
7. Spacecraft concepts – considered range of demonstrated Mars surface lander missions that could provide payload accommodation and meet other constraints. Used Team X and LM to evaluate key capabilities including launch, EDL, science and engineering payload accommodation, power, and operational capabilities.
8. Concept of operations – evaluated options for drilling and direct transfer to instruments vs. transfer to intermediate storage containment for later analysis. Worked with science representatives, Team X, and current mission operations experts on timeline and appropriate margins.

3 TECHNICAL CONCEPT

The MLE technical concept includes a baseline and threshold science payload, an engineering payload for drilling and sample delivery, and a spacecraft based on proven entry and operations on Mars that provide a robust concept for a New Frontiers-class life science mission.

3.1 INSTRUMENT PAYLOAD DEFINITION APPROACH

This section discusses the science payload options evaluated based on the Science Traceability Matrix (STM; Table 1-2), with input from the science representatives and other instrument experts. Instruments packages are broken down by groups—A, B, C, D—based on the STM. Specific instruments associated with meeting the STM capabilities have been identified and within each group, a reference capability, in terms of engineering resources, e.g., mass, energy, volume, interfaces concept of operations, and an estimated cost, was established. Appendix B contains the detailed tables of the data used to define the instrument group capabilities and characteristics.

3.1.1 SCIENCE PAYLOAD OPTIONS

Through a process of evaluating science instrument capabilities, and characteristics, including mass, cost, and power, two mission capabilities were derived. Table 3-1 shows the measurement capabilities associated with the baseline and threshold missions. In order to accommodate this range of payload options, a bounding set of characteristics in each group, A–D, was defined (Table 3-2) and used to develop a bounding set of constraints on the engineering payload (drilling and sample delivery system) and spacecraft. Based on inputs from the science advisory team, the only difference between the baseline and threshold is a reduction in the B2 and B3 measurements. The "Representative Instrument(s)" in Table 3-2 are there to provide insight into the type of instruments that could provide the desired measurements and help provide a basis for a representative set of bounding engineering characteristics, but are not intended to limit the future options for the science payload.

Table 3-1. Primary science measurements capabilities needed to meet baseline and threshold missions.

#	Measurement Description	Baseline	Threshold
A1	Sample extraction and detection of organics	X	X
A2	Detect and structurally characterize, amino acids, fatty acids, etc.	X	X
A3	Quantify the relative abundances of any amino acids to glycine	X	X
A4	Quantify enantiomeric excess (ee) of at least three chiral amino acids	X	X
A5	CO_2, CH_4, and other trace gases	X	X
A6	H, C, O, N, S isotopic measurements	X	X
B1	Evolved volatile gases from pyrolysis; combustion of total organic carbon (TOC)	X	X
B2	Analysis of both inorganic and small organic cations and anions	X	partial
B3	Silicate, oxide, salt, amorphous phase characterization	X	partial
B4	Major and minor element chemistry	X	X
C1	Temperature profile of the borehole temperature as a function of time	X	X
C2	Downhole imaging only	X	X
C3	Conductivity profile of borehole resistivity	X	X
D1a	Temperature, pressure	X	X
D1b	Fluxes of water vapor (abundance) and dust between the surface atmosphere	X	X
D1c	Surface wind stress	X	X
D2	Longwave (LW) and shortwave (SW) radiative fluxes at surface	X	X

Table 3-2. Science instrument engineering characteristics by mission option.

Mission Level	Baseline (A–D)				Threshold (A–D)			
Instrument Capabilities	GCMS, EGA, TLS	Chem, Min + Conduct	Downhole, temp, conduct, imaging*	Temp/Press, wind stress, H_2O flux, rad flux	GCMS, EGA, TLS	Chem, Min	Downhole, temp, conduct, Imaging*	Temp/Press, wind stress, H_2O flux, rad flux
Representative Instrument(s)	DRaMS w/EGA + Mini-TLS	Chem/MinX + MECA and EGA (part of Obj. A)	Engineering sensors and imager	Anemometer + TLS + MEDA temp/ press/TIRS	DRaMS w/EGA + Mini-TLS	APXS+ EGA (part of Obj. A)	Engineering sensors and imager	Anemometer + TLS +MEDA temp/ press/ TIRS
Technology Readiness Level (TRL)	5–6	5+	5–9	5+	5-9	9	5–9	5+
Current Best Estimate (CBE) Mass Dry Allocation (kg)	35	14	2	3	35	5	2	3
Exterior Size (cm)	50×40×30	40×30×20	Scaled to drill	20×20×10	50×40×30	30×20×20	Scaled to drill	10×10×10
Max Avg Power (W)	250	60	5	1	250	40	5	1
Max Data Volume Allocation (Mb/sol)	200	100	10	8	200	100	10	8
Energy Allocation (Wh/analysis cycle)	400	400	10	3	400		10	3
Sample Access	Internal Carousel	Internal Cartridge	Borehole	Atmosphere	Internal Carousel	Internal Cartridge	Borehole	Atmosphere
Cost by Group ($M FY25)	**$85**	**$60**	**$5**	**$12**	**$85**	**$7**	**$5**	**$12**
Total Cost by Mission	**$162**				**$109**			

*APXS = Alpha-Particle X-ray Spectrometer; Chem = Chemistry; DRaMS = Dragonfly Mass Spectrometer; EGA = Evolved Gas Analyzer; GCMS = Gas Chromatograph Mass Spectrometer; MECA = Microscopy, Electrochemistry, and Conductivity Analyzer; Min = Mineralogy; MOMA = Mars Organic Molecule Analyzer; TLS = Tunable Laser Spectrometer. *Mass for downhole is for imager, temp. and conductivity is in drill mass, cost includes imager and testing for temp. and conductivity measurements.*

3.2 ENGINEERING PAYLOAD (DRILL AND SAMPLE DELIVERY SYSTEM)

3.2.1 *TRADE SPACE*

A trade space was evaluated to determine the sampling system architecture. The trades were fundamentally between a system like the ExoMars segmented system with sample delivery directly from the drill to instruments or a single drill stem with an alternative sample delivery system. The evaluation followed the process illustrated in Figure 3-1, with the items in the bolded boxes being the elements selected for the reference concept based on compatibility with the science payload, heritage, complexity, reliability, and cost. Single-stem and multi-stem drilling systems have different advantages and disadvantages. The multi-stem design allows for a compact drill system such as the ExoMars drill system, which is designed to acquire samples from a depth of 2 m using 3 extension rods (Van Winnendael et al. 2005; ESA 2012). A coiled drill stem is an alternative single-stem solution, which could acquire samples from tens of meters deep, but would be more complex than a rigid stem solution (Mank et al. 2021; Zacny et al. 2018). A single-stem system with a rigid drill stem is limited in sampling depth by the lander deck stowage length. The 2-meter rigid single-stem drill system, described below, was selected since it is less complex and fits across the lander deck.

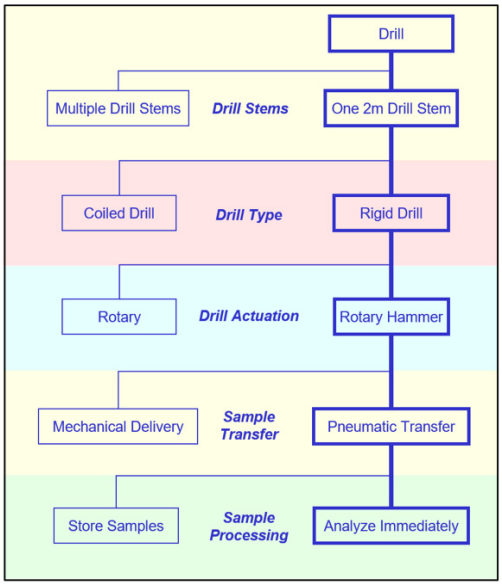

Figure 3-1. Engineering payload architecture.

Penetration into the surface can be accomplished with rotary and rotary-hammer drilling. A rotary-hammer adds mechanical complexity versus a rotary-only drill, but a rotary-hammer drill requires significantly lower energy (Zacny et al. 2013) and has been used on both MSL and M2020. Therefore, rotary-hammer drilling was selected.

Sample transfer from the bottom of the hole could be achieved by mechanical delivery as is done with the ExoMars drill, where the drill is pulled up completely from the hole and articulated to the point where the sample is dropped into a sample handling system for distribution to science instruments. Pneumatic sample transfer (using a noble gas) has been shown to be effective in low pressure environments (Zacny et al. 2013) and was chosen for this study. For the TRIDENT (The Regolith and Ice Drill for Exploration of New Terrains) design, the drill is pulled just to the surface (it is not articulated away from the existing hole and doesn't have a risk associated with reentering the hole), where cuttings are brushed into a sample container and pneumatics are used to carry the powdered sample to the science instruments on the lander.

The mechanisms for compressing and using in-situ gas for pneumatic sample transfer were considered because they could provide a nearly unlimited supply of gas, based on the MOXIE (Mars Oxygen In-Situ Resource Utilization Experiment) design. However, since the pneumatic sample transfer requires a very small volume of gas, it was decided that a tank and valve system, with >3× margin for 10 cycles of sample delivery would provide a less complex and lower cost system.

Operations concepts were compared for storing samples for later analysis versus immediate analysis of an acquired sample. Storing samples for later analysis would add significant complexity since the sample chambers would need to be sealed for stowage and later unsealed for analysis, while maintaining the samples at close to downhole temperature. Immediate sample analysis, consistent with current instrument approaches, was selected.

A key factor in the design and operations of this system is maintaining sample integrity, i.e., preserving the sample state and purity from acquisition downhole to delivery to the instruments (after which maintaining sample quality is the responsibility of the respective instruments). The pneumatic system would be operated at the appropriate time of day to maintain temperatures and would also allow for flushing of the sample delivery tube to help assure no cross-contamination between samples at desired depths.

Prior missions and testing indicate challenges associated with achieving needed reliability in drilling. Results from the Mars Phoenix mission show that sampling and sample transfer of samples that include ice can be affected by the daytime surface temperature. This proposed mission concept mitigates this by planning for sampling at night and early dawn when the cold temperature keeps the ice frozen and handles as a solid (options to provide shadowing can also be considered) The drill bit temperature is monitored and drilling is controlled to keep the change in ice temperature below 10°C. The InSight mission mole was designed to penetrate to a maximum 5-meter depth but was only able to penetrate to its 0.4-meter body length due to unexpected properties of the regolith. The MLE approach provides a drill that has been demonstrated to be robust to the uncertainties in the subsurface environment. Many drilling validation experiments have been performed, including in a Mars chamber, lunar chamber, and field experiments in the arctic, Greenland, Atacama desert, Antarctica, and RioTinto (Zacny et al. 2010; Zacny et al. 2011; Zacny et al. 2013). Drilling robustness is enhanced by the 3 degree of freedom (3-DoF) drill deployment arm being able to position the drill at alternative drilling locations if drilling in the one required hole is unsuccessful.

Details on the heritage, including testing in relevant environments is contained in Appendix D. Details of the downhole sensing capabilities are also discussed.

3.2.2 BASELINE ENGINEERING PAYLOAD

The drilling and sample transfer system is based on the high heritage of the TRIDENT drill system and PlanetVac pneumatic sample transfer system in development by Honeybee Robotics to be flown in 2022 on the Polar Resources Ice Mining Experiment-1 (PRIME1) lander (Intuitive Machines) and in 2023 on the Volatiles Investigating Polar Exploration Rover (VIPER) lunar rover. Table 3-3 shows all the key engineering parameters, including mass and cost associated with the baseline engineering payload. Figure 3-2 shows the configuration of the proposed landed system with key drill and sample delivery system elements.

Table 3-3. Drilling and sample transfer system parameters.

Payload Accommodation Requirements	Drill	Arm	Biobarrier	Drill Avionics	Gas Sample Transfer	Instrument Camera
CBE Mass (kg)	20	7	3	7	8	0.9
CBE Average Power (W)	100	50	-	30	10	5
CBE Average Energy (Wh)	200	25	-	60	10	2.5
CBE Data Rate(s) (bps)	25	10	n/a		10	<12.6 Mb / image
Thermal Control Requirements	Keep samples cold				Keep samples cold	
Accommodation Requirements	Deck; deploys off side	Deck	On deck covering drill	On Deck	Mounted on drill	Mounted on arm
CBE Dimensions (L×W×H in m)	2.7 m × 0.3 m × 0.3 m	1 m × 0.1 m × 0.1 m	3 m × 0.15 m diameter	0.3 m × 0.25 m × 0.2 m	0.3 m × 0.2 m × 0.2 m + tubing	
CBE Cost ($M FY25)	$16	$8	$3	$7	$7	$5
Basis of Estimate	Honeybee Trident Drill	Icebreaker Boom	Auger bio-barrier	Honeybee TRIDENT system	Honeybee PlanetVac	IDC
TRL	7	6	9	7	7	9
Basis of TRL	Honeybee Trident for lunar missions: VIPER and PRIME1	Icebreaker Boom; other options MSL and M2020 boom	Phoenix	Honeybee TRIDENT for lunar missions	CLPS19, MMX	IDC
Total Mass (kg)	**46**					
Total Energy (Wh/sol)	**300**					
Total Cost ($FY25)	**$46**					

CLPS = Commercial Lunar Payload Services; IDC = InSight Deployment Camera; MMX = Martian Moon eXploration

- Two meter drill is deployed from bio-barrier (not shown) using 3-DoF robotic arm
- Drill cuttings are moved by auger flutes to the surface, at depth the drill string is retracted and material is brushed off the auger tip into a chamber for transport to the instruments by a puff of gas from the pneumatic system (using a noble gas supply)
- At the instrument(s) a feature diverts the material in the gas flow into the instrument carousel
- The drill reenters the hole and drills to the next depth

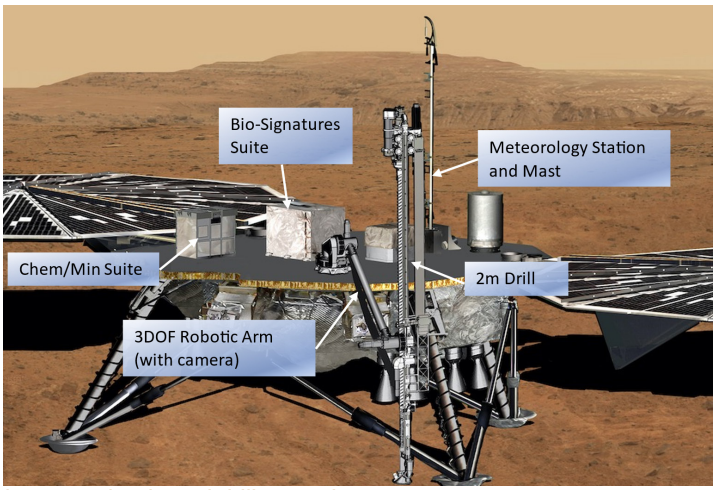

Figure 3-2. Deployed drill and representative science payloads and drill operations summary.

3.3 MISSION DESIGN AND CONCEPT OF OPERATIONS

3.3.1 MISSION DESIGN OPTIONS OVERVIEW

The MLE mission design is based on a ballistic launch with a baseline launch readiness date (LRD) of 2035, with backups in 2037 or 2039. The entry conditions for the three prime LRDs are assumed to be the following:

- Ls arrival: 0–90 (earlier is better)
- Landing: 40–45 N
- Max entry speed: <6.1 km/s (Vinf <3.7 km/s) (InSight was 6 km/s)
- Altitude: <−3 km Mars Orbiter Laser Altimeter (MOLA)
- Entry flight path angle: −11.5 to −12.5 (InSight was −12 deg)
- Landing ellipse major axis: ~10 km

Table 3-4 shows the summary results of the mission characteristics for the baseline, 2035, and backup LRDs. An earlier LRD of 2033 was also briefly evaluated and is programmatically viable but would require some additional work in the mission operations strategy.

The launch conditions have been evaluated and show the following:

- Can launch on any launch vehicle (LV) consistent with New Frontiers call (e.g., Falcon Heavy Recoverable, Vulcan)
- Launch mass capability >2,000 kg
- Large margins, could allow up to C3 = 40 km^2/s^2

Table 3-4. 20-day launch periods.

	2035	2037	2039
Arrival Ls	0	22	75
C3 (km^2/s^2)	23.1	18.4	37.5
VHP (km/s)	3.1	3.7	3.7
Entry Speed (km/s)	5.83	6.19	6.19
Type	II	I	II
1st Launch Date	5/17/2035	8/11/2037	7/28/2039
Cruise (days)	284	199	290
Arrival Date (fixed)	2/25/2036	2/26/2038	5/13/2040
DLA (°)	-29	43	-11
Max N Reachable	68N	55N	72N

DLA = Declination of Launch Asymptote;
VHP = Hyperbolic Excess Velocity

The entry, descent, and landing (EDL) performance based on these conditions is discussed in Section 3.3.2.

The options for landing sites and the issues associated with landing site selection are discussed in Section 3.3.3.

3.3.2 CRUISE AND EDL CONCEPT OF OPERATIONS

Cruise is expected to be a nominal ballistic trajectory with characteristics shown in Figure 3-3.

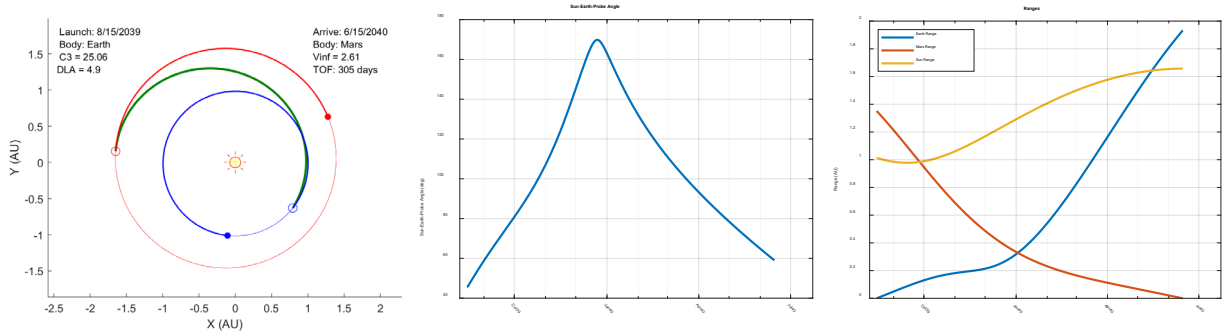

Figure 3-3. Representative cruise trajectory, Sun-Earth-probe angle and ranges for worst case, 2039.

Table 3-5 shows the differences in the vehicle characteristics for EDL between Phoenix, InSight, and MLE (the CBE/MPV [maximum possible value] numbers refer to lowest and highest values used for design ranges). The most significant mass difference between InSight and MLE is in the entry system due to the selection of the 3.65 m aeroshell (vs. 2.6 m for InSight) to provide volume for the drill and good EDL performance characteristics, including ballistic coefficient, heating rates, and parachute deploy conditions. The thrust-to-weight are in family with Phoenix and InSight.

Table 3-5. Vehicle characteristics for EDL. CBE/MPV used for min/max range.

	Unit	Values	PHX	InSight	MLE
Max Wet Entry Mass	kg	CBE/MPV	572/606	606/625	952/1203
Entry Ballistic Coefficient		min/max	62/67	67/69	55/70
On-chute Ballistic Coefficient		min/max	7.4/7.9	7.6/8.1	6.6/8.4
Max Wet Lander Mass	kg	CBE/MPV	363/426	366/435	460/645
Lander Thrust/Weight		min/max	2.0/2.4	2.3/2.4	2.0/2.5

Figure 3-4 shows the EDL timeline, which is consistent with the performance of Phoenix and InSight in all the key parameters. Appendix E contains details of the EDL performance analysis performed by LM and a table with specific comparisons of key EDL metrics with Phoenix and InSight.

Given the relatively large landing error ellipse for a ballistic entry and the expectation that a smaller target error will be needed, guided entry will be implemented for this mission. LM has assessed and factored in the changes needed, and cost to add guided entry, including thruster

locations, ballast, software, and simulations. The knowledge of the needed changes comes from their own experience with Phoenix, which had guided entry in the baseline but was descoped as not necessary given the large Phoenix landing area. JPL's experience with such a capability on MSL and M2020 will also be applied.

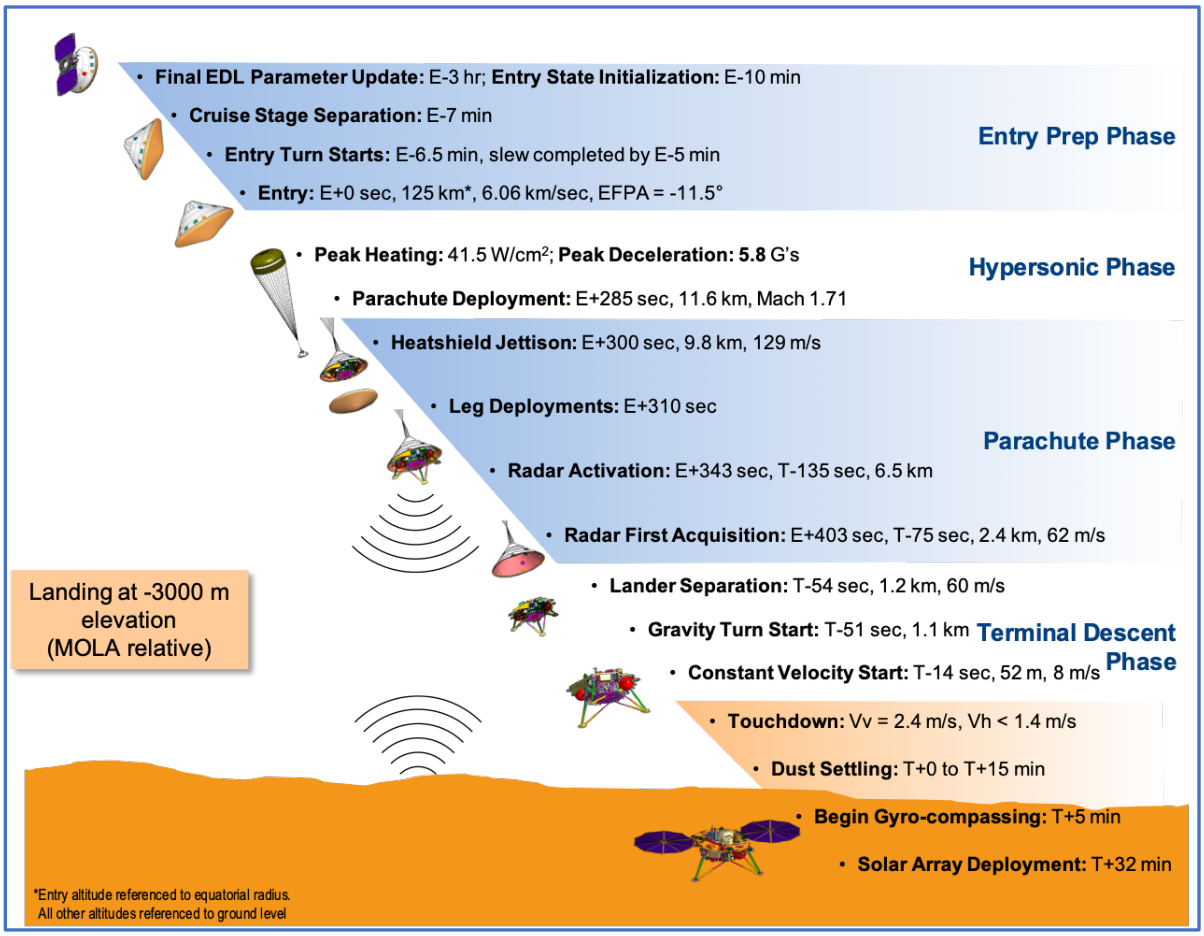

Figure 3-4. EDL concept of operations showing key parameters. Guided entry phase not shown.

3.3.3 MLE LANDING SITES

A range of landing sites have recommended for consideration by the science advisory group. All are at −3.5 km MOLA or lower including:

- Arcadia Planitia, 40°N
- Utopia Planitia, ~45°N
- Phlegra Montes, 35°N

The expected landing site constraints for a safe MLE landing assumes slopes <15 deg, 30 cm rock clearance, and low rock abundance. The most recent detailed safe landing analysis for an MLE-type mission was conducted for a SpaceX Red Dragon lander (Golombek et al. 2021), which was a legged lander study with similar landing site constraints to MLE including mid-latitudes, with near surface water, <−3 km MOLA, ~10 km landing ellipse. Studies of Arcadia Planitia using HiRISE (High Resolution Imaging Science Experiment), TES (Tropospheric Emission Spectrometer), THEMIS (Thermal Emission Imaging System), and Viking rock distribution data showed multiple sites (6–12) in the Sinuous Unit that look like credible landing sites for MLE. Further study of landing site options and landing site criteria should be conducted pre-Phase A and a primary and back-up landing site identified.

3.3.4 MISSION DESIGN REFERENCE CONCEPT

Table 3-6 shows the summary mission design conditions for the worst case of the 2035 and 2037 LRDs.

Table 3-6. Mission design scenarios.

Parameter	Value	Units
Entry Velocity	< 6.1	km/s
Entry Flight Path Angle	−12.5	deg
Max C3	24	km^2/s^2
Mission Lifetime	10 mo. cruise + >24 on surface	mos
Maximum Eclipse Period	(N/A in cruise, ~12 h on surface)	min
Launch Site	KSC or VAFB	
Total Entry Mass **with** contingency (includes instruments)	~1203	kg
Propellant Mass **with** contingency	116	kg
Launch Adapter Mass **with** contingency	70 (estimated0	kg
Total Launch Mass	~1300 kg	kg
Launch Vehicle	Falcon Heavy Recoverable	Type
Launch Vehicle Lift Capability	>2025	kg
Launch Vehicle Mass Margin	725	kg
Launch Vehicle Mass Margin (%)	36	%

3.3.5 CONCEPT OF OPERATIONS SUMMARY

The MLE surface concept of operations is based on the following:

- Baseline arrival: Ls = 0 (with Ls as late as 75 being accommodatable)
- Various mid-latitude landing sites are available
- 30 sol post landing checkout and commissioning phase
- Single drill hole (with options for other holes depending on need, time, performance, and instrument capabilities)
- Reconnaissance using instrument deployment camera before and during drilling
- Deploy drill using 3-DoF arm
- Drilling scenario assumes drilling in 20 cm increments with sample delivered to instruments from depth (duration from warm up to sample delivery, 1–2 hours, allocate 1 sol for drilling and data download, time of day is a consideration with night or early morning preferred for sample integrity)
- Sample transferred to two instruments set by pneumatic system
- Sample is processed and analyzed by two instrument sets, allocate 1 sol for each analysis (based on SAM and Chem/Min capabilities)
- Assuming typical AM/PM ground contact opportunities with each sampling and analysis sol bracketed with ground-in-the-loop and overnight activities completed nominally to proceed with the next sol's drilling. Therefore, no additional time for ground in the loop.
- Repeat 10 cycles, down to 2 m

Summary of timeline with margins for drilling:

- 30 sol checkout plus nominal minimum science timeline of 3 sols × 10 sites = 30 sols for a total of 60 sols. Add 100% margin for assumed total mission duration of 120 sols.
- Have assumed worst-case power condition for all mission options is at Ls=150, which provides up to a ~230 sol total surface timeline for the 2035 mission (another 100 sols of margin). For the 2039 mission option, with an arrival of Ls=75 deg, the total surface timeline has ~150 sols (for an additional 30 days of margin).

This timeline is comparable to that of Phoenix, which was faced with similar goals in terms of the number samples and similar engineering and operational considerations. Phoenix delivered samples

from ~14 separate acquisitions within its 90-day prime mission (see Table 2 from (Arvidson et al. 2009). This provides a basis for confidence for the overall timeline estimate.

The meteorology measurements for Objective D only, have an operational timeline of a full Mars year, ~668 sols, with power discussed in Section 3.4.

Phase	Duration (sols)	Activity
Post Landing Checkout, preparation to drill and analysis.	30	Engineering
1st Drill and analysis cycle	3	Science
9 more cycles	27	Science
2x margin for more time for first hole and/or another hole	60	Margin
Meteorology	668	Science

Figure 3-5. Operations timeline.

Figure 3-5 shows the overall operations timeline. The assumed key mission operations, flight system, and ground data system characteristics to support the three mission operations phases are summarized in Table 3-7.

Table 3-7. Mission operations, flight system, and ground data system characteristics by phase.

Downlink Information	Cruise	Surface Science	Meteorology
Number of Contacts per Week (peak science)	2	>21 (min. 3 per sol)	7
Number of Weeks by Mission Phase, weeks	40	16	~100
Downlink Frequency Band, GHz	8.4	8.4 (X-band), 0.4 (UHF)	8.4 (X-band), 0.4 (UHF)
Capable Downlink per Pass per Orbiter, Mb	NA	50	<10
Transmitting Antenna Type(s) and Gain(s), DBi	MGA; LGA	Helix, LGA	Helix, LGA
Transmitter Peak Power (RF), watts	18 (X-band)	10 (UHF), 18 (X-band),	10 (UHF), 18 (X-band)
Downlink Receiving Antenna Gain, DBi	79.37 in X/Ka Mode	79.37 in X/Ka Mode	79.37 in X/Ka Mode
Min Daily Data Volume, (Mb/sol/orbiter)	NA	100	<10
Uplink Information	**Cruise**	**Surface Science**	**Meteorology**
Number of Uplinks per Day	2	7	7
Uplink Frequency Band, GHz	7.2	7.2	7.2
Telecommand Data Rate, kbps	2	2	2
Receiving Antenna Type(s) and Gain(s), DBi	DSN 34 M BWG	DSN 34 M BWG	DSN 34 M BWG

BWG = beam waveguide; DSN = Deep Space Network; LGA = low-gain antenna; MGA = medium-gain antenna; UHF = ultra-high frequency

3.4 FLIGHT SYSTEM

3.4.1 KEY FLIGHT SYSTEM DRIVERS

The key drivers for the flight system based on the baseline payload, with margin, are:

- Accommodate a science and engineering payload of 150 kg based on a CBE of 100 kg, i.e., with 50% margin. For reference, the comparisons to Phoenix and InSight are:
  - Science payload for Phoenix was ~46 kg and for InSight was ~41 kg, as flown, compared to 54 kg CBE for MLE
  - Engineering payload for Phoenix was ~13 kg and for InSight was ~11 kg, as flown, compared to 46 kg CBE for MLE
- Accommodation of 2.75 m drill assembly (capable of drilling to 2 m depth)
- Landing within ~10 km ellipse at mid-latitude in spring to accommodate solar powered mission, based on InSight heritage, with good timeline margins
- High heritage in the overall concept from Phoenix/InSight (and others) but with expected changes in the aeroshell, parachute, sizing of the propulsion system, strengthening the primary structure

3.4.2 SPACECRAFT AND EDL OPTIONS

Several options were considered for the mission and flight system (FS) (Figure 3-6). High-level trades were made that arrived at the elements highlighted in yellow and constitutes the mission architecture summary.

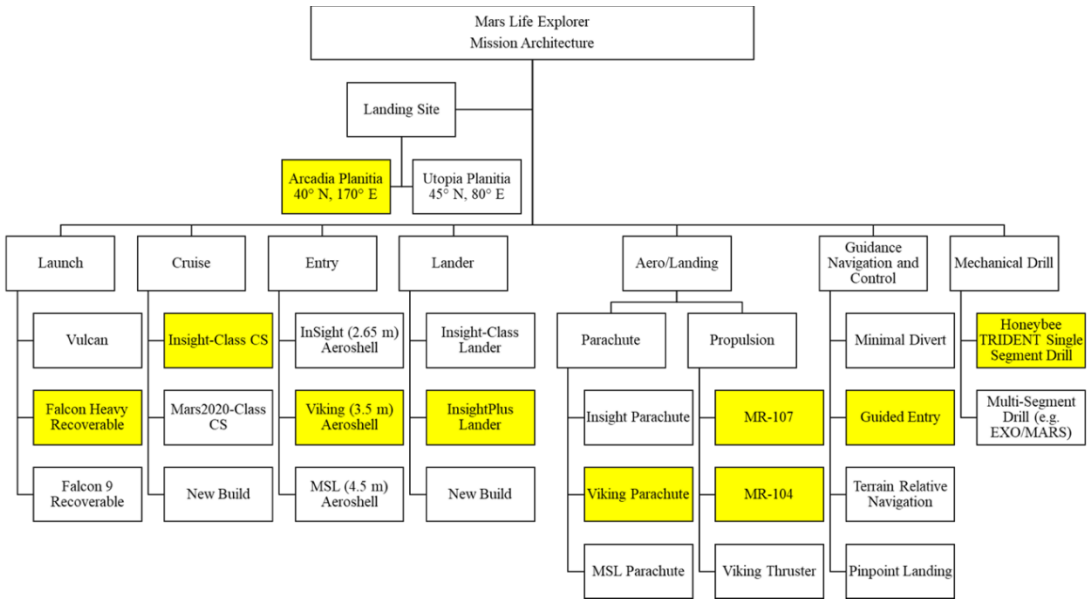

Figure 3-6. Flight System options considered in trade studies.

3.4.3 SPACECRAFT REFERENCE CONCEPT

Based on A-Team, Team X, and LM studies, an enhanced InSight-based spacecraft has been defined including an InSight-type cruise stage, an entry system with a 3.65 m aeroshell, and a static InSight-type propulsive lander. Figure 3-7 shows the section cut through the FS and accommodation of the drill and biobarrier. Figures 3-8 and 3-9 show the landed configuration including drill and representative instruments. The detailed block diagram, highlighted for heritage is shown in Figure 3-10. Table 3-8 shows the mass (with comparison to InSight as launched) summary with margins for maximum expected value (MEV) and MPV, with MPV considered the allocation. The total margin is calculated by formula: (MPV/CBE)−1, and is consistent with the high heritage of many elements and shown in Appendix G.

Table 3-8 provides the key characteristics of the FS. Table 3-9 is the mass summary for launch, entry, and landing. As mentioned in Section 3.3.3, the most significant mass difference is in the entry system due to the selection of the 3.65 m aeroshell and Viking size parachute to provide volume for the drill and good EDL performance characteristics.

The MLE flight system is based on the successful InSight/Phoenix platform. The design is a highly centralized flight system that discards hardware no longer needed for the next mission phase. Cruise stage-only hardware, such as star trackers, cruise solar arrays, and cruise telecom, is discarded prior to entry. The heatshield is discarded after the hypersonic phase is over and the parachute has deployed. The backshell is released once radar lock on the ground surface establishes that the correct height for lander separation has been reached.

The flight element that lands carries all the functions needed for powered descent as well as to support the payloads for the surface science mission. This includes landed power and telecom elements, the spacecraft computer, and avionics, as well as thermal provisions to keep those systems within thermal constraints during surface operations. All propulsion hardware is on the lander including for guided entry. The cruise thrusters are scarfed through the backshell

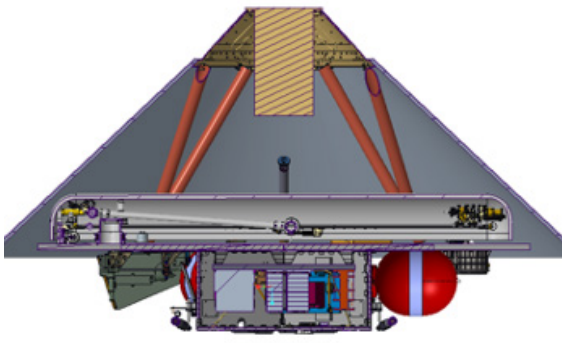

Figure 3-7. Cutaway side-view of aeroshell with lander with the drill and bio-barrier showing clearance.

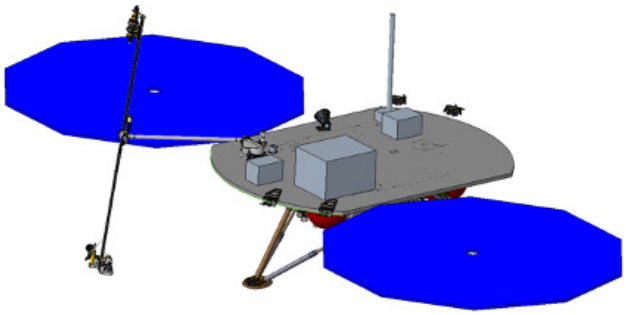

Figure 3-8. Lander configuration with drill deployed (biobarrier not shown).

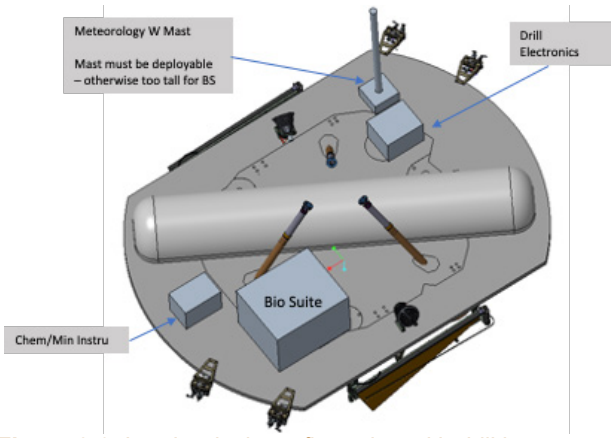

Figure 3-9. Lander deck configuration with drill in biobarrier and instruments positioned.

eliminating the need for a separate cruise propulsion system. The Miniature Inertial Measurement Unit (MIMU) is used to propagate attitude and position knowledge all the way to the ground and is thus also on the lander.

The propulsion system is derived from Phoenix and InSight. There are 12 MR-107 300N thrusters plus an additional 3 MR-104 445N thrusters for terminal descent, which together provide 150% more thrust than Phoenix or InSight. The 116 kg of propellant is stored in three fuel tanks (with heritage from XSS-11) mounted similarly to Phoenix and InSight. The plumbing is also increased to allow for the higher flow rate.

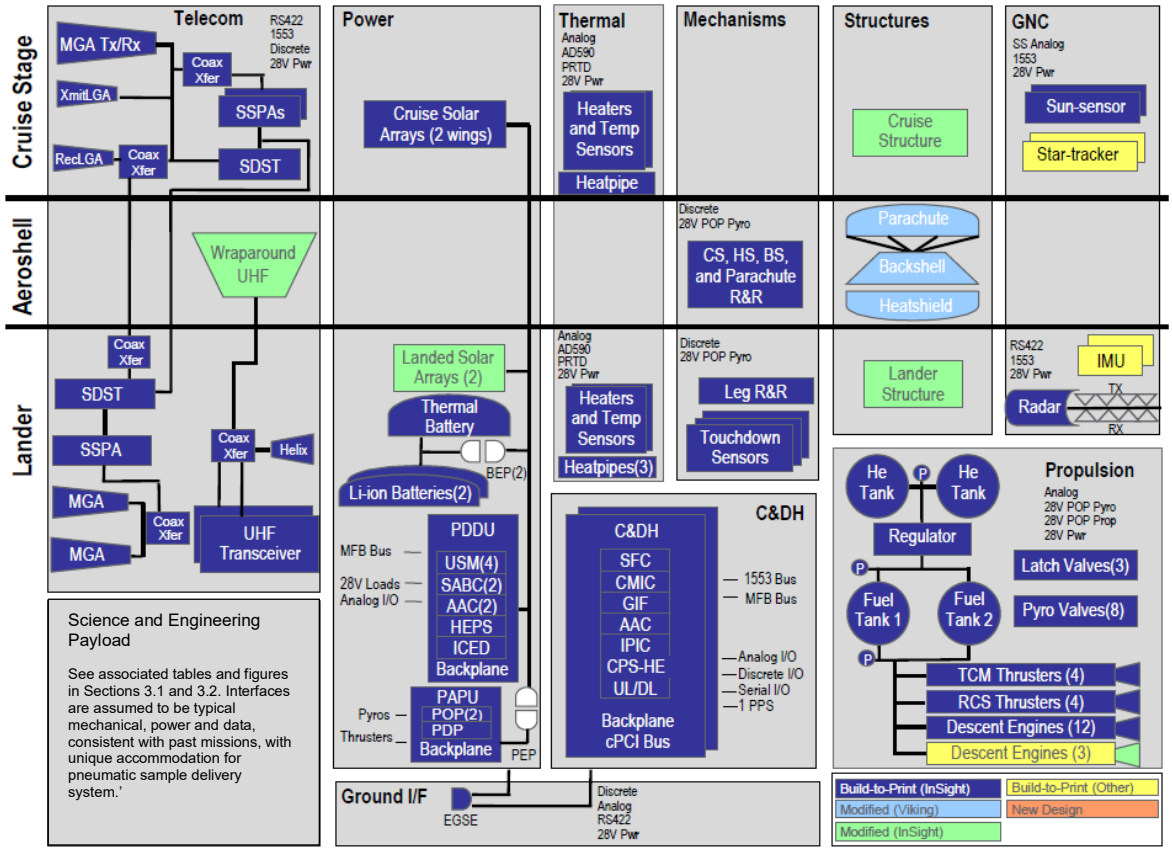

Figure 3-10. Flight system functional block diagram including heritage.

Table 3-8. Flight system element characteristics.

Flight System Element Parameters (as appropriate)	Value/Summary, units
General	
Design Life, months (Cruise, ~10 months); Sample surface ops w/margin: ~4 month; 24 for meteorology instrument only)	34
Structure	
Structures material (aluminum, exotic, composite, etc.)	Aluminum
Number of articulated structures (solar arrays)	2
Number of deployed lander structures (3 legs, 2 solar arrays)	5
Aeroshell diameter, m	3.65
Thermal Control	
Type of thermal control used	Passive; Active during hibernation mode
Propulsion	
Estimated delta-V budget, m/s	250
Propulsion type(s) and associated propellant(s)/oxidizer(s)	Hydrazine/He Pressurant
Number of thrusters and tanks	4 (TCM); 15 (Entry); 4 (ACS)
Specific impulse of each propulsion mode, seconds	218 (TCM); 232 (Entry); 170 (ACS)
Attitude Control	
Control methods	3-axis (Cruise); aerobraking, guided entry, parachute, landing thrusters (EDL)
Control reference (solar, inertial, Earth-nadir, Earth-limb, etc.)	Inertial
Attitude control capability, degrees	1.0
Attitude knowledge limit, degrees	0.1
Agility requirements (maneuvers, scanning, etc.)	Aero-maneuver during entry
Articulation/#–axes (solar arrays [SAs], antennas, gimbals, etc.)	3-axis boom for drill deploy, 2 axis for SAs
Sensors	MIMU, star tracker
Command & Data Handling	
Flight element housekeeping data rate, kbps	33.3
Data storage capacity, Mbits	128,000
Power	
Type of array structure (rigid, flexible, body mounted, deployed, articulated)	Flexible, deployed Ultraflex
Array size, meters x meters	2 x 5.8 m^2
Solar cell type (Si, GaAs, Multi-junction GaAs, concentrators)	Multi-junction GaAs
Expected power generation at Beginning of Life (BOL) and End of Life (EOL), watts	2043 (BOL); 1961 (EOL)
Battery type (NiCd, NiH, Li-ion)	Li-Ion
Battery storage capacity, amp-hours	80

ACS = Attitude Control System; TCM = trajectory correction maneuver

Table 3-9. Flight system mass summary for launch, entry, and lander (with InSight comparison for reference).

Launch Total	CBE	Cont %	MEV	MPV	Total Margin %	Selected InSight (as built)
Launch Flight System w/o Payload	852	8%	919	1039	22%	572
Payload	100	18%	118	150	50%	52
Launch Dry	**952**	**9%**	**1037**	**1189**	**25%**	624
Lander Fuel	**116**	**0%**	**116**	**116**	**0%**	66
Launch Wet Total	**1068**	**8%**	**1153**	**1305**	**22%**	690
Entry Flight System Subtotal	772	8%	834	937	21%	
Payload	100	18%	118	150	53%	
Entry Dry Total	**872**	**9%**	**952**	**1087**	**25%**	544
Flight System Subtotal	352	6%	373	415	18%	
Payload	100	18%	118	150	53%	
Dry Lander Total	**452**	**9%**	**491**	**565**	**25%**	354

The spacecraft core structure is the same configuration as Phoenix and InSight, but several enhancements allow the higher payload mass to be carried. The side panels are thickened to carry the heavier fuel tanks. The deck is enlarged to accommodate the larger payloads and provide access to the backshell for the cruise rocket engine modules (REMs), as well as to accommodate the larger

solar arrays. The aeroshell is of the same style as Phoenix and InSight, but the size is increased to the Viking diameter of 3.65 m to accommodate the drill and other payloads on the deck.

The thermal control system is identical to InSight. Except for electric heaters, the thermal control system is passive. Software thermostat zones are used in cruise and mechanical thermostats are used during the surface mission, since the computer is often in sleep mode. Heat pipes spread heat on the cruise stage and dump heat from the lander thermal enclosure during cruise. Martian gravity disables the thermal enclosure heat pipes during the landed phase to keep the lander warm.

The power system is a direct energy transfer 28V+8V/−6V system, also similar to InSight. MLE arrays are approximately twice the area of the InSight arrays, but well within the build experience of the vendor. Given the latitude of the landing sites, additional trades on actively or permanently tilted arrays may allow further size/cost reductions. The two Li-Ion batteries are nameplate 25 amp hours (same as InSight) but have been demonstrated to nearly 40 amp hours each. The 5 m^2 cruise arrays, like InSight, are fixed, and are off-pointed during cruise as needed for telecom. Like InSight, energy margin is greatest during the surface mission. Margin drops off due mainly to dust buildup until the 30% margin limit is crossed for the baseline on sol ~230 for the Ls=0 landing date.

The telecom system is nearly identical to InSight. A dual-string X-band system is used for cruise. One of those strings is landed for backup and direct-to-earth emergency links during the surface mission. The lander also carries redundant UHF transceivers for primary data return through relay orbiters. Nominally, the UHF system is capable of >50 Mbits per pass, per orbiter. Flight experience on InSight and Phoenix demonstrated >200 Mb/sol depending on number of orbiters and number of scheduled passes and energy margin. The UHF system also provides an EDL comm link to any overhead orbiters during EDL.

The guidance, navigation, and control (GN&C) subsystem is identical to InSight and Phoenix, with the addition of guided entry to reduce the landing error ellipse. Star trackers provide inertial reference during cruise and inertial measurement units (IMUs) provide attitude propagation during cruise and EDL as well as gyro-compassing after landing. To save costs and enhance redundancy, a redundant landing radar is baselined on MLE. This allows a more relaxed and lower cost parts program while simultaneously providing for a backup to the primary radar.

The spacecraft avionics are also heritage from InSight. The dual-string avionics provide redundancy. The IPIC card memory (128 Gbits flash) is at least twice that of InSight (more may be possible depending on memory standards when MLE goes through development). The command and data handling (C&DH) system has the same nighttime mode as InSight, allowing it to conserve power during part of the day. Nominally, the baseline assumes the spacecraft is awake and operating 7 hours per sol, plus two 20-minute UHF passes per sol, plus a 5-minute wake-up every 2 hours to check on the battery state of charge. Longer awake times, including night or early dawn operations, can be accommodated through different energy management strategies, including battery margin. Phoenix demonstrated continuous around-the-clock operations on at least 1 sol. It has been determined that the spacecraft can provide the needed energy to maintain the health of the spacecraft assuming an InSight mission 1-year environment but with lower dust accumulation through either a more easily wind cleaned array design and/or addition of a rotation axis actuator to tilt the array.

3.4.4 ASSEMBLY, INTEGRATION, AND TEST

The spacecraft assembly, test, and launch operations (ATLO) plan is designed to safely integrate the spacecraft subsystems and payloads, and then execute a thorough system verification to ensure mission success. The generous 21-month ATLO schedule (nearly identical activities were conducted in 16 months on Phoenix and InSight) includes 3 months of funded program margin to minimize schedule risks; margin not consumed by programmatics will be utilized in rerunning mission sequence tests and performing additional off-nominal and stress tests. In addition, the program schedule includes 2 months or more of margin on all deliveries to ATLO. ATLO uses flight ground data system (GDS) and mission operations hardware, tools, processes, and products.

At ATLO start, initial assembly and integration begins with the primary structure, propulsion subsystem, and harness. ATLO testing also begins with a flight software build that has been verified in the STL. Each subsystem with electrical functionality (e.g., C&DH, electric power system [EPS], attitude and articulation control system [AACS], telecom, propulsion, thermal) is integrated. These initial integration and functional tests verify a set of spacecraft requirements and validate component-level fault-protection responses. Once all subsystems are safely integrated and fully functional at the system level, the payload elements are integrated with the spacecraft bus.

Each flight instrument will be integrated on the lander body using dedicated assembly and test procedures. Additional attention to cleanliness and maintaining cleanliness will be expected and will be defined as part of the Planetary Protection Implementation Plan (see Section 3.5). Once mechanical integration is complete, an initial power turn-on and function test will be conducted, with the instrument operated strictly through onboard avionics and flight software. There will also be an opportunity for payload-to-payload calibration testing whenever the vehicle is in landed configuration.

Once all payloads are integrated, the pre-environments deployments are tested. The flight system is then run through all environmental testing, first in launch cruise configuration and then in the landed configuration. Flight like-deployments throughout the environmental campaign ensure deployments still function after the relevant environments have been experienced. After environments, any necessary refurbishments are conducted and the spacecraft is readied for shipment to the launch site. At the launch site, the spacecraft goes through a final series of system-level testing and deployments. Then ordnance and fuel is loaded and the spacecraft is integrated with the launch vehicle.

3.4.5 BASELINE FLIGHT SYSTEM

The baseline flight system for costing is based on the following baseline payload and mission parameters:

- Total payload, used for FS sizing, assumed to be: 150 kg (MPV). This number is based on the following, with the proviso that the amount of margin needed would be based on actual systems proposed and the heritage, i.e., if the Honeybee system, as discussed, were proposed it would likely not need 50% reserves, based on heritage.
  - Science payload: CBE 54 kg + 50% mass margin = 81 kg
  - Engineering payload based on Honeybee design: CBE 46 kg + 50% mass margin =69 kg
- Mission design LRD 2035, with 2037 and 2039 as backup and 2033 as an option for further study
- Spacecraft and EDL: InSight-derived with most significant changes in the aeroshell, parachute, propulsion, and structure subsystems to accommodate the larger and heavier payload
- Nominal mission operations: assume 30 sols post landing to prepare for drilling and 90 sol subsurface science phase, with margin, and a full Mars year operations of the meteorology station

3.5 PLANETARY PROTECTION STRATEGY

MLE would develop and implement a Planetary Protection Implementation Plan based on mission science objectives, the latest NPR (currently NPR 8715), and negotiations with the NASA Planetary Protection Officer. The assumed categorization, derived from the Committee on Space Research (COSPAR) Planetary Protection Policy (2017), is IVb. In general, the surface bioburden and the procedures employed for cleaning and assay will be similar to past missions (including Phoenix, InSighter, Curiosity and Perseverance) to the surface of Mars. However, it is expected that new practices for both cleaning, measuring, and monitoring cleanliness will be developed and proposed for NASA acceptance to improve the accuracy and confidence in meeting an assumed categorization of IVb. The MLE strategy for implementing IVb would be consistent with the subsystem-level COSPAR bioburden policy and applied to those hardware elements that would contact Mars material for delivery to the instruments. More specifically, it is expected that the current spore-based bioburden approach will continue but will be more limited in scope and cost, and that new

approaches (e.g., nanopore genomics and proteomics), while more sophisticated in terms of sensitivity to other biologic entities (e.g., viruses and prions) are expected to be able to be conducted within the current anticipated Planetary Protection (PP) budget. It is understood that these new analytical methods are advancing rapidly for commercial and government applications and are expected to be available to meet NASA needs for MLE (Danko et al. 2021).

For MLE, one potential strategy is to treat the drill and sample delivery system in a similar way to the Phoenix arm, which was IVb and was cleaned and contained in a biobarrier. The use of new cleaning and measurement techniques to assure meeting the IVb levels are expected to work with the assumed drill and biobarrier but verification of any new processes will need to be worked either pre-project or early in the project. Consideration will be given to biobarrier supplementation or replacement by denaturing techniques applied in transit or on the surface of Mars such as ultraviolet (UV), heat, and chemical oxidation. Appropriately high levels of cleanliness would be needed for the biosignature instrument(s) to meet the science objectives and are expected to be facilitated by the new cleaning and measurement processes.

For reference, M2020 was IVb for specific hardware. For hardware associated with the sample return elements and tubes, an even higher level of cleanliness was required for backward planetary protection, which may be pertinent for study by MLE. Innovative measurement techniques under development are expected to make verification of the appropriate level of biological cleanliness faster and easier to implement, and are expected to be applied to Mars Sample Return (MSR), which, while not carrying life detection instruments, is tentatively planning on meeting a better than IVa level of cleanliness specifically for the inside of orbiting sample container.

3.6 RISK LIST

Table 3-10 provides a risk list of implementation and mission risks, with risk ratings and mitigations. The mission risk likelihood and consequences shown are assumed to be representative of the rating of such risks at the time of a specific mission and instrument proposal.

Table 3-10. Risk list (per NASA standard 5×5 risk rating)

Risk	Status	L×C	Mitigation
Science payload costs exceed range	Implementation, Mitigated	G (2, 2)	Basis of likelihood of 2 is expectation of high heritage from third-generation MS and TLS. Threshold mission reduces risk in chemistry/minerology with high TRL instrument. Recommend budget reserves at 60%. (Estimated cost risk ~$80M, covered by reserves)
Engineering payload costs exceed range	Implementation, Mitigated	G (1×3)	Basis of likelihood of 1 is expectation of high heritage from two flight missions to the moon plus knowledge gained from ExoMARS. Have set large implementation budget reserves of 50%. (Estimated cost risk ~$20M, covered by reserves)
Bus costs exceed range	Implementation, Mitigated	G (1×3)	Basis of likelihood of 1 is due to high heritage from InSight for lander and EDL. Have set large implementation budget reserves of 50%. (Estimated cost risk ~$50M, covered by reserves)
Engineering payload requires significant redesign	Mitigate	Y (2×3)	Utilize experience from upcoming 2022 and 2023 lunar missions and Perseverance to validate drill and delivery systems. “Test, Test, Test” is already key to drill and delivery system development (Estimated cost risk ~$10M, covered by reserves)
Entry system mass growth	Mitigate	Y (2×3)	EDL margins are good based on the intentionally robust sizing of the aeroshell and parachute. if mass grows beyond margins, options exist to refine EDL analysis and possibly increase aeroshell or parachute size to accommodate. (Estimated cost risk $15M, covered by reserves)
EDL system requires modification due to issues with landing site selection	Mitigate	Y (2×3)	Baselined guided entry to reduce landing ellipse to provide high probability of landing safely in area with ice within 1 m of surface. Use of Terrain Relative Navigation (TRN) and precision landing (i.e., camera, additional propellant) could be additional mitigation if precise landing sites are identified from future observations and/or analysis. Study as part site selection process. (Potential cost impact $20M)
Not getting to ice due to no ice at site or problem with drill, sample delivery	Mission	Y (1×5)	Baselining guided entry helps targeting various safe landing sites with high probability of ice within <1 m. Recommend in pre-Phase A establishing the criteria for site selection, with option for higher latitude missions or precision landing. Emphasize drill testing in representative environments.
Ambiguous science result	Mission	Y (1×5)	Specify life-science instrument capabilities and performance to provide variety of complementary measurements to assure verifiable results

3.7 CONCEPT MATURITY LEVEL

Per Table 3-11, the overall MLE concept meets Concept Maturity Level (CML) 4 with spacecraft and engineering payload at CML 5.

Table 3-11. Concept Maturity Level (CML) definitions.

	CML 4 Criteria	MLE Study Status
Science	Preliminary instrument/mission-level reqmts quantified (e.g., range and resolution, accuracy and precision of: instrument intensity, wavelength, phase/polarization; mission observing positions, frequencies, durations)	STM includes key measurement accuracies. Not specifying specific instruments, basing representative payload on existing or underdevelopment systems
	Preliminary baseline vs. threshold science	Defined
Engineering	Preliminary design at the subsystem level, including the "what" and "how" (e.g., optics, detectors for instruments; ACS, C&DH, FSW for spacecraft; profiles for science, communications, trajectory, power)	High heritage in engineering payload and S/C, meets CML 5 criteria
Implementation	Potential subsystem-level suppliers and contributors (engineering and science) project Phase (A–F) durations by month	Assuming industry participation in engineering payload and S/C
Cost	Preliminary subsystem-level cost estimates to WBS Level 4 (e.g., 05.04.01, 05.04.02, 05.04.03...)	Have model and analogy costs estimates for comparison and industry provided estimates where appropriate

3.8 TECHNOLOGY MATURITY AND DEVELOPMENT PLAN

This study is not recommending specific instruments or instrument suites, especially for biosignature. However, a number of options were identified that are currently at TRL 5 that would benefit from technology funding for completing an engineering model level of maturity for the appropriate environment tests to achieve TRL 6, including such instruments as Mini-TLS and ChemMinX. There may also be options for new capabilities for more sophisticated pre-front-end systems for performing wet chemistry processes, such as being worked for ExCALiBR (Extractor for Chemical Analysis of Lipid Biomarkers in Regolith) and SCHAN (Supercritical CO_2 and Subcritical H_2O Analysis). Some technology work may be appropriate for meeting cleanliness and verification of cleanliness (related to PP discussion in Section 3.5).

For chemistry and mineralogy, the needed technologies are already in work by the representative instruments.

For meteorology, the needed technologies are: TLS in specific water wavelengths, which is under development.

For the engineering payload, possible technology issues may exist for meeting cleanliness and verification of cleanliness (related to PP discussion in Section 3.5).

For the spacecraft, there are no new technologies.

4 DEVELOPMENT SCHEDULE AND SCHEDULE CONSTRAINTS

Based on an assumed New Frontiers-class schedule, the 2035 Mars opportunity is achievable with a robust schedule including funded reserves.

4.1 HIGH-LEVEL MISSION SCHEDULE

Based on possible New Frontiers (NF) opportunities, the study evaluated 2035, 2037, and 2039 launch readiness options for mission design purposes. For implementation purposes, the first mission launch readiness date (LRD) of May 2035 is assumed. An earlier LRD in 2033 is programmatically possible but more work on the mission design is necessary.

4.2 DEVELOPMENT SCHEDULE AND CONSTRAINTS

The development schedule for MLE is based on a Principal Investigator (PI) led, JPL managed, NF-class implementation with an industry partner for spacecraft development; assembly, integration, and test (AI&T) and supporting operations. As discussed in Section 3, there are three different science instruments/suites to be developed, tested, delivered, and integrated. In addition, there is an engineering payload, provided by industry to perform drilling and sample delivery, which includes engineering downhole sensors that provide science data, to be developed, tested, and integrated. The assumed design and implementation of the spacecraft draws heavily from InSight experience (per Section 3.4). The AI&T activities are assumed to be based on a typical flow of integration, functional testing, and environmental testing, followed by launch site operations and launch. There will be an overlay of Planetary Protection (PP) operations, per a typical Mars Planetary Protection Implementation Plan, including current and future cleaning and assay techniques, with special focus on those elements that contact the samples and the science instruments.

For the purposes of developing a robust schedule, the study team assumed that MLE would be part of a NF6-like program. Based on NF5 and a typical 5-year NF cycle selection for flight, NF6 was assumed to be June 2029. With a May 2035 launch and Phase D running from launch to L+30 days, and with inputs from industry and comparisons with other missions of this class and complexity, the following schedule is robust, including JPL-required funded reserves. Based on inputs from industry, a shorter schedule could also be implemented but for the purposes of this study, additional schedule time in Phase C/D was assumed. Table 4-1 and Figure 4-1 present the MLE schedule phase durations and top-level schedule.

- Phase A: July 2028–June 2029 (12 months)
- Extended-A/Bridge: July 2029–April 2030 (10 months)
- Phase B: May 2030–August 2031 (16 months)
- Phase C: September 2031–September 2033 (25 months)
- Phase D: October 2033–June 2035 (21 months; includes launch + 30 days)
- Phase E/F: July 2035–April 2038 (34 months; 10 months cruise (1 month included at end of Phase D) + 24 months of meteorology (4 months of drilling and analysis done in parallel) + 1-month closeout)

Table 4-1. Key phase duration.

Project Phase	Duration (Months)
Phase A – Conceptual Design	12
Extended A – Bridge	10
Phase B – Preliminary Design	16
Phase C – Detailed Design	25
Phase D – Integration & Test (includes Launch + 30 days)	21
Phase E – Cruise Mission Operations	9
Phase E – Surface Mission Operations	24
Phase F – Closeout	1

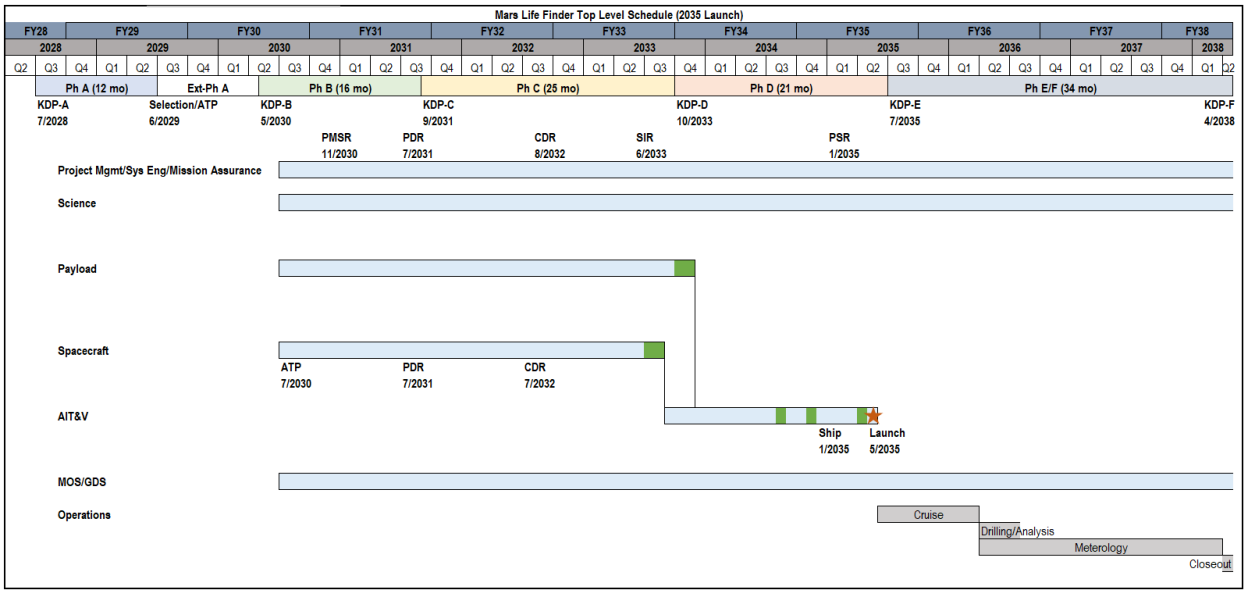

Figure 4-1. MLE top-level schedule.

In order to assess the credibility and feasibility of the MLE schedule, an analysis was conducted to compare historical competed mission durations as well as Mars mission durations between milestone reviews. The durations between milestone reviews have been observed to be a more stable measure of schedule adequacy compared to overall phase length. Table 4-2 presents the results of this schedule analysis. MLE pushed the System Integration Review (SIR) and start of AI&T earlier for a longer SIR−PSR (Pre-Ship Review) period than most other missions based on the experience of Mars 2020.

Table 4-2. MLE schedule validation.

Missions	PMSR–PDR	PDR –CDR	CDR–SIR	SIR–PSR	PSR–Launch	Total PMSR–Launch
MLE	8	13	11	19	4	55
Average	10	10	18	14	4	56
Phoenix	11	8	4	13	4	40
MRO	6	10	10	13	4	43
Juno*	10	9	10	13	5	47
Deep Impact	9	11	19	13	4	56
InSight**	6	9	37	8	3	63
Mars 2020	17	11	12	23	6	69

**Juno (Normalized): 2 months removed from PMSR (Project Mission System Review) to PDR (Preliminary Design Review) and 2 months from PDR to CDR (Critical Design Review) due to funding delays*

***InSight duration reported at launch (includes launch delay)*

5 MISSION LIFE-CYCLE COST

The MLE baseline mission cost has been estimated in a number of ways and provides a range consistent with a $1.1B FY25 New Frontiers-class cost including 50% reserve. This plan also provides a basis for flexibility in the reserves strategy that would allow for science enhancements for future mission proposers.

5.1 COSTING METHODOLOGY AND BASIS OF ESTIMATE

The MLE study team developed its cost estimate using JPL's cost estimation process for early formulation. The technical design and project schedule were used as the main inputs into the development of the cost estimate. Rather than providing a single estimate, the MLE study team developed a "study point estimate" with additional estimates that provide a range based on valid estimation techniques to provide confidence in the baseline and threshold estimates. The cost information contained in this document is of a budgetary and planning nature and is intended for informational purposes only. It does not constitute a commitment on the part of JPL and/or Caltech.

The MLE cost is organized, defined, and estimated according to the NASA Standard Work Breakdown Structure (WBS), which is compliant with NPR 7120.5E. Per study ground rules, costs presented in this section are in fiscal year 2025 dollars unless otherwise noted.

The baseline mission cost point estimate was developed using the Team X Institutional Cost Models (ICMs) with informal comparison to industry model based estimates. Additionally, the Phase E/F operations cost estimate was developed using burn rates derived from the planned InSight costs at launch (reported in CADRe; see Appendix F for detail on the Phase E–F cost derivation).

Three main methods were used to validate the baseline mission cost estimate range: (1) analogy mission and wrap factor-based costs, (2) hardware-based cost model SEER-H, and (3) NASA's Project Cost Estimating Capability (PCEC). Table 5-1 includes the technique used to estimate each WBS in each method. See Appendix F for additional detail on historical mission costs used, wrap factor derivation, and cost model inputs and analyses.

Team X is a JPL concurrent engineering design process created in 1995. Team members represent all JPL technical and science disciplines. The Team X ICM suite has been approved by JPL implementing organizations and is consistent with JPL institutional ground rules. The ICMs have been developed based on historical actuals and individual model runs are tailored to most closely represent the scope and complexity of the technical implementation. Additionally, the concurrent design environment of Team X enabled the team to perform design-to-cost trades. Based on the study assumption of a major industry partner, industry model-based cost estimates for the spacecraft, system integration and test, and mission operations and ground data system developed by Team X were discussed and compared, and in some cases, adjustments were made to the Team X numbers. Planetary Protection (PP) costs have been included and were compared to actuals reported in Mars 2020 for reasonableness. Additionally, an analogy scaled cost pass-through for the drilling and sample transfer and science payload estimates were used. Note that these estimates are strictly used for informational purposes only and are not to be considered as a commitment by any institution nor should it be considered as a selection of a potential supplier.

The analogy methodology used historical mission costs to estimate the payload, spacecraft and operations with analogies sourced from Phoenix, MSL, and InSight CADRes. Wrap factors were applied to WBS 01 Project Management, WBS 02 Project Systems Engineering, WBS 03 Mission Assurance, WBS 04 Science, WBS 05.01/05.02 Payload Management and Payload Systems Engineering, WBS 06.01/06.02 Spacecraft Management and Spacecraft Systems Engineering, and WBS 07/09 Mission Operations System and Ground Data System. The wrap factors were derived from the average of InSight, Mars Reconnaissance Orbiter (MRO), Phoenix, MSL, Juno, Dawn, and Gravity Recovery and Interior Laboratory (GRAIL).

Table 5-1. MLE cost estimating methodology.

WBS	Element	Study Point Estimate	Analogy Based	SEER	PCEC
	Phase A	pass through	pass through	pass through	pass through
	Phase B–D				
01	Project Management	Team X ICM	wrap factor	SEER	PCEC
02 + 12	Systems Engineering + MDNav	Team X ICM	wrap factor	SEER	PCEC
03	Mission Assurance	Team X ICM	wrap factor	SEER	PCEC
04	Science	Team X ICM	wrap factor	wrap factor	PCEC
05	Payload				
05.01+05.02	PL Mgmt/SE	Team X ICM	wrap factor	SEER	PCEC
	Sampling System	Industry Est.	Phoenix RA/BB(2)	SEER	SEER
	Payload for Sci Obj A-D	Scaled Pass Thru	MSL SAM(3)	Cost to Mass Scaled	NICM
	Instrument Camera	NICM	InSight IDC(4)	SEER	NICM
06+10	Spacecraft & AITV				
06.01+06.02	S/C Mgmt/SE	Team X ICM	wrap factor	SEER	PCEC
06.16+10	S/C +I&T Contract	Team X with Industry Model inputs	InSight S/C +AITV(5)	SEER	PCEC
	Lander				
	EDL				
	Cruise				
	AITV				
07/09	MOS/GDS	Team X ICM	wrap factor	wrap factor	PCEC
	A–D less reserves				
	A–D Reserves	50% Reserves	50% Reserves	50% Reserves	50% Reserves
	A–D with reserves				
	LV	pass through	pass through	pass through	pass through
	A–D with reserves and LV				
	E/F less reserves	InSight Burn Rate Derived(1)	InSight Planned Phase E(1)	MOCET	SOCM
	E/F Reserves	25% Reserves	25% Reserves	25% Reserves	25% Reserves
	Total E–F				

(1) InSight burn rate derived operations estimate detailed in Appendix F
(2) Phoenix RA/BB estimate sourced from Phoenix end of mission (EOM) CADRe and escalated to FY25. Additionally, estimate was compared to robotic arm assemblies on OSIRIS-REx and InSight (See Appendix F)
(3) MSL SAM estimate sourced from Launch CADRe and escalated to FY25 (see Appendix F)
(4) InSight IDC estimate sourced from Launch CADRe and escalated to (see Appendix F)
(5) InSight S/C & AIT&V estimate sourced from Launch CADRe and escalated to FY25 (see Appendix F). Note that these costs include the 2-year launch delay.

The SEER-H parametric model uses hardware specifications (as noted in Appendix G, Master Equipment List) as the primary input. The parametric model is used to estimate the development (Phase B–D) cost of a given mission concept. For WBS elements not estimated by SEER, wrap factors based on historical competed missions were used. Wrap factors were used for science and mission operations/ground data system. For the purposes of this study, the science payload was estimated from a regression analysis based on flown Mars instruments cost versus mass, corroborated by knowledgeable scientists in the field. For the Phase E operations costs, the Mission Operations Cost Estimation Tool (MOCET) was used.

NASA PCEC contains a collection of Cost Estimating Relationships (CERs) derived from a database of historical NASA missions. PCEC estimates all WBS except for the payload instruments. Therefore, the SEER modeled estimate was used for the Sampling System and the NASA Instrument Cost Model (NICM) System Model was used for the science payload and the Instrument Camera (which is integrated with the drilling system). For Phase E operations costs, the Space Operations Cost Model (SOCM) was used.

Reserves were applied at 50% for Phase A–D development (excluding launch vehicle LV) and 25% for Phase E–F operations (excluding tracking costs) as guidelined by NASA for this study. A placeholder of $5M FY25 was used for Phase A based on the New Frontiers 4 AO (inflated to FY25

from FY15). The concept is baselining the Launch Service Option 4, which is identified as $275M ($240M inflated to FY25 from FY20) in the Decadal Mission Study Ground Rules.

5.2 COST ESTIMATES

The study point estimate as well as validation results for the baseline point design are presented in Table 5-2. The A–D point estimate, as well as the validation estimates, support a New Frontiers-class categorization for the Baseline MLE concept, with a range from approximately $1.1–1.2B with 50% reserves.

The science payload presents the element of highest cost uncertainty at this stage of formulation due to the range of possible instrument types and heritage. Therefore, various cost estimation techniques were used to inform the potential cost of the science instrument suite as well as to provide confidence in the study point estimate. The study point estimate was derived from a combined set of instruments which have either flown or are currently in development (Table 3-2). The modeled validation range is based by an estimate derived from a regression analysis formed from 39 flown Mars instruments cost versus mass ($146M FY25). The results of this analysis for the representative baseline science package of 54 kg (including the downhole engineering instruments) and 50% reserve, for a total of 81 kg, can be seen in Figure 5-1. An analogy estimate of MSL SAM (estimate of $150M FY25) was used to bound the upper end. Finally, the NICM System cost model, which yielded an estimate of $124M FY25, was run to represent a parametrically derived estimate. The estimated range is approximately $124-160M.

The MLE study team uses the study point estimate and an historical profile model to create the mission cost funding profile seen in Table 5-3. The funding profile assumes the 12-month Phase A duration, 10-month Bridge/Extended Phase A duration, and a 62-month Phase B–D duration with no more than 25% of the Phase A–D Principal Investigator Mission Managed Cost (PI-MMC) cost spent prior to Key Decision Point (KDP) C (consistent with typical New Frontiers constraints).

Table 5-2. MLE Baseline mission point estimate and validation cost model range.

WBS	Element	Study Point Estimate	Cost Analogies/Wraps	SEER	PCEC
	Phase A	5	5	5	5
	Phase B–D	802	726	788	772
01	Project Management	103	80	107	90
02 + 12	Systems Engineering + MDNav				
03	Mission Assurance				
04	Science	15	19	20	13
05	Payload	227	193	199	177
05.01+05.02	PL Mgmt/SE	19	14	11	11
	Sampling System	41	25	38	38
	Payload for Sci Obj A–D	162	150	146	124
	Instrument Camera	5	4	5	5
06+10	Spacecraft & AITV	397	386	408	421
06.01+06.02	S/C Mgmt/SE	39	20	28	29
06.16	S/C Contract	312	320	328	365
10	AIT&V	47	46	53	27
07/09	MOS/GDS	60	48	52	71
	A–D less reserves	807	731	793	777
	A–D Reserves	404	366	396	388
	A–D with reserves	**1,211**	**1,097**	**1,189**	**1,165**
	LV	275	275	275	275
	A–D with reserves and LV	1,486	1,372	1,464	1,440
	E/F less reserves	96	91	82	100
	E/F Reserves	24	23	21	25
	Total E–F	120	114	103	125
	Total A–F	1,606	1,486	1,567	1,565

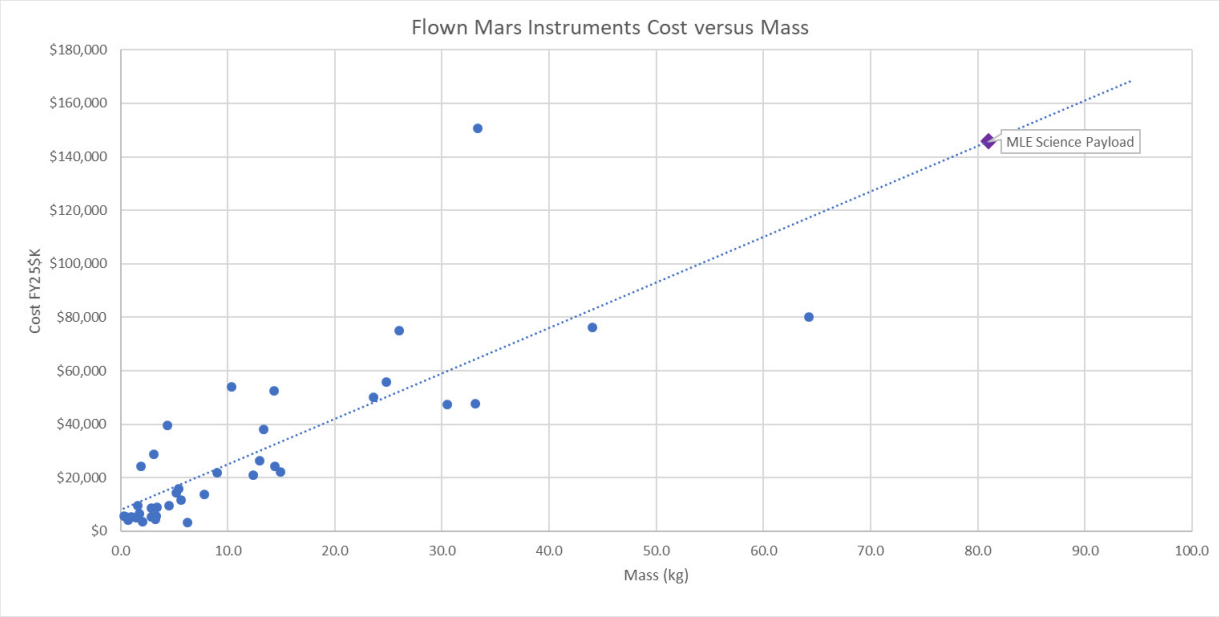

Figure 5-1. Historical Mars instruments cost versus mass.

Table 5-3. MLE cost by fiscal year RY$M.

Element	FY28	FY29	FY30	FY31	FY32	FY33	FY34	FY35	FY36	FY37	FY38	RY$M	FY25$M
Phase A	1	4	0	0	0	0	0	0	0	0	0	6	5
Phase B–D	0	0	69	171	207	211	177	136	0	0	0	971	802
Phase B–D Reserves	0	0	34	86	104	106	89	68	0	0	0	488	404
Total A–D Development Cost	**1**	**4**	**103**	**257**	**311**	**318**	**266**	**204**	**0**	**0**	**0**	**1465**	**1211**
LV	0	0	25	62	63	65	66	51	0	0	0	333	275
A–D with Reserves and LV	**1**	**4**	**128**	**319**	**374**	**383**	**333**	**255**	**0**	**0**	**0**	**1798**	**1486**
Phase E/F	0	0	0	0	0	0	0	20	72	20	14	125	96
Phase E–F Reserves	0	0	0	0	0	0	0	5	18	5	3	31	24
Total E–F Cost	**0**	**0**	**0**	**0**	**0**	**0**	**0**	**25**	**90**	**25**	**17**	**156**	**120**
Total Mission Cost A–F	**1**	**4**	**128**	**319**	**374**	**383**	**333**	**280**	**90**	**25**	**17**	**1954**	**1606**

The baseline mission cost estimate was used as a point of departure to develop the threshold cost estimate (Table 5-4). The science payload cost was adjusted to reflect the Threshold estimate presented in Table 3-2. The primarily level-of-effort WBS (WBS 01, 02, 03, 04, 05.01, 05.02, 06.01, 06.02, 07/09) were scaled down to maintain the same wrap factor ratios as the Baseline. Table 5-4 presents the baseline and threshold cost estimates with the 50% A–D reserves posture.

Table 5-4. Baseline versus Threshold study cost estimate.

WBS	Element	Threshold	Baseline
	Phase A	5	5
	Phase B-D	728	802
01	Project Management	93	103
02 + 12	Systems Engineering + MDNav		
03	Mission Assurance		
04	Science	14	15
05	Payload	169	227
05.01+05.02	PL Mgmt/SE	14	19
	Sampling System	41	41
	Payload for Sci Obj A - D	109	162
	Instrument Camera	5	5
06+10	Spacecraft & AITV	397	397
07/09	MOS/GDS	55	60
	A–D less reserves	733	807
	A–D Reserves (50%)	366	404
	A–D with reserves	**1,099**	**1,211**
	LV	275	275
	A–D with reserves and LV	1,374	1,486
	E/F less reserves	96	96
	E/F Reserves (25%)	24	24
	Total E–F	120	120
	Total A–F	1,494	1,606

An additional bottom-up reserves assessment is shown in Table 5-5, which used a reserves posture more consistent with the actual basis of estimate (including heritage), more typical reserves carried on wrap-factor-based WBS items such as engineering and management, and a higher reserve on the science payload. The results of this analysis shows an average A–D reserves level of 38%.

Table 5-5. MLE bottom-up cost reserves assessment.

WBS	Element	Study Point Estimate	% Reserves	Reserves $	Total w/ Reserves
	Phase A–D	807	38%	306	1113
	Phase A	5	0%	0	5
	Phase B–D	802	38%	306	1108
01	Project Management	103	20%	21	123
02 + 12	Systems Engineering + MDNav				
03	Mission Assurance				
04	Science	15	20%	3	18
05	Payload	227	62%	141	368
05.01+05.02	PL Mgmt/SE	19	20%	4	23
	Sampling System	41	35%	14	56
	Payload for Sci Obj A-D	162	75%	122	284
	Instrument Camera	5	25%	1	6
06+10	Spacecraft & AITV	397	34%	133	531
06.01+06.02	S/C Mgmt/SE	39	20%	8	46
06.16+10	S/C +I&T Contract	359	35%	126	484
07/09	MOS/GDS	60	20%	8	69

Table 5-6 uses both a 38% and 50% level of reserves to illustrate a further basis for a range on the MLE cost, providing greater flexibility to manage cost risk and the potential for greater science investigation opportunity.

Table 5-6. Summary of mission options, reserves and total costs (FY25$M).

	CBE	Bottom Up Reserves		Total	50% A–D Reserves		Total
Development (A–D) Baseline	$807	38%	$306	**$1,113**	50%	$404	**$1,211**
Development (A–D) Threshold	$733	38%	$278	**$1,011**	50%	$366	**$1,099**
Launch Vehicle	$275			**$275**			**$275**
Operations (E/F)	$96	25%	$24	**$120**	25%	$24	**$120**
Full Lifecycle for Baseline	$1,178		$330	**$1,508**		$428	**$1,606**

Appendices

A ACRONYMS

AAC	Analog Acquisition Card
AACS	Attitude and Articulation Control System
AC	Analog Acquisition Card
ACS	Attitude Control System
AI&T	Assembly, Integration, and Test
AITV	Assembly, Integration, Test, and Validation
APXS	Alpha-Particle X-ray Spectrometer
ASI MET	Atmospheric Structure Instrument/Meterology Package
ATLO	Assembly, Test, and Launch Operations
ATM	Atmospheres
ATS	Air Temperature Sensor
BB	Biobarrier
BOL	Beginning of Life
BS	Backshell
BTP	Build to Print
BWG	Beam Waveguide
C&DH	Command and Data Handling
C3	Characteristic Energy
CADRe	Cost Analysis Requirements Document
CBE	Current Best Estimate
CDR	Critical Design Review
CER	Cost Estimating Relationship
CheMin	Chemistry and Mineralogy
CMIC	C&DH Module Interface Card
CML	Concept Maturity Level
COSPAR	Committee on Space Research
COTS	Commercial off the Shelf
CPS-HE	C&DH Power Supply - High Efficiency
CRISM	Compact Reconnaissance Imaging Spectrometer for Mars
CS	Cruise Structure
CSR	Concept Study Report
CTX	Context Camera
DHMR	Dry Heat Microbial Reduction
DL	Downlink
DLA	Declination of Launch Asymptote
DoF	Degree of Freedom
DRaMS	Dragonfly Mass Spectrometer
DSN	Deep Space Network
DSP	Dielectric Spectroscopy Probe
EDL	Entry, Descent, and Landing
EE	Enantiomeric Excess
EFPA	Entry Flight Path Angle

EGA-MS	Evolved Gas Analyzer / Mass Spectrometer
EGSE	Electrical Ground Support Equipment
EM	Engineering Model
EMILI	Europan Molecular Indicators of Life Investigation
EOL	End of Life
EPS	Electric Power System
ESA	European Space Agency
ExCALiBR	Extractor for Chemical Analysis of Lipid Biomarkers in Regolith
FORJ	Fiber Optic Rotary Joint
FS	Flight System
FY	Fiscal Year
GCMS	Gas Chromatograph Mass Spectrometer
GDS	Ground Data System
GIF	GN&C Interface Card
GN&C	Guidance and Navigation Control
GRAIL	Gravity Recovery and Interior Laboratory
GRC	Glenn Research Center
GRS	Gamma Ray Spectrometer
HE	High Efficiency
HEO	Human Exploration and Operations
HEOMD	Human Exploration and Operations Mission Directorate
HEPS	High-Efficiency Power Supply Card
HiRISE	High Resolution Imaging Science Experiment
HP^3	Heat Flow and Physical Properties Package
HS	Heat Shield
HW	Hardware
I&T	Integration and Test
I/F	Interface
I/O	Input/Output
ICC	Instrument Context Camera
ICE	Independent Cost Estimate
ICE-SAG	Ice and Climate Evolution Science Analysis Group
ICM	Institutional Cost Model
ICU	Instrument Control Unit
IDA	Instrument Deployment Arm
IDC	(InSight) Instrument Deployment Camera
IDD	Instrument Deployment Device
IDS	Instrument Deployment System
IFG	InSight Fluxgate Magnetometer
IMP	Imager for Mars Pathfinder
IMU	Inertial Measurement Unit
InSight	Interior Exploration using Seismic Investigations, Geodesy and Heat Transport
IPIC	InSight Payload Interface Card
IR	Infrared

ISRU	In Situ Resource Utilization
JAXA	Japan Aerospace Exploration Agency
JPL	Jet Propulsion Laboratory
KDP	Key Decision Point
KSC	Kennedy Space Center
LGA	Low-Gain Antenna
LIBS	Laser Induced Breakdown Spectrometer
LIDAR	Light Detection and Ranging
LM	Lockheed Martin
LRD	Launch Readiness Date
LV	Launch Vehicle
LVDS	Low Voltage Differential Signaling
LW	Longwave
M2020	Mars 2020
Ma_MISS	Mars Multispectral Imager for Subsurface Studies
MAG	Magnetometer
MAHLI	Mars Hand Lens Imager
MARCI	Mars Color Imager
MARDI	Mars Descent Imager
MARIE	Martian Radiation Environment Experiment
MastCam	Mast Camera
MAVEN	Mars Atmosphere and Volatile EvolutioN
MCS	Mars Climate Sounder
M-E	Modified Existing Design
MECA	Microscopy, Electrochemistry, and Conductivity Analyzer
MEDA	Mars Environmental Dynamics Analyzer
MEL	Master Equipment List
MEPAG	Mars Exploration Program Analysis Group
MER	Mars Exploration Rover
MEV	Maximum Expected Value
MFB	Multiple Feedback
MFEX	Microrover Flight Experiment
MGA	Medium-Gain Antenna
MICA	Microfluidic Icy-World Chemistry Analyzer or Minerals Identified through CRISM Analysis
MIMU	Miniature Inertial Measurement Unit
MIR	Midwave Infrared
MLE	Mars Life Explorer
MLPS	Mid- and Long-wave Infrared Point Spectrometer
MM-E	Minor Modification to Existing Design
MOC	Mars Observer Camera
MOCET	Mission Operations Cost Estimation Tool
MOLA	Mars Orbiter Laser Altimeter
MOMA	Mars Organic Molecule Analyzer

MOS	Mission Operations System
MOXIE	Mars Oxygen In-Situ Resource Utilization Experiment
MPV	Maximum Possible Value
MRO	Mars Reconnaissance Orbiter
MS	Mass Spectrometer
MSL	Mars Science Laboratory
MSR	Mars Sample Return
NASA	National Aeronautics and Space Administration
NF	New Frontiers
NGIMS	Neutral Gas and Ion Mass Spectrometer
NICM	NASA Instrument Cost Model
NSI	NASA Standard Initiator
NTE	Not to Exceed
ODY	(Mars) Odyssey
ONC	Optical Navigation Camera
OTS	Off the Shelf
OWLS	Ocean Worlds Life Surveyor
PAH	Polycyclic Aromatic Hydrocarbon
PAPU	Pyro & Propulsion Unit
PCEC	Project Cost Estimating Capability
PDDU	Power Distribution Drive Unit
PDR	Preliminary Design Review
PHX	Phoenix
PI	Principal Investigator
PI-MMC	Principal Investigator Mission Managed Cost
PL	Payload
PMIRR	Pressure Modulator Infrared Radiometer
PMSR	Project Mission System Review
PPB	parts per billion
ppbw	parts per billion by weight
PPS	Pulse Per Second
PRIME1	Polar Resources Ice Mining Experiment-1
PS	Pressure Sensor
PSADS	Planetary Science and Astrobiology Decadal Survey
PSD	Planetary Science Division
PSDS	Planetary Science Decadal Survey
PSR	Pre-Ship Review
R&R	Retention and Release
RA	Robotic Arm
RAD	Radiation Assessment Detector
RAT	Rock Abrasion Tool
RCS	Reaction Control System
REA	Rocket Engine Assembly
REM	Rocket Engine Module

RF	Radio Frequency
ROM	Rough Order of Magnitude
RTD	Resistance Temperature Detector
Rx	Receive
RY	Real Year
S/C	Spacecraft
SA	Sonic Anemometer
SA	Solar Array
SABC	Solar Array & Battery Control Card
SAM	Sample Analysis at Mars
SARA	Sample Acquisition and Return Assembly
SCHAN	Supercritical CO2 and Subcritical H2O Analysis
SDST	Small Deep Space Transponder
SE	Systems Engineering
SEER	System Evaluation and Estimation of Resources
SEP	Solar Energetic Particle
SFC	Spaceflight Computer
SHARAD	Shallow Radar
SIMPLEx	Small Innovative Missions for Planetary Exploration
SIR	System Integration Review
SKG	Strategic Knowledge Gap
SOCM	Space Operations Cost Model
SSI	Surface Stereo Imager
SSPA	Solid-State Power Amplifier
STATIC	Suprathermal and Thermal Ion Composition
STL	Structures Test Laboratory
STM	Science Traceability Matrix
SW	Shortwave
SW	Software
SWEA	Solar Wind Electron Analyzer
SWIA	Solar Wind Ion Analyzer
SWIR	Short-Wave Infrared
TAGSAM	Touch-And-Go Sample Acquisition Mechanism
TCM	Trajectory Correction Maneuver
TECP	Thermal and Electrical Conductivity Probe
TEGA	Thermal and Evolved Gas Analyzer
TES	Tropospheric Emission Spectrometer
THEMIS	Thermal Emission Imaging System
TIRS	Thermal Infrared Sensor
TLS	Tunable Laser Spectrometer
TOC	Total Organic Carbon
TPS	Thermal Protection System
TRIDENT	The Regolith and Ice Drill for Exploration of New Terrains
TRL	Technology Readiness Level

TRN	Terrain Relative Navigation
Tx	Transmit
UHF	Ultra High Frequency
UL	Uplink
ULDL	Uplink Downlink
USM	Universal Switch Module
V&V	Verification and Validation
VAFB	Vandenberg Air Force Base
VHP	Hyperbolic Excess Velocity
VIPER	Volatiles Investigating Polar Exploration Rover
VNIR	Visible and near-infrared
WBS	Work Breakdown Structure
WTS	Wind and Thermal Shield
XRD	X-ray Diffraction
XRF	X-ray Fluorescence

B SCIENCE INSTRUMENT OPTIONS

This appendix provides detailed science instrument data tables used to define reference instrument capabilities and characteristics in Section 3.1. Also included in this appendix are detailed instrument information used to populate these tables and related publication references. The upper portion of each table within this Appendix provides specific key engineering information such as mass, volume, average max power during operation, maximum energy per sol, data volume, and sample access (i.e., how the instrument engages with a sample). Also included are the best estimates available for cost, which were obtained from various sources, generally without formal documentation due to propriety or other sensitivities. The lower portion of each table (i.e., below the thick black line) identifies with an 'X' if an instrument (or suite) is capable of addressing the corresponding Science Objective, all of which are abbreviated here under "Measurement Description" (with corresponding number; e.g., A1) but are laid out in full detail in the STM (Table 1-2). Each figure also shows a color coding used by the study team to highlight possible options for combining instruments to meet objectives.

Table B-1 lists the primary science measurement capabilities needed to meet Objective A in the Science Traceability Matrix (STM) and some of the capabilities required to meet Objective B. These measurement capabilities are then associated with existing instruments, such as the Sample Analysis at Mars (SAM; flying on Mars Science Laboratory [MSL]), Mars Organic Molecule Analyzer (MOMA; to fly on ExoMars), and others as part of an approved mission, such as the Dragonfly Mass Spectrometer [DRaMS], or proposed for future missions, such as the Ocean Worlds Life Surveyor [OWLS] and SCHAN instruments. In addition to the six Objective A measurements, the first two Objective B priority measurements are included, given that these constitute a key part of meeting the highest biosignature priorities.

For input to Table 3-2 the study uses an approach of defining a representative set of capabilities and characteristics for each Objective instrument set and providing a "Representative Instrument" label as descriptive. For the Objective A instrument suite baseline, the study team chose for a Representative Instrument label an assumed future generation MS system called DRaMS+Mini-TLS. However, for the mass, power, volume and data rate the chosen numbers are associated with SAM to drive the spacecraft capabilities. For cost, the study team chose the sum of our best knowledge of the CBE for DRaMS and Mini-TLS. There is no reduction in the scope of the Objective A instrument capabilities for the threshold mission.

Table B-1. Science instruments capable of the various measurements needed to meet Objective A and their engineering characteristics.

	Instrument Options	DRaMS*	MOMA MS	SAM MS w/EGA w/TLS	OWLS[2]	EMILI[3]	SCHAN[8]	ExCALiBR	TLS-MSL	TEGA	Mini-TLS
	Function	Biodetection Suite	Biodetection Suite	Biodetection Suite	Biodetection Suite	Biodetection Suite	Biodetection Suite	"Biomarker Extraction and Sample Processing"	Gas Analyzer	Gas Analyzer	Gas Analyzer
	TRL	5	7+	9	5	5	4	5	9	9	6
	CBE Mass Dry [kg]	21	11.5	33	28	16.4 [4]	20	25	4.37	14.9	2.3
	Exterior Size [cm]			55.3 × 42.1 × 31	50 × 34 × 45	35 × 30 × 20 [5]	55U	70 × 30 × 30	-		120 cm3
	Avg. Power Value [W]		82	63.8	60/42 [6]	84 [6]	45	35	68	74	24
	Data Volume (Mb/sol)		240	240		320	40	2			
	Energy (Wh/Sol)			400		293	200	850			
	Sample Access	Internal Carousel	Internal Carousel	Internal Carousel	Internal Carousel	Internal Carousel	Internal Carousel	Internal Carousel	Needs Gas Transfer System	Internal Crucible	Needs Gas Transfer System
	Cost Total [$M FY25]	**$65**	**$110**	**$138**		**$65**			**$36**	**$23**	**$20**
Priority	**#**	**Measurement Description**									
1	A1	Sample Extraction and Detection of organics	X	X	X	X	X	X	X			
1	A2	Detect and structurally characterize, amino acides, fatty acids, etc	X	X	X	X	X	X				
1	A3	Quantify the relative abundances of any amino acids to glycine	X	X	X	X	X	X				
1	A4	Quantify enantiomeric excess (ee) of at least three chiral proteinogenic amino acids	X	X	X	X	X	X				
1	A5	CO_2, CH_4, and other trace gases	X [1]		X		X			X		X
1	A6	H, C, O, N, S isotopic measurements			X					X		X
2	B1	Evolved volatile gases from pyrolysis; combustion of TOC			X		X			[9]	X	[9]
2	B2	Analysis of both inorganic and small organic cations and anions				X	X[7]					

Assume green as baseline, with purple and yellow as alternates (all with mini-TLS)

Footnotes:

1. Applicability not for Mars; CO_2 is a different; potential indirect measurement using MS (not expected to be PPB)
2. (OCEANS subsystems + extractor module) – does NOT include separate mass spec.; OWLS: does not have gas analysis currently; FULL OWLS also includes microscopy
3. EMILI does not have combustion capability.
4. Does not include the mass spectrometer
5. Assuming all in one box
6. 60 = avg power for EXTRACTOR; 42 = average power for the three subsystems that comprise OCEANS
7. Includes the OCEANS subsystem capabilities
8. No pyrolysis system on SCHAN, nor are they set up to do evolved gases; assumes mass spectrometer is included.
9. True for the evolved gases portion ONLY if connected to something like the SAM EGA

Table B-2 lists the primary science measurements capabilities needed to meet Objective B in the STM. For input to Table 3-2, for the baseline chemistry/meteorology, the capabilities of a CheMinX best met the objectives with MECA providing a conductivity measure to strengthen meeting Objective B2. For the baseline mission mass, the mass of CheMinX and the high Technology Readiness Level (TRL) of MECA, was used and set at a bounding 14 kg. The other engineering characteristics were set at CheMinX levels. Given the assumed high cost for the chemistry and mineralogy instrument suite, the decision was made, based on inputs from the science advisory group, to descope the threshold mission objectives to B3 and B4 and assume a high TRL, low cost APXS.

Table B-2. Science instruments capable of the various measurements needed to meet Objective B and their engineering characteristics.

	Instruments	CheMinX	MECA	MICA	CheMin	APXS	MLPS [5]
	Function	Mineraology (XRD, XRF)	Conductivity Analyzer	pH, Eh, conductivity	Mineraology (XRD)	Major Minor Chemistry	Mineralogy (IR)
	TRL	5+	9	5	9	9	5/6 [6]
	CBE Mass Dry [kg]	5	7.8	1.5	10.2	1.64	2
	Exterior Size [cm]	27.5 × 16.2 × 19		10 × 11.5 × 17	26.3 × 30.2 × 30	18.0×x 12.7 × 6.2	
	Avg. Power Value [W]	60 [1]	25	5 (peak = 10 W)	30.13	6.33	10
	Data Generation Rate [kbps]		10	[3]	8000	9.6	
	Data Volume (Mb/sol)	100	72		200	69	
	Energy (Wh/Sol)	450	50	5 [4]	500	13	20
	Sample Access	Internal Cartridge	Internal Carousel	Europa Lander sample carousel	Internal carousel	Hover above sample	sense illuminated sample
	Cost Total [$M FY25]	**$45**	**$15**	**$19**	**$50**	**$7**	**$11**
Science Priority	**#**	**Measurement Description**					
2	B2	Analysis of both inorganic and small organic cations and anions	partial	X	X	partial		partial
2	B3	Silicate, oxide, salt, amorphous phase characterization.	X [2]	partial	partial	partial	X	partial
2	B4	Major and minor element chemistry	X				X	

Assume green as baseline, with purple as alternative and yellow with APXS as 2nd alternative

Footnotes:

1. Assumes an 8-hour operation; currently working towards a detector design that does not require active cooling, which would reduce TRL but decrease estimated power consumption to 30 W.

2. A combination XRD/XRF is one of the few instruments that will allow you to establish quantitative mineralogy and crystal structure allowing comparisons against XRF chemistry allowing determination of amorphous composition. Moessbauer has better direct insight into amorphous composition, but only for Fe-minerals

3. MICA generates approx 0.75MB (6Mbits) per sample

4. MICA requires 0.5 hours to process a sample

5. Was deemed TRL 6 for SIMPLEx call (~$9.5M)

Table B-3 lists the primary science measurements capabilities needed to meet Objective C in the STM. Based on review of past, present, and future implementations by Honeybee and others, the study team decided to use the model of a small set of engineering sensor-based instruments that are already under development at Honeybee to provide all three desired measurements (C1, C2, C3) for the baseline and threshold missions. See Appendix D for details on the instrumentation options in the auger currently being implemented by Honeybee that could be adapted for MLE. Given the relatively low mass of the downhole elements, a 1 kg CBE is assumed. Energy needs are also very low. Initial CBE cost assumption of $3M was used.

Table B-3. Science instruments capable of the various measurements needed to meet Objective C and their engineering characteristics.

	Instrument	Phoenix Temp Sensor	Honeybee Drill Temeperature Sensor	MLPS Downhole	Honeybee Drill Imager	Phoenix Electrical Conductivity Sensor	Honeybeee Conductivity Sensor plus Heater
	Function	Downhole Temp Profile	Downhole Temperature Profile	Mineralogy (IR)	Downhole Imager	Downhole Conductivity Profile	Downhole Conductivity Profile
	TRL	9	6	5/6 [6]	?	9	6
	CBE Mass Dry [kg]	0.0002	0.001	2	0.5	0.0005	1
	Exterior Size [cm]						
	Avg. Power Value [W]	0.4	0.5	10	5	0.1	10
	Data Generation Rate [kbps]					1	
	Data Volume (Mb/sol)						
	Energy (Wh/Sol)	0.8	1	20	10	0.2	20
	Sample Access	Borehole	Borehole	Borehole	Borehole	Borehole	Borehole
	Cost Total [$M FY25]		**$1**	**$11**	**$1**		**$1**
Science Priority	**#**	**Measurement Description**					
3	C1	Temperature profile of the borehole temperature as a function of time.	X	X			
3	C2	Downhole imaging only				X	
3	C3	Conductivity profile of borehole resistivity					X	X

Assume green as baseline, purple as alternatives

Table B-4 lists the primary science measurements capabilities needed to meet Objective D. Based on the importance of meeting the D1b measurement and the low mass and cost of meeting the other measurements, the study team decided to use the model of a single instrument suite that could provide all the desired measurements of the STM for the baseline and threshold missions. Given the desire to operate for a full Martian year, low energy use will be important, so a predicted use of 3 Whr/sol was specified. A mast is assumed with properties appropriate for the instruments on it but of a similar design to other masts. The CBE cost is assumed to be the sum of the current estimates, $3M. It has been verified that the S/C can provide the needed energy to maintain the health of the S/C and downlink data from the instrument assuming a one Mars year environment like InSight has experienced but with lower dust accumulation through either a more easily wind-cleaned array design and/or addition of a rotation axis actuator to tilt the array. Tolerance of a high Tau long duration storm such a Opportunity experienced will not be built into the S/C capabilities.

Table B-4. Science instruments capable of the various measurements needed to meet Objective D and their engineering characteristics.

		Instrument	Sonic Anemometer w/ TLS	M2020 MEDA-PS[2]	M2020 MEDA-ATS	M2020 MEDA-TIRS
		Function	Wind Speed/Direction & Water Vapor Abundance	Pressure	Temperature	Up/Down Radiative Flux
		TRL	5	9	9	9
		CBE Mass Dry [kg]	1.075	0.04	0.05	0.1
		Exterior Size [cm]	SA: 600 cm^3 TLS: 10 × 10 × 5	6.2 × 5.0 × 1.7	5.75 × 2.75 × 6.75	6.25 × 5.75 × 5.75
		Avg. Power Value [W]	1	0.015	0.015	0.1
		Data Generation Rate [kbps]	0.6	0.03	0.03	0.03
		Data Volume (Mb/sol)	5	3	3	0.3
		Energy (Wh/Sol)	2	1	1	0.2
		Sample Access	Atmosphere w/ Mast	Atmosphere	Atmosphere	Atmosphere
		Cost Total [$M FY25]	**$10**	**$1**	**$1**	**$1**
Science Priority	**#**	**Measurement Description**				
4	D1a	Temperature, pressure	Partial	X	X	
4	D1b	Fluxes of water vapor (abundance) and dust between the surface atmosphere	X			
4	D1c	Surface wind stress. [1]	X			
4	D2	LW and SW radiative fluxes at surface				X

Assume green as baseline

Footnotes:

1. At different elevations or 3-D winds at high frequency; best is 3-D winds at high frequency; backup is at different elevations

2. Instrument Control Unit + Pressure Sensor = 14 × 14 × 13; This seems reasonable for the PS + ICU for MEDA; it may be reasonable for the PS + ICU for the combined sensors shown here, too

Science Instrument Abstract Excerpts and Figures used to Develop Measurement and Capabilities Tables

Sample Analysis at Mars (SAM):

Abstract Excerpt: "The Sample Analysis at Mars (SAM) investigation of the Mars Science Laboratory (MSL) addresses the chemical and isotopic composition of the atmosphere and volatiles extracted from solid samples. The SAM investigation is designed to contribute substantially to the mission goal of quantitatively assessing the habitability of Mars as an essential step in the search for past or present life on Mars. SAM is a 40 kg instrument suite located in the interior of MSL's Curiosity rover. The SAM instruments are a quadrupole mass spectrometer, a tunable laser spectrometer, and a 6-column gas chromatograph all coupled through solid and gas processing systems to provide complementary information on the same samples. The SAM suite is able to measure a suite of light isotopes and to analyze volatiles directly from the atmosphere or thermally released from solid samples. In addition to measurements of simple inorganic compounds and noble gases SAM will conduct a sensitive search for organic compounds with either thermal or chemical extraction from sieved samples delivered by the sample processing system on the Curiosity rover's robotic arm." (Mahaffy et al. 2012)

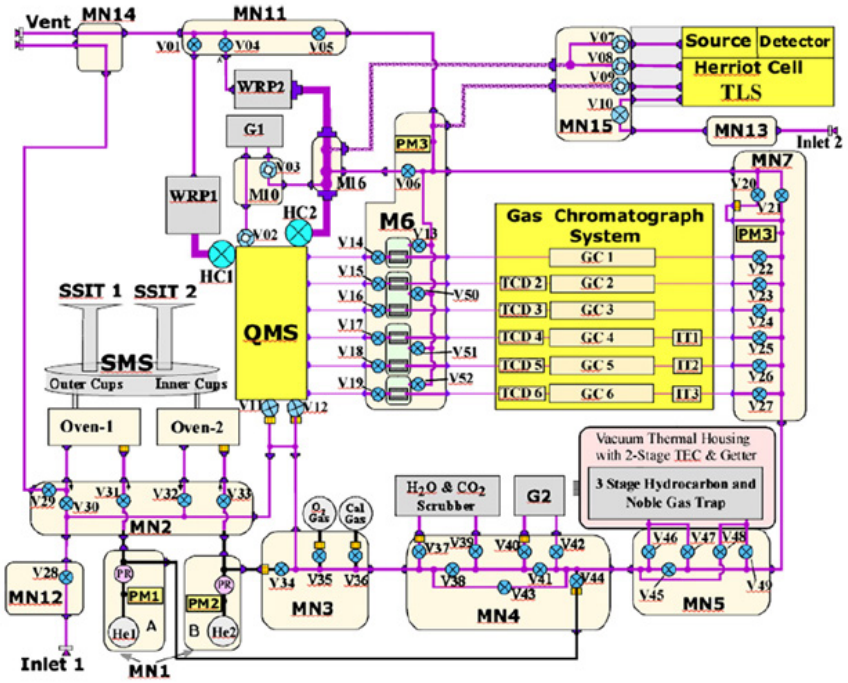

Table 5 SAM required data sets, performance, and implementation

Required data sets	Required performance	Implementation & performance
Inventory of *volatile organic compounds* in rocks and soils Signatures of *refractory carbon* and its $^{13}C/^{12}C$ ratio Distribution of *molecular weights* and *chemical structures* for organic compounds	*Organics Analysis* • Volatile organics to 1–10 ppb (by mass) • Polar and non-polar organics (from saturated hydrocarbons to carboxylic acids • Complex organics to >20 C/molecule • Refractory organics to ppm (by mass)	*Gas Chromatograph Mass Spectrometer* • Unit QMS mass resolution 2–535 Da • 6 GC columns to separate polar and non-polar compounds & derivatized compounds (Table 9) • Inert He carrier gas
Oxidation state distribution for organic compounds Inventory of specific molecular classes (*amino acids, amines, carboxylic acids*)	*Atmospheric composition* • Noble gas mixing ratios to <15 % • Major species & trace species to ppm mixing ratios • Ability to sample atmosphere at any time of day	*Mass Spectrometer* • Dynamic range $\sim 10^9$ • Sensitivity $>10^{-2}$ (cnts/sec)/(part/cc) • 0.02 transition time to any m/z value • 0.1 Da scans for peak shape determination • ~25 Da band scans to capture GC transients
Inventory and temperature profile of *volatile inorganic compounds* released from solids *Methane abundance* and its variation in the atmosphere and its $^{13}C/^{12}C$ *ratio* *Seasonal and diurnal variation* of major and minor atmospheric species Atmospheric mixing ratios of noble gases Xe, Kr, Ar, and Ne Isotopic composition of atmospheric noble gases Xe, Kr, Ar, and Ne	*Isotopic Analysis* • $\delta^{13}C$ to 5 per mil in CO_2 and 10 per mil in CH_4 • $\delta^{18}O$ to 5 per mil in H_2O and CO_2 • $\delta^{17}O$ to 10 per mil in H_2O and CO_2 • Noble gas isotopes from <10–20 per mil • C isotopic composition of refractory organics by combustion to CO_2 *Evolved Gas Analysis* • Mineral classes (carbonates, sulfates, clays, etc.) with ppm sensitivity • Features (e.g. peak T) in EGA profiles to ±20 °C	*Tunable Laser Spectrometer* • Separate methane (IC) and CO_2 (NIR) lasers • Wavelength shift in NIR laser for H_2O isotopes • Performance given in Table 10 *Gas & solid processing* • Turbomolecular pumps • Heated transfer lines ($T \geq 135$ °C) • Controlled solid sample heating ambient to 900 to 1100 °C in inert quartz cups • Solvent extraction & derivatization • Combustion with O_2 • Getters & scrubbers to remove selected gases

Mars Organic Molecule Analyzer (MOMA):

Abstract Excerpt: "The Mars Organic Molecule Analyzer (MOMA) instrument onboard the ESA/Roscosmos ExoMars rover (to launch in July, 2020) will analyze volatile and refractory organic compounds in martian surface and subsurface sediments. In this study, we describe the design, current status of development, and analytical capabilities of the instrument. Data acquired on preliminary MOMA flight-like hardware and experimental setups are also presented, illustrating their contribution to the overall science return of the mission." (Goesmann et al. 2017)

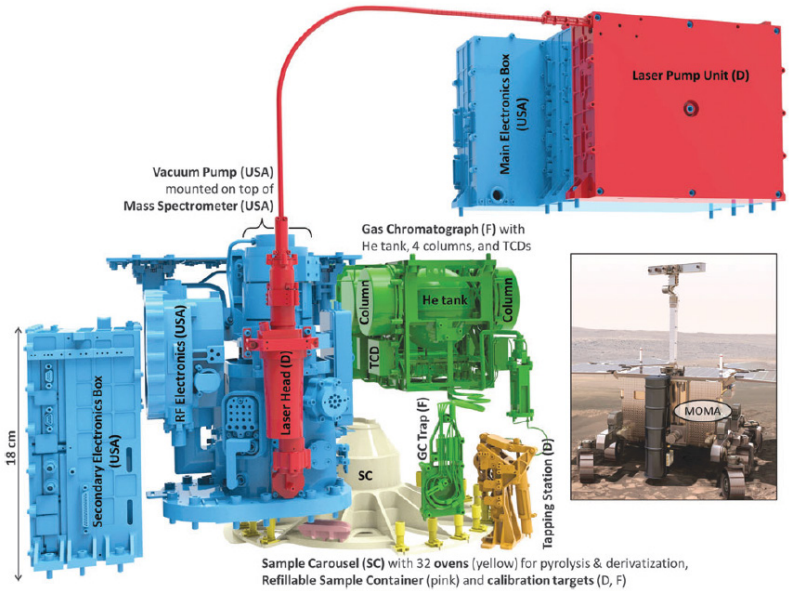

FIG. 1. The different parts of MOMA and their contributors (France (F), Germany (D), United States) are displayed in the figure above. The LPU that controls the LH is mounted as a slice on the MEB (top right). Sample carousel (SC) and refillable sample container are not part of MOMA. LH, Laser Head; LPU, Laser Pump Unit; MEB, Main Electronic Box; MOMA, Mars Organic Molecule Analyzer.

TABLE 1. MAIN CHARACTERISTICS OF THE MARS ORGANIC MOLECULE ANALYZER INSTRUMENT

Mass	*11.5 kg w/o margin*
Average power	65 W (LDMS) 82 W (GCMS)
Maximum power	133 W (LDMS) 154 W (GCMS)
Operational temperature range	(–40 + 20)°C (upper value limited by laser)

GCMS = Gas Chromatography–Mass Spectrometry; LDMS = Laser Desorption Mass Spectrometry.

TABLE 5. PERFORMANCE REQUIREMENTS OF MOMA-MS SUBSYSTEM

Specification	*Pyr/GCMS mode*	*LDMS mode*
Targeted biosignatures	Volatile organics (*e.g.*, alkanes, amines, alcohols, carboxylic acids)	Nonvolatile organics (*e.g.*, macromolecular carbon, proteins), inorganic species
Mass range	50–500 u	50–1000 u
Limit of detection	≤nmol analyte[a] (SNR[c] > 10)	≤pmol mm^{-2} analyte[b] (SNR[c] ≥3)
Resolution (FWHM[d])	≤1 u	≤2 u
Single scan dynamic range	≥100 over 50–1000 u	
Mass isolation	±5 u precision over 50–1000 u	
Accuracy	Observed mass ±0.4 u actual mass	
Instrument drift	<0.4 u over 30 min	
Operational P	4 to 8 torr of Mars atmosphere	
Operational T	–40°C to +20°C	
Nonop T	–50°C to +60°C	
Survival T	Up to +145°C	

[a]pyr/GCMS analyte: PFTBA.
[b]LDMS analytes: Rhodamine 6G and Angiotensin II.
[c]SNR of mass peak.
[d]FWHM of mass peak.
FWHM = Full-Width Half Maximum; PFTBA = perfluorotributylamine; SNR = Signal-to-Noise Ratio.

Dragonfly Mass Spectrometer (DRaMS):

Abstract Excerpt: "DraMS is a linear ion trap mass spectrometer, most closely related to the Mars Organic Molecule Analyzer (MOMA) [9], part of the ExoMars Rosalind Franklin Rover set to launch in 2022. For solid sample analysis, DraMS features two modes: Laser Desorption Mass Spectrometry (LDMS) for the broad compositional survey of surface materials including refractory organics, and Gas Chromatography Mass Spectrometry (GCMS) for the separation and identification of key prebiotic molecules and measurement of enantiomeric excesses (if present). LDMS mode allows for structural disambiguation of surface molecules using ion isolation and tandem mass spectrometry (MS/MS). GCMS mode uses pyrolysis or derivatization to volatilize, separate, and identify molecules of interest. Much of the gas processing system (valves, pyrolysis oven, etc.) and electronics are also inherited from the Sample Analysis at Mars (SAM) instrument onboard Curiosity [10]." (Trainer et al. 2021)

Table 1. DraMS Specifications

Characteristic	Predicted Performance
Mass Sensor	Linear Ion Trap
Mass Range	**15 – 1950** Da [a]
Mass Resolution	**0.4** – 3 Da (FWHM) [b]
Mass Accuracy	**± 0.4 Da**
Ion polarity	Positive and Negative ion detection [c]
Limit of detection	**100 ppbw** organics in surface sample
GC Columns	Two; General and Chiral separation

Bold = Exceeds requirements
[a] Composite range, individual modes access a subset of this range
[b] Resolution decreases above required maximum mass range (550 Da), impacts LDMS mode.
[c] Negative ion detection only in LDMS mode

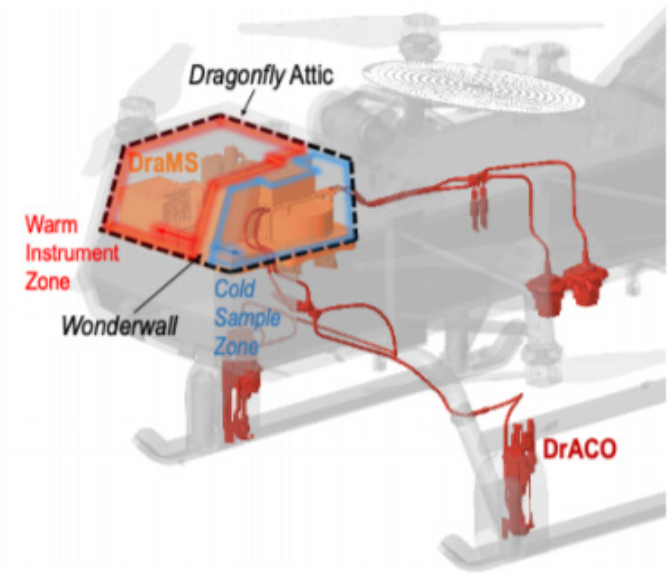

Figure 1. The *Dragonfly* "Attic" Cold Zone and Warm Zone.

Europan Molecular Indicators of Life Investigation (EMILI):

Abstract Excerpt: "The Europan molecular indicators of life investigation (EMILI) is an instrument investigation designed to address the top science objectives of a future Europa lander mission, such as documented by the recent Europa Lander Science Definition Team (SDT). EMILI seeks to detect and characterize potential organic molecular biosignatures, which may be present only at ultralow (nM) concentrations. EMILI also characterizes key aspects of the mineralogical context of the samples collected from the Europan near-subsurface to discern the provenance and degree of radiative or oxidative processing they have undergone. Here we present selected EMILI instrument features, including recent prototype mass spectrometer (MS) developments, and preliminary results." (Willis et al. 2019)

Also see Brinckerhoff et al. (2018).

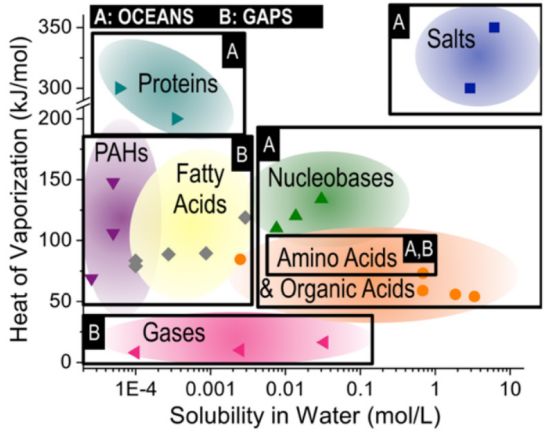

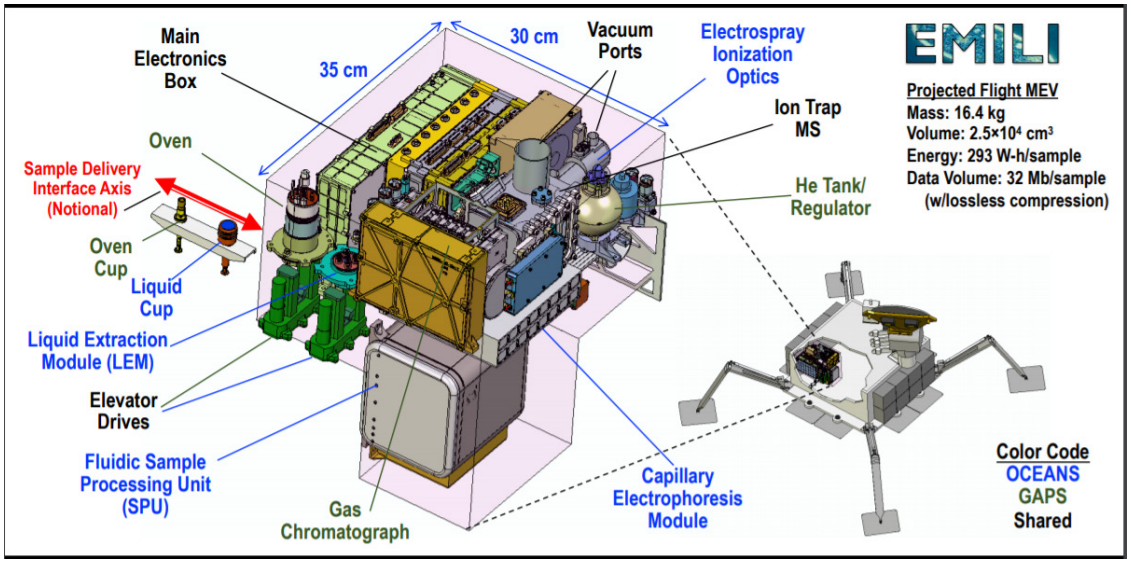

Ocean Worlds Life Surveyor (OWLS):

Abstract Excerpt: "The Ocean Worlds Life Surveyor (OWLS) instrument suite is designed to search for signs of life by combining the complementary lines of evidence provided by organic chemical analysis and microscopy. Organic chemical analysis in OWLS is performed by the Organic Capillary Electrophoresis Analysis System (OCEANS). OCEANS is designed to search for biological patterns in the distributions of classes of organic molecules such as amino acids, nucleic acids, and carboxylic acids, as well as higher molecular weight polymers such as small peptides or fatty acids. OCEANS achieves this by coupling the high efficiency separation capability of capillary electrophoresis (CE) with three different detection modes: • Conductivity (C4D) to detect small common di- and tri-carboxylic acid metabolites that could be present when active organisms are in a sample. • Laser induced fluorescence (LIF) for highly sensitive detection of amino acid, specifically determining the distribution of amino acid type and chirality. • Electrospray ionization mass spectrometry (ESI-MS) to broadly survey for organic molecules over the mass range from 75 – 500 m/z, as well as target nucleic acids and fatty acids. An upstream sample extraction system allows for variable temperature extraction followed by bulk characterization to provide information on the pH, eH, and dominant salts in the sample. Bulk characterization of the sample allows for appropriate preparation by the microfluidic processing ahead of CE separation." (Chong et al. 2019)

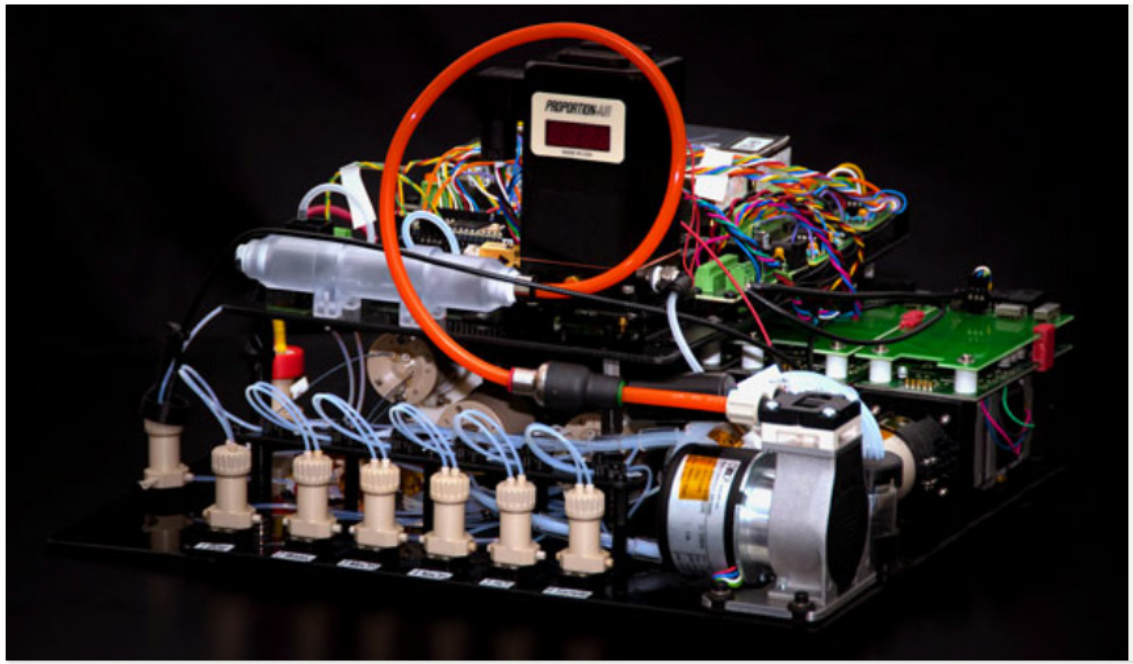

JPL's first complete brassboard prototype for end-to-end capillary electrophoresis analysis using a hollow glass capillary as the separation element. This design has been validated and is the first system capable of directly interfacing with mass spectrometry detection.
+ Larger image

Supercritical CO_2 and Subcritical H_2O Analysis (SCHAN):

"SCHAN is capable of detecting a wide range of hydrophobic molecules such as polycyclic aromatic compounds, fatty acids, pigments, sterols and glycerides with detection limits as low as 20 parts per trillion (ppt) (3). Nonpolar biomarkers are extracted with scCO2 at 40 °C at 22 MPa, or at higher temperatures (100 °C) which has been proven to be efficient for recovering adsorbed amino acids (16, 17). Analysis of both inorganic and small organic cations (e.g., alkali metals, amines and alkanolamines) and anion (e.g., perchlorates, chloride, organic acids) is unmatched by ion chromatography analysis with conductivity measurements (18). Detection limits of ca. 10 ppb is obtained for virtually any small ionic analyte." (Lin et al. 2021)

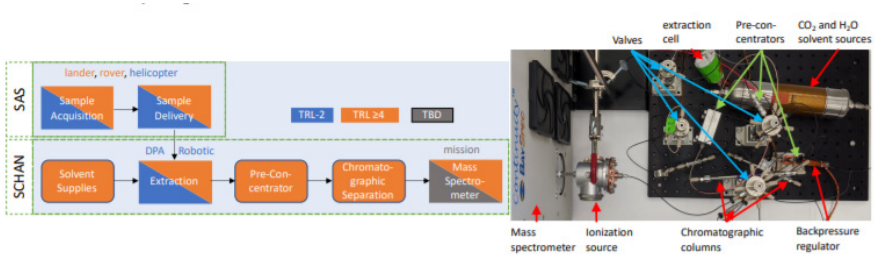

Figure 2. The DREDGE-M system consists of 7 major components as shown on the left. The SAS can be on either a mobile platform or the same lander where extraction and analysis components reside. A picture of the breadboard SCHAN instrument is shown on the right. The estimated mass for SAS is 21 kg (incl. drill) and 12 kg for SCHAN.

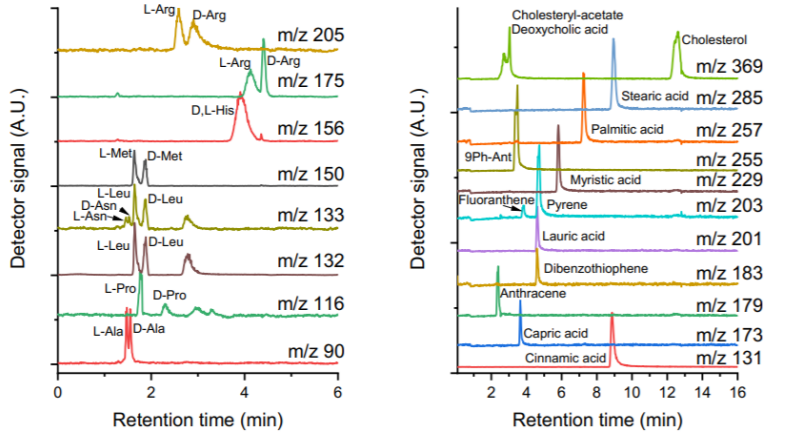

Figure 4. SCHAN is able to resolve complex mixtures that contain e.g. enantiomeric amino acids and lipids such as polycyclic aromatic compounds, fatty acids and sterols at ppb-level. The chromatographic separation resolves species based on chirality or their chemical structure and the mass spectrometer differentiates based on molecular weight.

Tunable Laser Spectrometer (TLS):

Abstract Excerpt: "The Tunable Laser Spectrometer (TLS) is one of three instruments that make up the Sample Analysis at Mars (SAM) suite on the Curiosity Rover that landed in August 2012. TLS is a two-channel tunable laser spectrometer (3.7 kg) using an Interband Cascade (IC) laser at 3.27 μm for methane measurements, and a near-IR tunable diode laser for measurements of water and carbon dioxide isotopes. To date, TLS has measured in CO2 the isotope ratios 13C/12C, 18O/16O , 17O/16O and 13C18O/ 12C16O; and in water the isotope ratios D/H and 18O/16O in both the atmosphere and gases evolved from pyrolysis of soils and rock samples." (Webster et al. 2013)

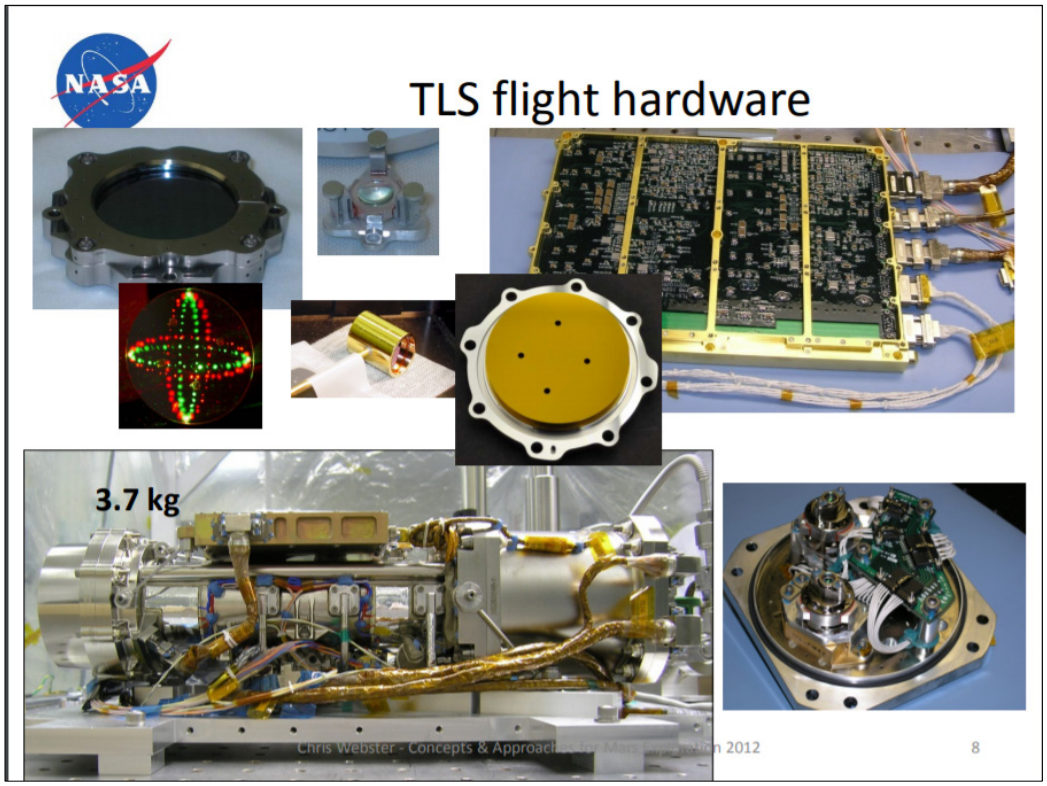

Miniature Tunable Laser Spectrometer (Mini-TLS):

See Webster et al. (2012).

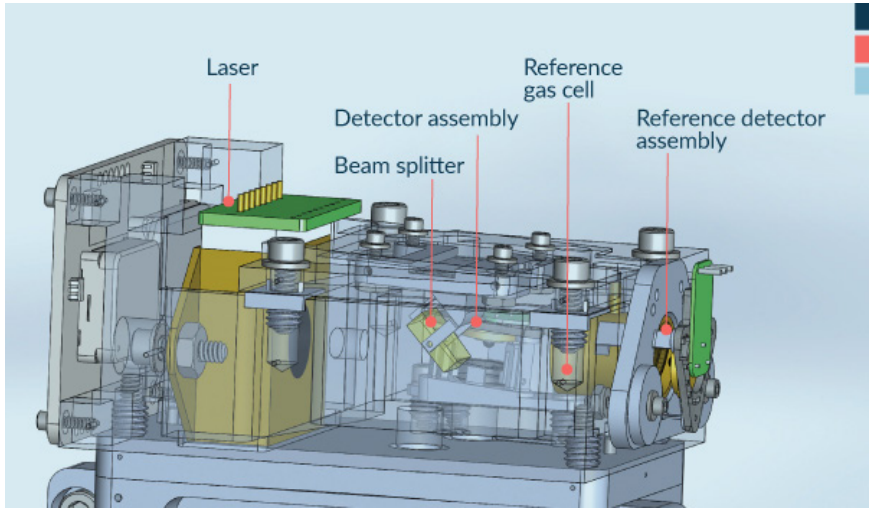

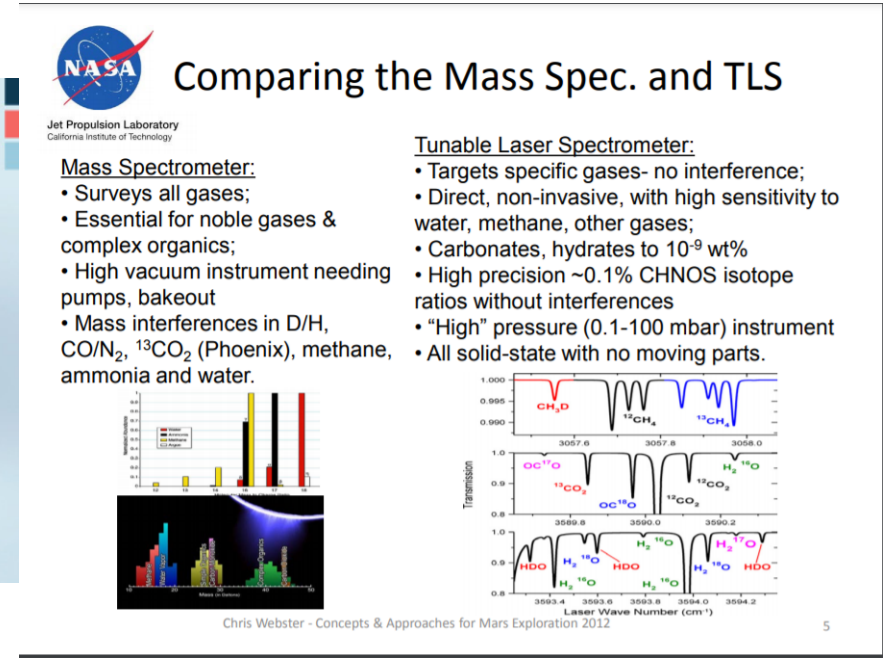

Thermal Evolved Gas Analyzer (TEGA):

Abstract Excerpt: "The Phoenix spacecraft that was launched to Mars in August 2007 landed safely on the Martian northern arctic region on May 25, 2008. It carried six experiments to study the history of water on the planet and search for organic molecules in the icy subsurface Martian soil. The spacecraft is a lander with an arm and scoop designed to dig a trench though the top soil to reach an expected ice layer near the surface. One of the instruments on board is the thermal evolved gas analyzer (TEGA), which consists of two components, a set of eight very small ovens that will heat samples of the ice soil mixtures from the trench to release imbedded gases and mineral decomposition products, and a mass spectrometer that serves as the analysis tool for the evolved gases, and also for measurements of the composition and isotopic ratios of the gases that comprise the atmosphere of Mars. The mass spectrometer is a miniature magnetic sector instrument controlled by microprocessor-driven power supplies. One feature is the gas enrichment cell that will increase the partial pressures of the noble gases in an atmosphere sample by removing all the active gases, carbon dioxide, and nitrogen, to improve the accuracy of their isotopic ratio measurements." (Hoffman et al. 2008)

Table 1. Instrument parameters

Mass analyzer	Magnetic sector-field
Electron source	Thermal emission type
Mass ranges	4, extending from 0.7 to 140 Da
Mass resolution	m/Δm = 140 (highest mass range, others appropriate to the mass range)
All components of the MS are packaged together	
Volume	24 × 23 × 18 cm
Mass	5.7 kg
Operating power	13 watt

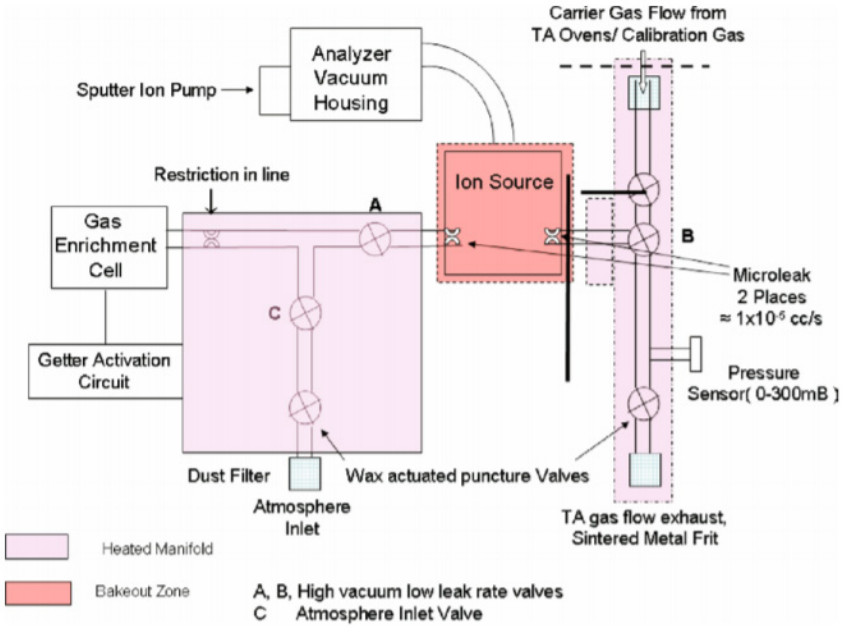

Figure 1. Drawing of the mass analyzer and associated gas manifold.

Extractor for Chemical Analysis of Lipid Biomarkers in Regolith (ExCALiBR):

ExCALiBR optimizes solvent extraction and concentration of lipids from regolith, rock powder, or icy materials for delivery to analytical instruments for molecular characterization. The ExCALiBR system will enable future organic surveys by extracting and concentrating lipids from approximately ~50 grams of sample using a fluidic and microfluidic sample processor made of materials compatible with the non-aqueous organic solvents. ExCALiBR bridges a critical gap by replicating traditional analytical laboratory sample processing procedures that have been used for over 70 years autonomously on a flight-instrument scale with fidelity to established lab techniques, overcoming challenges common to natural samples such as low organic concentration and organic-mineral molecular interactions. See Wilhelm et al. (2020).

Parameter	Specifications
Sample Input Size	50 g
Number of Samples	3 (plus one blank)
Extraction Type	Organic solvent techniques based on traditional geolipid analysis
Target Molecules	Mid to high molecular weight lipids (e.g., fatty acids, *n*-alkanes, polycyclic isoprenoids, PAHs)
Extraction Temperature & Pressure	0°C-120°C; 8.6 atm
Final Lipid Extract Volume	100 µL
Comminution Output Particle Size	>75% of particles <100 µM
Mass	25 kg
Power (Average)	35 W
Energy	850 Wh/sol
Volume	60 x 25 x 20 cm = 30 L
Analytical Instrument Compatibility	e.g., GC-MS, LD-MS, LC-MS, Raman SERS

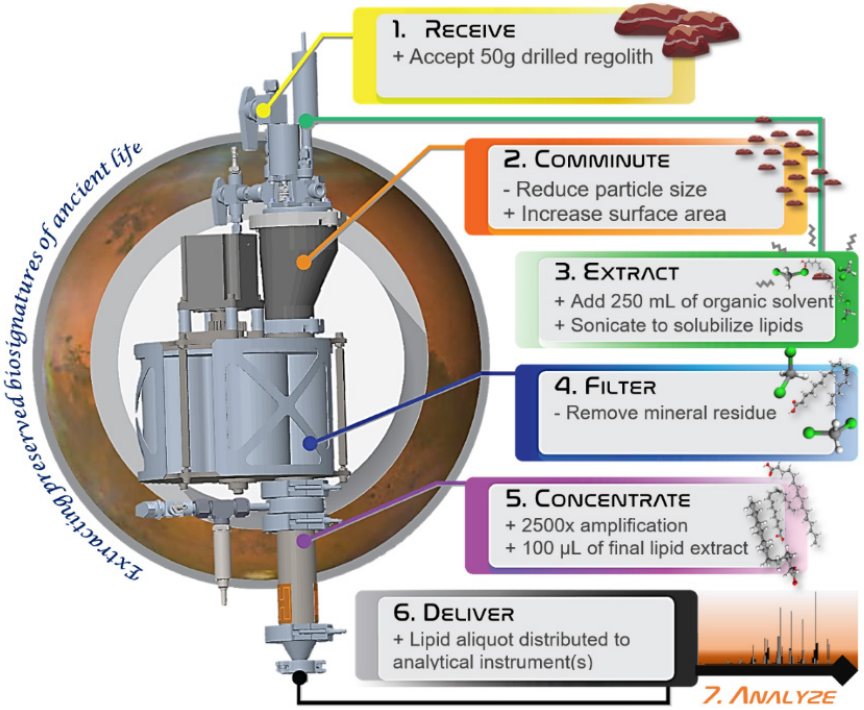

Next Generation CheMin X- Ray Diffractometer (CheMinX):

Abstract Excerpt: "CheMinX, a next-generation XRD/XRF instrument, is based on similar principles as MSLCheMin, but benefits from a decade of advancements in geometry design and subsystem miniaturization [22]. The XRD measurement of CheMinX is similar to MSL-CheMin, but uses different components and a different layout to optimize its geometry. Diffracted photons are collected by a CCD in direct illumination, critical for energy-selective detection of XRD photons in Mars' radiation environment. Whereas MSL-CheMin uses APXS bulk sample compositions, CheMinX uses an internal Silicon Drift Detector (SDD) to provide a concurrent XRF measurement of the sample. CheMinX sample cells are redesigned for a more compact and lower cost sample handling subsystem. A fixed tuning fork is combined with multiple single-use cells in a cartridge/dispenser arrangement to address the issue of clogged sample cells experienced with MSL-CheMin. A preliminary mechanical design of CheMinX is shown in Figure 2." (Rampe et al. 2020)

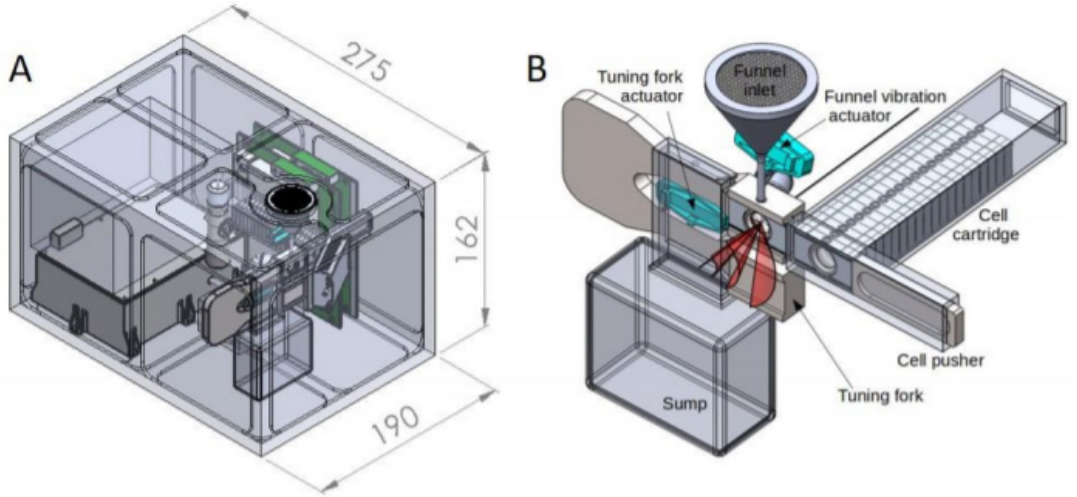

Figure 2. Preliminary mechanical design of the CheMinX flight instrument. (A) Instrument with dimensions (in mm), projected mass is 5 kg. (B) Sample handling subsystem for the vibrated sample method based on single-use cells in a cartridge dispenser system. This sampling subsystem is being developed as part of a NASA PICASSO19 grant awarded to P. Sarrazin.

Microscopy, Electrochemistry, and Conductivity Analyzer (MECA):

Instrument Requirements Section Excerpt: "The WCL science objectives have been translated into specific design requirements. Six of these pertain to the determination of inorganic ionic species and electrochemical properties, as follows:

1. The WCL is designed to measure the concentration of the anions Cl^-, Br^-, and I^- and the cations Na^+, K^+, Mg^{2+}, and Ca^{2+} in a particle-free aqueous solution with a pH from 3 to 10. To satisfy this requirement, it is necessary that the minimum detectable concentration be the greater of 10^{-5} M or 1% of the total ion concentration. It is also critical that in such solutions the presence of HCO_3^-, SO_4^{2-}, NH_4^+, Fe^{n+}, or other constituents of the leaching solution not interfere with the measurement.
2. The WCL is designed to detect SO_4^{2-} in solution at concentrations greater than 10^{-4} M and to determine its concentration at levels between 0.01 and 0.06 ± 0.01 M.
3. The WCL is designed to determine the pH of a sample/water mixture between pH 0–12 with an accuracy of ±0.5 pH units.
4. The WCL is designed to measure the reduction/oxidation potential between 1000 and −1000 mV with an accuracy of ±20 mV.
5. The WCL is designed to measure the electrical conductivity of the solution between 0.01and 100 mS cm^{-1}.
6. The WCL is designed to run a cyclic voltammogram between ±1000 mV to an accuracy of ±1 mV.

In addition, each WCL is designed to be able to perform these analyses for at least 90 min to study possible progressive changes as the liquid H_2O interacts with the soil, under agitation provided by a stirring motor. The WCL has the ability to monitor and control the temperature to ±1°C between 0 and 40°C, although most experiments are planned for the temperature range of between 5 and 10°C." (Kounaves et al. 2009)

Microfluidic Icy-World Chemistry Analyzer (MICA):

Abstract Excerpt: "MICA will use electrochemical sensors to quantitatively measure key chemical properties of Europan surface materials. The measurements will help evaluate habitability (SDT mission Goal 2) and provide sample context to other instruments in the search for evidence of potential biosignatures (SDT mission Goal 1). Although Europa's subsurface ocean is estimated to be tens of kilometers below the surface, determining its nature can be accomplished by analyzing materials that have been brought to the surface by either ice shell activity or ejection by plumes. Water-rock interactions necessary for habitability can only be discerned by analyzing dissolved salts in ionic form. The relative and absolute abundances of such ions as Na+ , K+ , Mg2+ , Ca2+, Cl- , SO4 2- , and CO3 2- can provide information on the depth and duration of water-rock interactions and the probable geologies and geochemistries involved. Enhanced levels of trace species such as Li+ and Zn2+, as well as transition metals with multiple oxidation states (e.g. Fe, Mn, Cu, Co) can be indicative of hydrothermal activity as well as constrain potential metabolic pathways of putative organisms." (Noell et al. 2019)

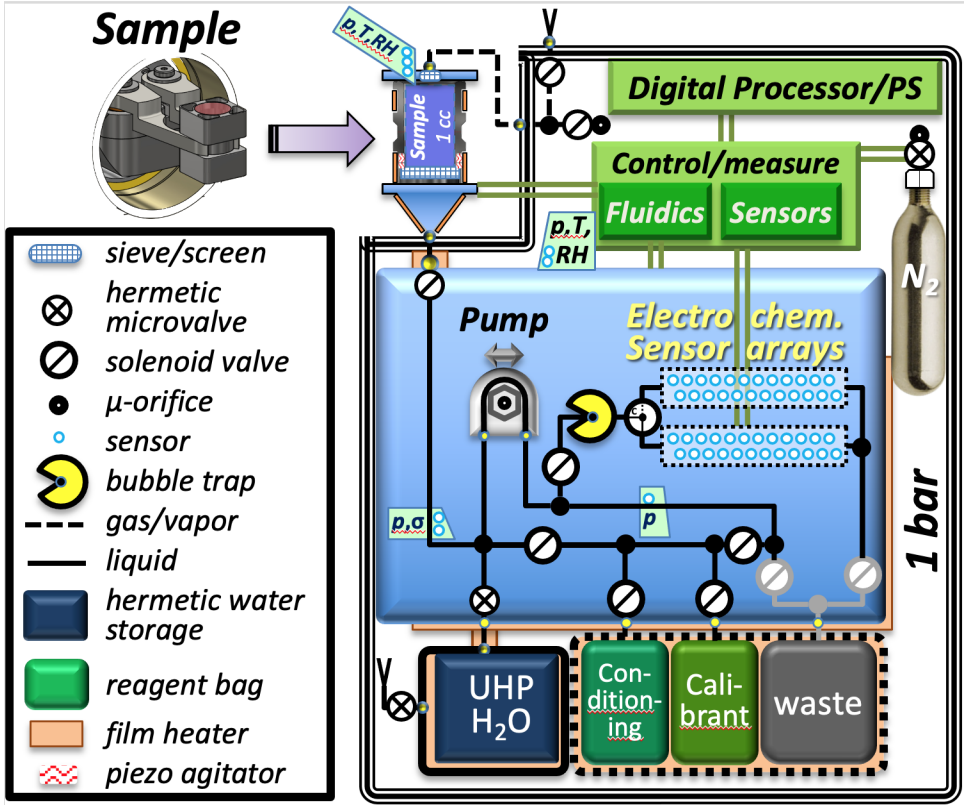

Microfluidic Wet Chemistry Laboratory (mWCL):

Abstract Excerpt: "The 2008 Phoenix lander mission provided the first successful soil analysis of the Martian surface. Utilizing the on board Wet Chemistry Laboratory (WCL) revealing the chemical composition and potential habitability of the planet. This was achieved by a simple array of ion selective electrodes (ISEs) which analyzed the geochemistry of the Martian soil providing invaluable information into not only the aqueous geochemistry but the history of Mars [1,2]. As such, similar technology can be utilized to assess the ocean composition of icy moons, such as Europa and Enceladus. A redesigned TRL9 Phoenix WCL array with microfluidic platform will allow analysis of either ejected plumes or liquid brine from the moons subsurface oceans. These analyses will provide essential data about the chemical energy, redox gradients, subglacial ocean geochemistry as well as the habitability of these icy ocean worlds." (Naz and Kounaves 2021)

CheMin Mineralogical Instrument (CheMin):

Abstract Excerpt: "The CheMin X-ray diffraction (XRD) and X-ray fluorescence (XRF) instrument on MSL will return accurate mineralogical identifications and quantitative phase abundances for scooped soil samples and drilled rock powders collected at Gale Crater during Curiosity's 1-Marsyear nominal mission. The instrument has a Co X-ray source and a cooled charge-coupled device (CCD) detector arranged in transmission geometry with the sample. CheMin's angular range of 5° to 50° 2θ with < 0.35° 2θ resolution is sufficient to identify and quantify virtually all minerals. CheMin's XRF requirement was descoped for technical and budgetary reasons. However, X-ray energy discrimination is still required to separate Co Kα from Co Kβ and Fe Kα photons. The X-ray energy-dispersive histograms (EDH) returned along with XRD for instrument evaluation should be useful in identifying elements Z > 13 that are contained in the sample. The CheMin XRD is equipped with internal chemical and mineralogical standards and 27 reusable sample cells with either Mylar® or Kapton® windows to accommodate acidic-to-basic environmental conditions." (Blake et al. 2012)

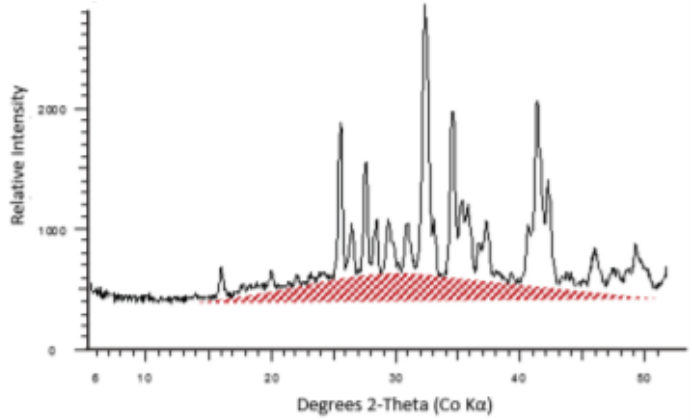

Figure 1. Rocknest CheMin XRD pattern illustrating the intensity contribution due to amorphous scattering (shaded).

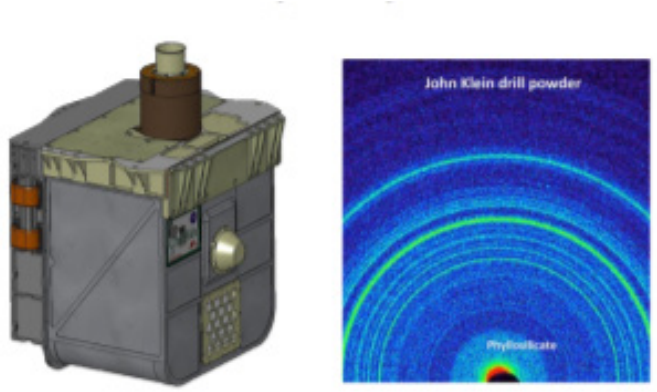

Figure 1: The MSL CheMin instrument (left) and 2D XRD data (right). Resolution is ~0.3° 2θ.

Alpha-Particle X-ray Spectrometer (APXS):

Introduction Excerpt: "The alpha particle X-ray spectrometer (APXS) permits the determination of the elemental chemical composition of rocks and soil by placing its sensor head against the sample, powering on the instrument, and commanding it to acquire spectra. It does not require any sample preparation and is thus well suited for in situ measurements of the surface constituents of objects in space (planets, comets and asteroids). Its working principle is based on the bombardment of the sample surface with alpha particles and X rays from radioactive sources (244Cm) and the measurement of the energy distribution of alpha particles, scattered by sample atoms in a backward direction, and of characteristic X rays, emitted by the sample atoms upon recombination of ionizations caused by the radiation from the sources, processes commonly referred to as "Rutherford backscattering" or RBS, "particle-induced X-ray emission" or PIXE, and "X-ray fluorescence" or XRF. One version of the instrument has been on board of the Sojourner rover of the NASA Mars Pathfinder (MPF) mission." (Rieder et al. 2003)

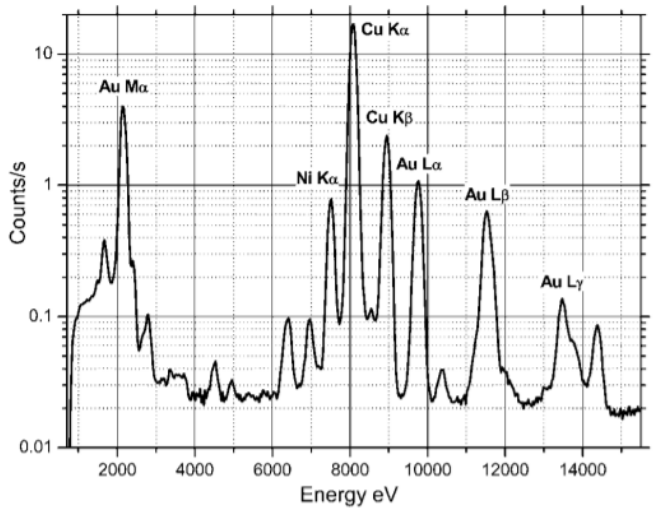

Figure 12. X-ray spectrum of the internal calibration target (backside of the doors) taken with the FM2 sensor head in CO_2 gas.

Table 1. APXS Sensor Head, Including Door Mechanics, Microswitches, an X-Ray Channel, Two Alpha Channels, and Tantalum Shielding

Parameter	Value
Length, mm	90
Diameter, mm	53
Mass, g	250
Power +12 V, mA	27
Power −12 V, mA	25

Table 2. APXS Main Electronics

Parameter	Value
Length, mm	170
Width, mm	100
Height, mm	10
Mass, g	120
Power +5 V, mA	60
Power −5 V, mA	40

SWIR-MIR Point Spectrometer (MLPS):

Poster Instrument Objective Excerpt: "To develop a small, scientifically capable, readily-replicable IR point spectrometer, miniaturizing by several factors a crucial (and proven) technique to enable assay of volatiles, minerals, organics, and ices from small satellites • A key element of the Intrepid (NEO-100) mission concept science payload, as well as a versatile instrument for many other CubeSat & SmallSat concepts (2U form factor) • Of size and capability suitable for mass-constrained landers and commercial opportunities • Surface volatile assessment (quantity, nature of the host materials) and mineralogy enabled by wavelength ranges SWIR (2 – 4 μm) and Thermal IR (5.5 – 12 μm) in a single instrument." (Ehlmann et al. 2019)

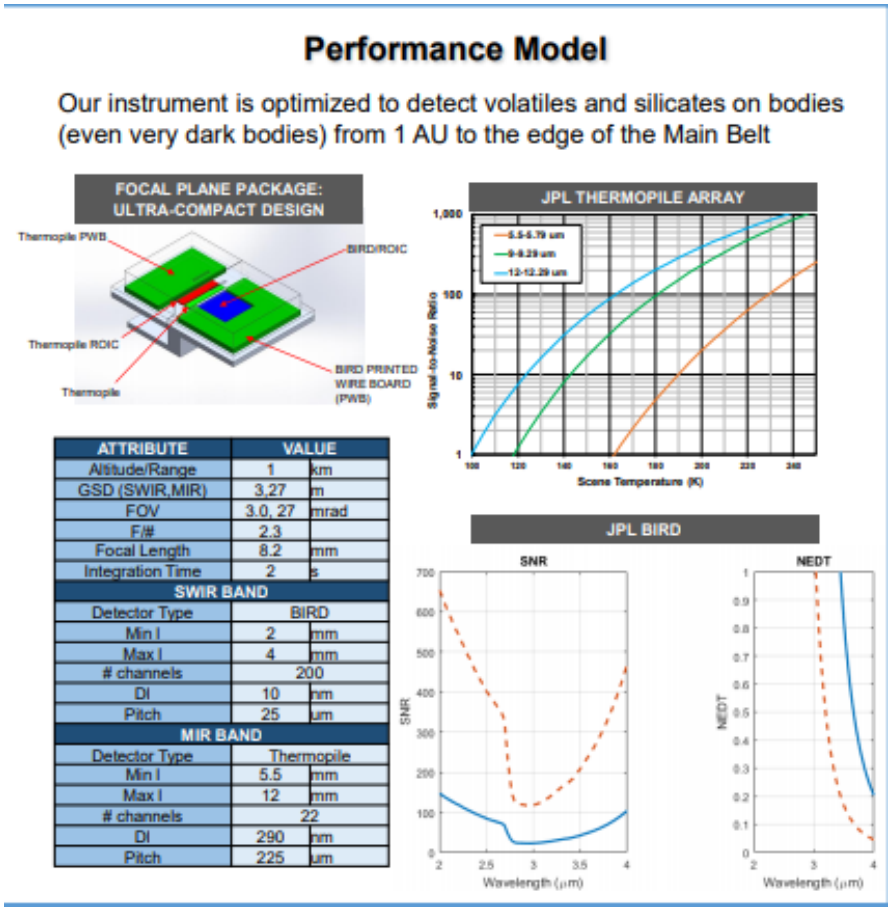

ATTRIBUTE	VALUE	
Altitude/Range	1	km
GSD (SWIR,MIR)	3,27	m
FOV	3.0, 27	mrad
F/#	2.3	
Focal Length	8.2	mm
Integration Time	2	s
SWIR BAND		
Detector Type	BIRD	
Min l	2	mm
Max l	4	mm
# channels	200	
Dl	10	nm
Pitch	25	um
MIR BAND		
Detector Type	Thermopile	
Min l	5.5	mm
Max l	12	mm
# channels	22	
Dl	290	nm
Pitch	225	um

Phoenix Temperature Sensor:

Journal Excerpt: "The payload shall be capable of measuring near surface temperature at three height levels over at least 0.8 vertical meters continuously at a frequency of 0.5 Hz, in the range 140 –280 K, with an absolute accuracy of ±1 K and a resolution of 0.5 K. The uncertainty in the calculated difference between any two concurrent thermocouple readings shall not exceed 0.3 K 2. Phoenix shall be capable of measuring surface barometric pressure at a frequency of 0.5 Hz over a range of 7 – 11 hPa with (design goal) 10 Pa accuracy and 0.1 Pa resolution." (Taylor et al. 2008)

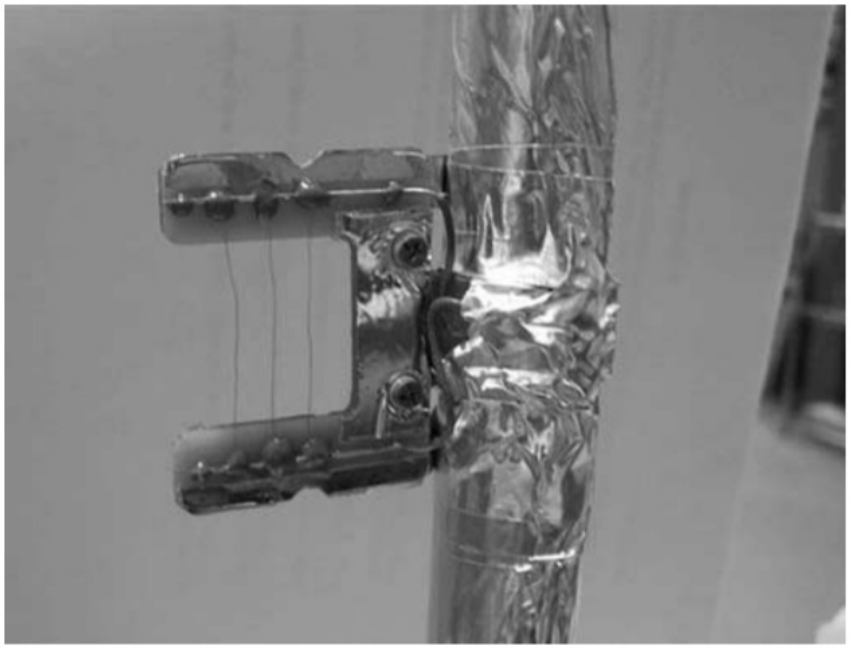

Figure 1. Phoenix MET thermocouples and C Frame.

Mars Multispectral Imager for Subsurface Studies (MaMISS):

Abstract Excerpt: "The Ma_MISS (Mars Multispectral Imager for Subsurface Studies) experiment is the visible and near infrared (VNIR) miniaturized spectrometer hosted by the drill system of the ExoMars 2020 rover. Ma_MISS will perform IR spectral reflectance investigations in the 0.4–2.2 mm range to characterize the mineralogy of excavated borehole walls at different depths (between 0 and 2 m). The spectral sampling is about 20 nm, whereas the spatial resolution over the target is 120 mm. Making use of the drill's movement, the instrument slit can scan a ring and build up hyperspectral images of a borehole. The main goal of the Ma_MISS instrument is to study the martian subsurface environment. Access to the martian subsurface is crucial to our ability to constrain the nature, timing, and duration of alteration and sedimentation processes on Mars, as well as habitability conditions. Subsurface deposits likely host and preserve H2O ice and hydrated materials that will contribute to our understanding of the H2O geochemical environment (both in the liquid and in the solid state) at the ExoMars 2020 landing site. The Ma_MISS spectral range and sampling capabilities have been carefully selected to allow the study of minerals and ices in situ before the collection of samples. Ma_MISS will be implemented to accomplish the following scientific objectives: (1) determine the composition of subsurface materials, (2) map the distribution of subsurface H2O and volatiles, (3) characterize important optical and physical properties of materials (e.g., grain size), and (4) produce a stratigraphic column that will inform with regard to subsurface geological processes." (De Sanctis et al. 2017)

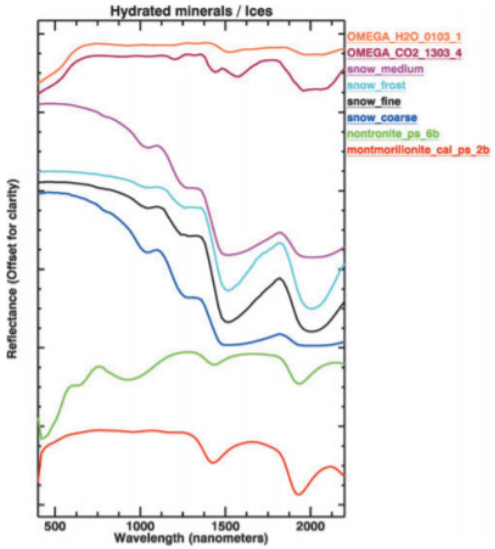

FIG. 1. Reflectance spectra of hydrated minerals (nontronite and montmorillonite, USGS Library), terrestrial snow at different grain sizes (USGS Library), and martian H_2O and CO_2 ices (Mex/OMEGA, from orbit 103 and 1303, respectively). All spectra have been convolved at the spectral resolution and sampling (20 nm) of Ma_MISS, in the range 400–2200 nm. Ma_MISS, Mars Multispectral Imager for Subsurface Studies.

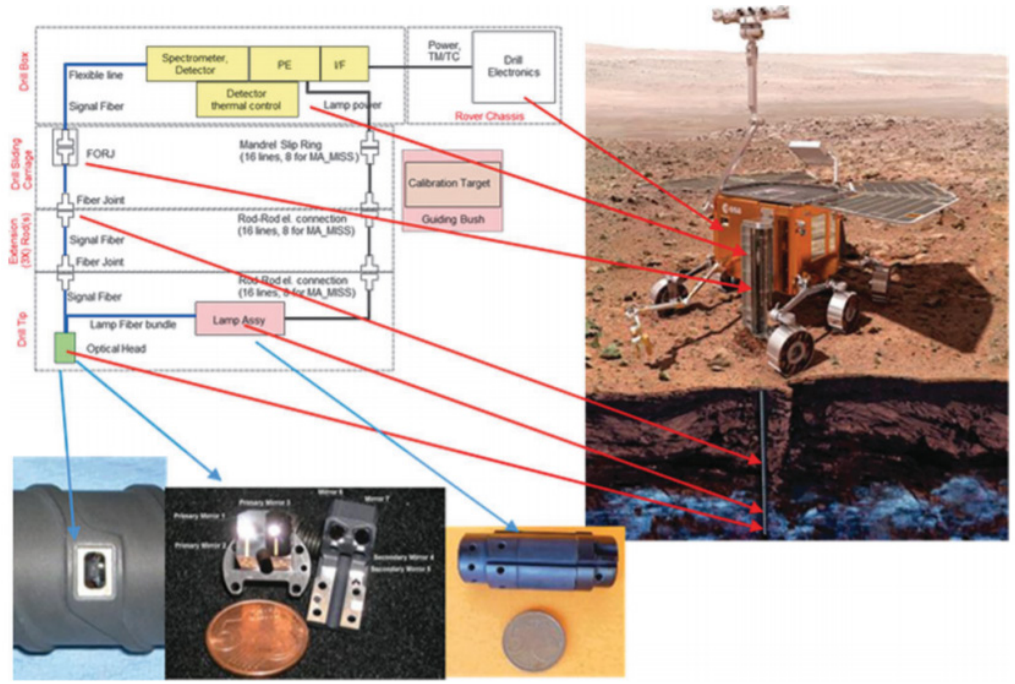

FIG. 2. Ma_MISS functional diagram (left side) and accommodation inside drill parts (right side). PE is the Proximity Electronics. I/F is the electrical/mechanical interface between Ma_MISS and drill.

Phoenix Thermal and Electrical Conductivity Probe (TECP):

Journal Excerpt: "The Thermal and Electrical Conductivity Probe (TECP) is a component of the Microscopy, Electrochemistry and Conductivity Analyzer (MECA) payload on the Phoenix Lander. TECP will measure the temperature, thermal conductivity, and volumetric heat capacity of the regolith. It will also detect and quantify the population of mobile H2O molecules in the regolith, if any, throughout the polar summer, by measuring the electrical conductivity of the regolith as well as the dielectric permittivity. In the vapor phase, TECP is capable of measuring the atmospheric H2O vapor abundance as well as augmenting the wind velocity measurements from the meteorology instrumentation. TECP is mounted near the end of the 2.3 m Robotic Arm and can be placed either in the regolith material or held aloft in the atmosphere. This paper describes the development and calibration of the TECP. In addition, substantial characterization of the instrument has been conducted to identify behavioral characteristics that might affect landed surface operations. The greatest potential issue identified in characterization tests is the extraordinary sensitivity of the TECP to placement. Small gaps alter the contact between the TECP and regolith, complicating data interpretation. Testing with the Phoenix Robotic Arm identified mitigation techniques that will be implemented during flight. A flight model of the instrument was also field tested in the Antarctic Dry Valleys during the 2007–2008 International Polar Year." (Zent et al. 2009)

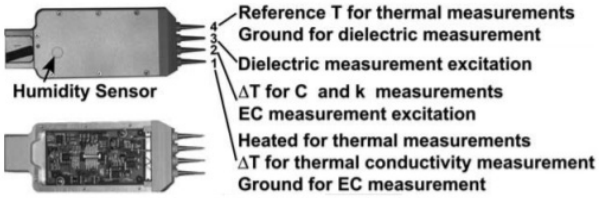

Figure 2. (top) Photograph of the Thermal and Electrical Conductivity Probe (TECP) instrument and (bottom) with the external cover removed to allow access to the electronics board. For each needle, the numerical designation and functionality is identified at right. The TECP is 118.76 mm in length. Its needles are 15 mm long.

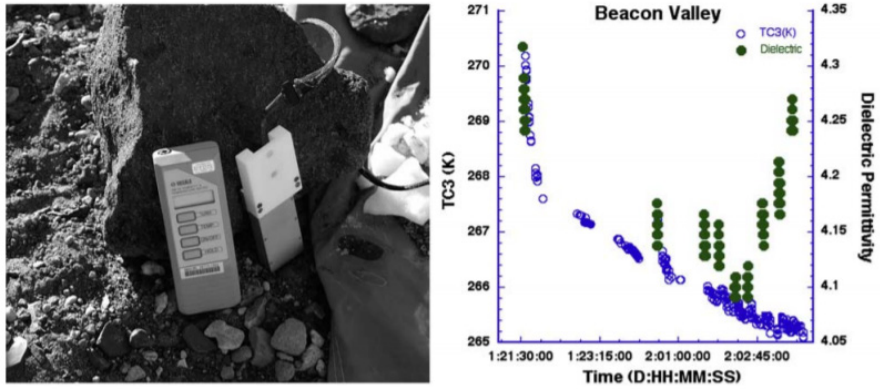

Figure 14. (left) The TECP deployed in Beacon Valley. (right) Needle 3 temperature and bulk dielectric permittivity recorded during the overnight hours of 2 January 2008.

Sonic Anemometer (Sonic Anemometer):

Abstract Reference: "An acoustic anemometer for use on Mars has been developed. To understand the processes that control the interaction between surface and atmosphere on Mars, not only the mean winds, but also the turbulent boundary layer, the fluxes of momentum, heat and molecular constituents between surface and atmosphere must be measured. Terrestrially this is done with acoustic anemometers, but the low density atmosphere on Mars makes it challenging to adapt such an instrument for use on Mars. This has been achieved using capacitive transducers and pulse compression, and was successfully demonstrated on a stratospheric balloon (simulating the Martian environment) and in a dedicated Mars Wind Tunnel facility. This instrument achieves a measurement accuracy of 5 cm/s with an update rate of >20 Hz under Martian conditions. VC 2016 Acoustical Society of America." (Banfield and Dissly 2005)

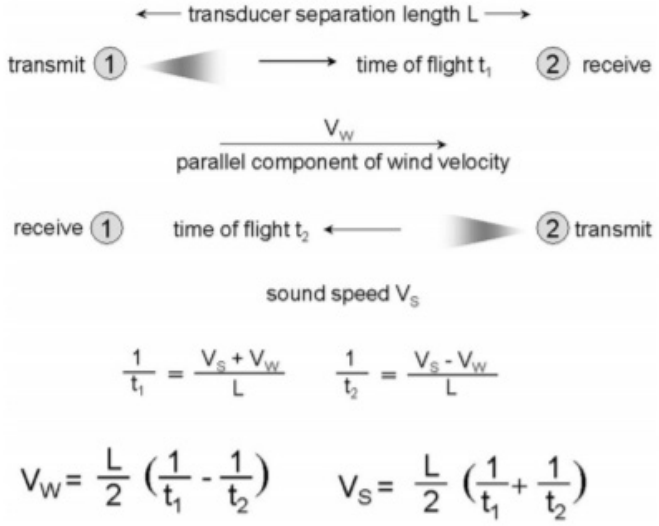

FIG. 1. Diagram showing the measurement technique used in acoustic anemometry as described in the text. The equations demonstrate how the wind speed and sound speed can both be retrieved from the average and difference of the upwind and downwind acoustic travel times.

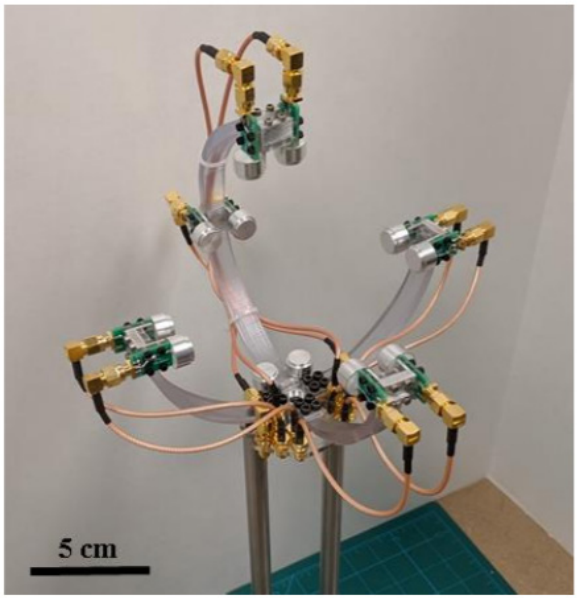

Fig 1: Acoustic anemometer prototype with 6 pairs of PUI piezoelectric ultrasound transducers.

Coupled Sonic Anemometer and Met TLS:

Overview: The TLS is integrated into the sonic anemometer to form a single instrument able to measure eddy fluxes at high frequency (20Hz) with an accuracy of ±2%.

Method: The integration requires synchronization of electronics, with care to avoid the TLS mechanically interfering with the wind measurement, and is necessary because the small eddy sizes near the surface demand that wind and gas measurements be collocated in order to accurately determine covariances.

Readiness: A version with only an H_2O channel has been deployed and demonstrated in field locations. Because the TLS measures gas abundance in the same path as the acoustic path using the same driving electronic clock, the eddy covariances needed for flux determination are obtained with minimal processing and flow directly from the data. The combined instrument is currently at TRL 5.

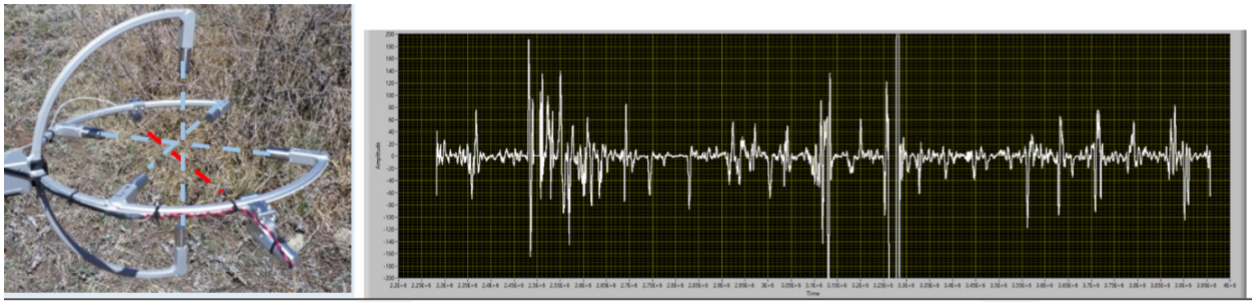

Figure 1. The integrated TLS and anemometer sensor head (left). The TLS path is highlighted by the dashed red line while the 3-D acoustic path is shown by the dashed blue lines. Real time instantaneous water covariance measurements from a field experiment as shown on the right.

Meteorological Tunable Laser Spectrometer(Met TLS):

Abstract Excerpt: "A newly developed tunable laser spectrometer (TLS) capable of simultaneously measuring many of the key photochemical species in planetary atmospheres is presented. The instrument consists of a low-power «10 mW) and low mass «50 mg) vertical cavity emitting laser source and photodetector, a mUlti-pass optical cell to provide a long absorption path in a compact design, and laser driving and digital signal processing electronics. The sensor takes advantage of two key technological developments: 1) a patented mUltiple-pass optical cell design that uses small mirrors and dense spot patterns to give a long optical path with a small footprint; and 2) a low power and compact electronics system. Designs for Mars and Venus are mature, allowing for deployment on probe or balloon missions to either planet, and deployment on landed spacecraft at Mars. The instrument is immune to the corrosive sulfuric acid environment of Venus and is capable of operating at temperatures of up to at least 370 K; the instrument is ideal for an atmospheric balloon investigation at altitudes of 50 km or higher. The large diurnal temperature range of Mars is not a challenge, and the optical design is robust against dust contamination. The major advantage of this system over previously developed TLS instruments is the multichannel gas measuring capability, an increase in path length and sensitivity without an increase in mirror size, a dramatic decrease in mass and power, and the robust nature of the design in a hostile environment. Most of the instrument components and electronics are at TRL-6 with the combined system at TRL-5. The instrument is currently in field tests and will undergo environmental Mars testing for qualification to TRL-6 by then end of 2014. Current best estimates of total instrument mass and power are 750 mW and 1 kg, respectively.

If the Martian air were saturated with water, the water vapor pressure associated with the warmest air temperatures would be in excess of 600 Pa. While this value exceeds the total atmospheric pressure on Mars, it nonetheless provides a hard physical upper limit of dynamic range for a Mars water vapor sensor. At the other extreme, we might imagine just 10% relative humidity at 150 K. Observations indicate that air in the polar hood regions is very cloudy, suggesting a value closer to 100%. A relative hwnidity of 10% at 150 K 4 corresponds to a vapor pressure of order 10-5 Pa. Thus, the total dynamic range for a water vapor sensor is no greater than 7 decades (600 Pa to 10-5 Pa). This corresponds to a water vapor mixing ratio of 10^{-8} to 10^{-1} . A resolution of ~10% water concentration or mixing ratio is adequate to address science objectives, but ~1 % resolution is a reasonable expectation, particularly at the higher concentrations. For laser emission at 1.877 11m under Mars atmospheric conditions, a fractional absorption of about 10-6 over a pathlength of 1 m (easily achievable with multiple mirror bounces) would be required to resolve a mixing ratio of 10^{-8} at T = 150 K. Fractional absorption of 10^{-5} -10^{-6} can be reached with diode laser WMS spectroscopy, which is therefore, adequate for the task." (Rafkin 2015)

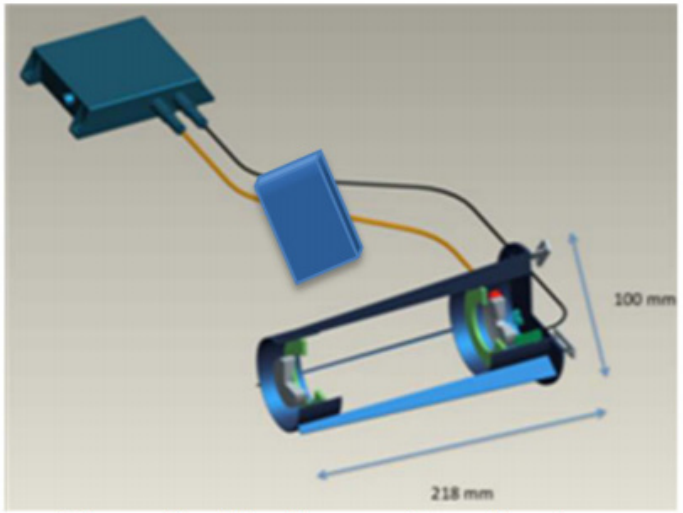

Figure 2 – The three major subsystems comprising the TLS instrument: CEB (top), LIB (middle), and OC (bottom).

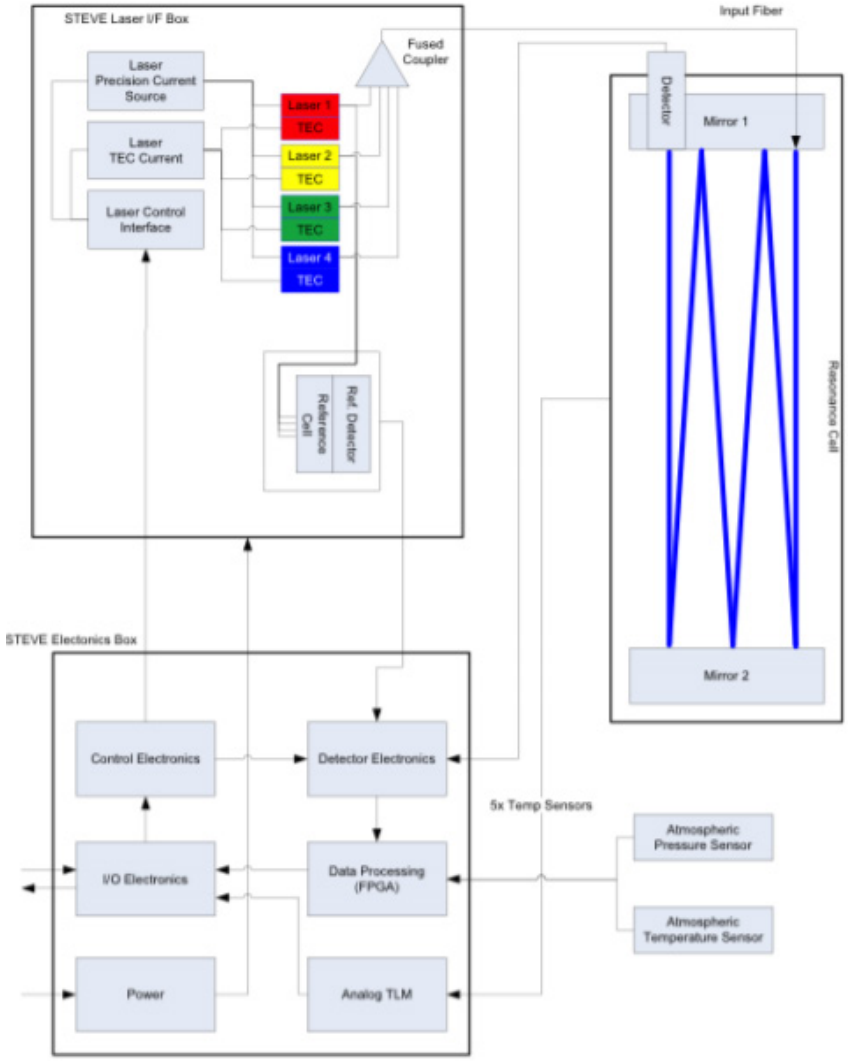

Figure 3 – The functional block diagram of the TLS instrument

Mars Environmental Dynamics Analyzer Thermal Infrared Sensor (MEDA-TIRS):

Mars 2020 MEDA TIRS is the first Martian IR radiometer that includes channels looking upward and downward, measuring the net thermal infrared radiation, the reflected solar radiation at the surface, as well as the atmospheric and surface skin temperatures using five different channels. TIRS is currently operating successfully on Mars, and is TRL 9.

For TIRS+ an additional channel would be needed to measure the downward solar radiation.

Abstract Excerpt: "The Mars Environmental Dynamics Analyzer (MEDA) is a suite of environmental sensors onboard NASA's Mars 2020 mission. The Thermal InfraRed Sensor (TIRS), developed at Centro de Astrobiología of Spain, is one of the six sensors comprising MEDA, and it will measure the net thermal infrared radiation and reflected solar radiation at the surface, as well as the atmospheric and surface skin temperatures using five different channels. In combination with MEDA's other sensors, TIRS will allow the quantification of the surface energy budget and the determination of key geophysical properties of the terrain such as the albedo and thermal inertia. Here we present a general description of the TIRS, its channels scientific requirements, and the mechanical and thermal design. Then, a detailed sensor mathematical model and a sensitivity analysis to model uncertainties are described. Some characterization test results to model parameters identification are included. Finally, accuracy and resolution calculus for each channel versus operational temperature is presented. The calculus is performed based on sensitivity equations, the practical tests results and the estimated values for different uncertainty sources." (Pérez-Izquierdo et al. 2018)

Table 1
TIRS Channels.

Channel	*Purpose*	*Spectral range*	*Pointing angles*
IR1	Downward LW	6.5–30 μm	Upward (+35°)
IR2	Air Temp	14.5–15.5 μm	Upward (+35°)
IR3	Upward SW	0.3–3 μm	Downward (-35°)
IR4	Upward LW	6.5–30 μm	Downward (-35°)
IR5	Ground Temp	8–14 μm	Downward (-35°)

Table 2
TIRS channels requirements.

Channel	*Dynamic range*	*Accuracy*	*Resolution*
IR1[a,b]	3.5–180 W/m^2	± (2.5 + 5% of the reading)W/m^2	± 0.9 W/m^2
IR2	173–293 K	± 5 K	± 1 K
IR3[a]	0–230 W/m^2	± (1 + 5% of the reading) W/m^2	± 1.2 W/m^2
IR4[a,b]	50–420 W/m^2	± (2 + 5% of the reading) W/m^2	± 2.1 W/m^2
IR5	173–293 K	± 5 K	± 1 K

[a] This requirement assumes a hemispherical FOV.
[b] This requirement assumes Stefan-Boltzmann emission.

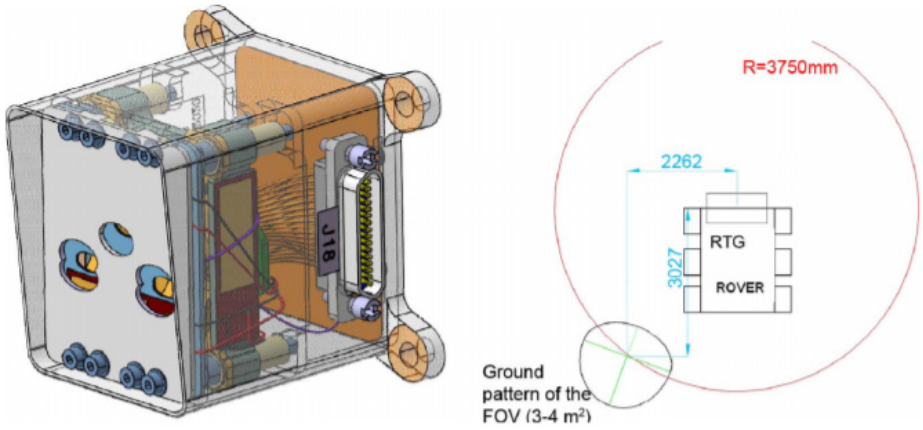

Fig. 2. (Left): TIRS sensor head. (Right): TIRS focused area.

Mars Environmental Dynamics Analyzer (MEDA):

Note: Study only considered portions of MEDA instrument suite, only the TIRS, pressure and temperature sensors are applicable.

Pressure sensor.
A Vaïsala pressure sensor has flown very successfully on MSL and Mars 2020. This is a small, lightweight, low-power and low-cost sensor that is at TRL 9.
Air temperature sensor.
Mars 2020 MEDA air temperature sensors (ATS) are thin-wire thermocouples with an accuracy of ~0.25K and response time of ~1s. One will be mounted as close to the surface as possible, with up to three more spaced evenly between the surface and near the top of the meteorological mast. These sensors are small, lightweight, low-power and low-cost, are currently operating successfully on Mars, and are TRL 9.

Abstract Excerpt: "NASA's Mars 2020 (M2020) rover mission includes a suite of sensors to monitor current environmental conditions near the surface of Mars and to constrain bulk aerosol properties from changes in atmospheric radiation at the surface. The Mars Environmental Dynamics Analyzer (MEDA) consists of a set of meteorological sensors including wind sensor, a barometer, a relative humidity sensor, a set of 5 thermocouples to measure atmospheric temperature at ∼1.5 m and ∼0.5 m above the surface, a set of thermopiles to characterize the thermal IR brightness temperatures of the surface and the lower atmosphere. MEDA adds a radiation and dust sensor to monitor the optical atmospheric properties that can be used to infer bulk aerosol physical properties such as particle size distribution, non-sphericity, and concentration. The MEDA package and its scientific purpose are described in this document as well as how it responded to the calibration tests and how it helps prepare for the human exploration of Mars. A comparison is also presented to previous environmental monitoring payloads landed on Mars on the Viking, Pathfinder, Phoenix, MSL, and InSight spacecraft.

To carry out the aforementioned investigations, MEDA has been designed as a set of separate sensors, each of them accommodated in the most suitable position possible, within rover constraints. The sensors are listed below and will be discussed in the following sections: – Air Temperature Sensor (ATS) – Pressure Sensor (PS) – Radiation and Dust Sensor (RDS), including SkyCam – Relative Humidity Sensor (HS) – Thermal Infrared Sensor (TIRS) – Wind Sensor (WS)." (Rodriguez-Manfredi et al. 2021)

Phoenix Robotic Arm (RA):

Abstract Excerpt: "The primary purpose of the Mars 2007 Phoenix Lander Robotic Arm (RA) and associated Icy Soil Acquisition Device (ISAD) is to acquire samples of Martian dry and icy soil (DIS) by digging, scraping, and rasping, and delivering them to the Thermal Evolved Gas Analyzer and the Microscopy, Electrochemistry, and Conductivity Analyzer. The RA will also position (1) the Thermal and Electrical Conductivity Probe (TECP) in the DIS; (2) the TECP at various heights above the surface for relative humidity measurements, and (3) the Robotic Arm Camera to take images of the surface, trench, DIS samples within the ISAD scoop, magnetic targets, and other objects of scientific interest within its workspace. The RA/ISAD will also be used to generate DIS piles for monitoring; conduct DIS scraping, penetration, rasping, and chopping experiments; perform compaction tests; and conduct trench cave-in experiments. Data from the soil mechanics experiments will yield information on Martian DIS properties such as angle of repose, cohesion, bearing strength, and grain size distribution. (Bonitz et al. 2008)

The Robotic Arm (RA) on the Mars 2007 Phoenix Lander is a 2.4 m long, low-mass, 4-degree-of-freedom arm (Figure 1) that carries on its end effector (Figure 2) the Icy Soil Acquisition Device (ISAD), Robotic Arm Camera (RAC), and the Thermal and Electrical Conductivity Probe (TECP). The ISAD consists of a scoop with two blades for acquiring dry and icy soil (DIS) samples, and a rasp for rapid acquisition of hard icy soils." (Bonitz et al. 2008; Arvidson et al. 2009; Smith et al. 2008).

Phoenix Biobarrier (Biobarrier):

Abstract Excerpt: "To prevent contamination of the Martian subsurface with Earth organisms per NASA planetary protection policy, the RA meets Category IV-B bio-burden requirement (NPR 8020.12B Planetary Protection Provisions for Robotic Extraterrestrial Missions, Revision B, 16 April 1999) in order to the meet this requirement, the RA was sterilized prior to final integration onto the lander and encased in a biobarrier (Figure 6). The biobarrier maintains sterilization during the journey to Mars and is deployed shortly after landing on the Martian surface." (Bonitz et al. 2008)

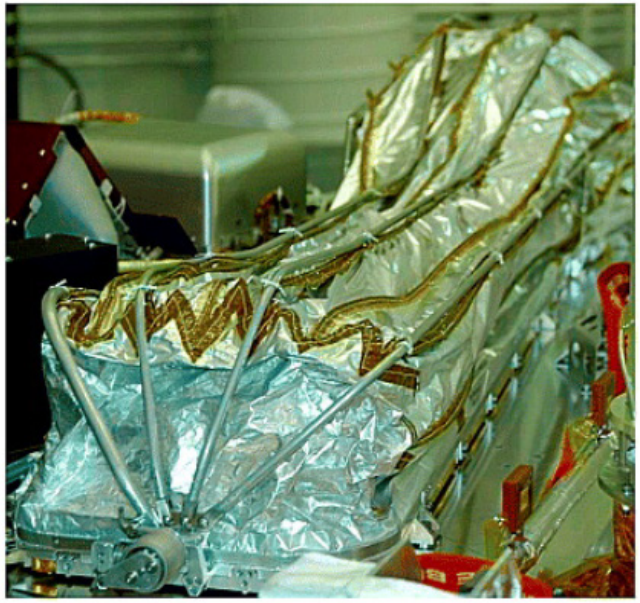

Figure 6 Open in figure viewer | PowerPoint

Robotic Arm encased in the biobarrier that maintains sterility to prevent contamination of the Martian subsurface with Earth organisms. The biobarrier is held in place by a series of latches that are released shortly after landing by a pyro-activated pin puller. Torsion springs at each end then rotate the ribs (right to left in the figure) to open the bag.

C TEAM X EXECUTIVE SUMMARY

Note: The Team X point design was early in the JPL Mars Life Explorer study. Some values listed in this Executive Summary differ from the values in the main body and other appendices of the final study report since the study matured. Differences are as expected for a planetary mission study. Where differences occur, the final report main body or other appendix values take precedence over the values listed here. This executive summary is included as further evidence that the concept study is New Frontiers class.

Mars Life Explorer

Customers: Brian Muirhead, Steve Matousek

Facilitator: Alfred Nash

Session Dates: 2-Mar-2021 – 4-Mar-2021 Mornings

Data Use Policy

- The information and data contained in this document does not include restricted information considered JPL/Caltech Proprietary, Proposal Sensitive, Third-party Proprietary, and Export Controlled. It may be made public as part of the Planetary Decadal survey
- The data contained in this document may not be modified in any way.
- Distribution of this document is constrained by the terms specified in the footer on each page of the report.

2

Study Participants

- Alfred Nash (Facilitator)
- William Jones-Wilson (ACS)
- Kevin Lo (ACS)
- Roger Klemm (CDS)
- Mariam Malek (CDS)
- Arby Argueta (CDS)
- Sherry Stukes (Cost)
- Alex Austin (Deputy Systems)
- Greg Welz (Ground Systems)
- Melora Larson (Instruments)
- Lemil Cordero (Mechanical)
- Reza Karimi (Mission Design)
- Laura Newlin (Planetary Protection)
- Ronald Hall (Power)
- Matthew Devost (Propulsion)
- William Smythe (Science)
- Mohammad Shahabuddin (Software)
- Jonathan Murphy (Systems)
- David Hansen (Telecom)
- Nick Emis (Thermal)
- Kevin Tan (Configuration)

Table of Contents

Executive Summary

Author: Alfred Nash
Email: Alfred.E.Nash@jpl.nasa.gov
Phone: (818) 458-0501

Executive Summary

Study Overview

- Goals
  - The purpose of the parent study is to obtain a detailed design, and more robust cost estimate, for a Mars Life Explorer mission to drill near-surface ice, at a detail level suitable for production of an independent cost estimate (ICE).
  - The goal of the study is to determine whether all of present Objectives A-D can go forward, including identification of potential descopes if the mission concept exceeds the NF cost cap of $1.1B (FY 25) phase B-D cost, without Launch vehicle (no launch vehicle nor phase E/F operations included in the $1.1B PI Managed Cost Cap (PIMCC)).
- Objectives
  - From customer supplied sample handling and instrumentation descriptions, as well as an industry supplied design approach,
    - Study team shall complete a design at the subsystem level and estimate the total mission cost.
    - Study team shall also recommend descopes if the mission concept exceeds the New Frontiers cost cap.

Executive Summary

Mission Architecture and Assumptions

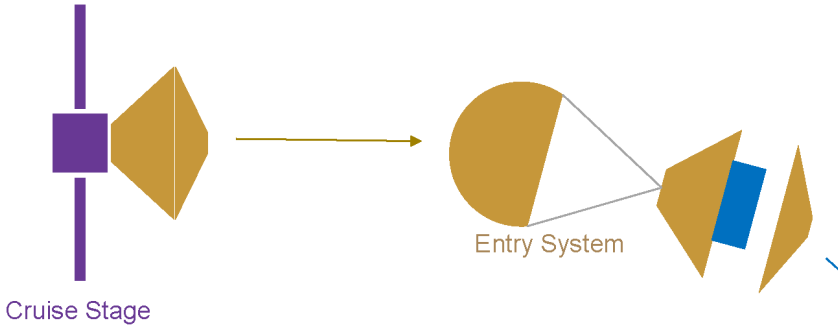

Mars Life Explorer uses an **InSight/Phoenix-like** architecture.

The primary **design** focus of this study was the **Lander flight element.**

The masses and costs of the **Cruise Stage** and **Entry System** were estimated at a flight element level (see Systems Report "Design Assumptions" slide for details).

7

Systems

Stack Summary

- The table below summarizes the launch stack and the elements in it
- Note that the Lander, Entry System, and Cruise Stage were sized such that they would have 30% Dry Mass Margin, calculated according to JPL Design Principles 8. There is additional un-allocated margin at the stack level (13% of the L/V capability). See Systems Report "Margin and Contingency Guidelines" for more.
- Note also that the Launch Vehicle capability below was already margined by the Mission Design chair (10% of the capability was held back)

Name	Dry Mass						Propellant	Wet Mass	Share of Launch
	CBE	Contingency	MEV	Allocation	JPL Margin	NASA Margin	Mass	Allocation	Allocation
	kg	%	kg	kg	%	%	kg	kg	%
Falcon Heavy Recoverable Capability								1819.8	100%
Additional Launch Vehicle Margin								234.8	13%
Cruise Stage + Entry System + Lander	999.0	19%	1192.1	1464.5	32%	23%	120.5	1585.0	87%
Cruise Stage	119.9	15%	138.2	171.5	30%	24%	0.0	171.5	9%
Entry System	429.3	16%	500.0	613.9	30%	23%	0.0	613.9	34%
Lander	449.7	23%	553.8	679.1	34%	23%	120.5	799.6	44%
Lander Payload	83.9	30%	109.1				0.0		
Lander Bus	365.8	22%	444.8				120.5		

CBE = "Current Best Estimate"
MEV = "Maximum Expected Value" = CBE * (1 + Contingency)

Dry Allocation = Wet Allocation – Propellant
JPL Margin = (Dry Allocation – CBE) / (Dry Allocation)
NASA Margin = (Dry Allocation – MEV) / (MEV)

"Share of Launch Allocation" is as fraction of "Falcon Heavy Recoverable Capability"

8

Executive Summary

Cost Findings

- The cost summary shown here is for the In-House Lander with 50% Phase A-D Reserves and 25% Phase E-F Reserves
- See the cost report for additional options

COST SUMMARY (FY2025 $M)	Generate ProPricer Input	CBE	Res.	PBE
Project Cost		$1024.4 M	36%	$1391.2 M
Launch Vehicle		$274.6 M	0%	$274.6 M
Project Cost (w/o LV)		$749.8 M	49%	$1116.6 M
Customer Specified Phase A		$5.0 M		$5.0 M
Development Cost Phases B-D		$716.3 M	50%	$1076.6 M
Phase B		$64.5 M	50%	$96.9 M
Phase C/D		$651.8 M	50%	$979.7 M
Operations Cost		$28.5 M	23%	$35.1 M

$1,081.6	Phases A-D
reserves (50%) added	
below	

9

Executive Summary

Conclusions, Risks, & Recommendations

- The mission concept closed well under the mass allocation, and under (but close to) the cost cap
- With regard to the flight system, there is nothing architecturally unique or risky about this mission (it is very similar to Phoenix and InSight)
  - The Entry System needs to be larger, which leads to some cost uncertainty but is certainly feasible (it is still much smaller than MSL/M2020)
  - A full assessment of the science payload, sampling system, and drilling system was outside the scope of this study (they were taken as pass-through designs from the customer)
- The mass of the lander was primarily driven by the mass of the payload
  - The power subsystem was driven by the need to keep the S/C warm *and* do a sample analysis. The "Sample Analysis Day" scenario was the highest-power one examined; even so, during that sizing sol, thermal power was the largest energy consumer (see Power report)

10

D SAMPLING SYSTEM

D.1 SAMPLING SYSTEM CONCEPT

The proposed sampling system is based on Honeybee Robotics The Regolith and Ice Drill for Exploration of New Terrains (TRIDENT), which is under development for deployment on two lunar missions, Volatiles Investigating Polar Exploration Rover (VIPER) and Polar Resources Ice Mining Experiment PRIME1 (Zacny et al. 2021). The rigid single-stem drill is stowed across the lander deck and is deployed using a 3 degree-of-freedom (DoF) deployment system (Technology Readiness Level [TRL] 4) as tested[1] for the previously proposed Icebreaker mission (Zacny et al. 2013). The TRIDENT drill enables sampling from 1-meter depth. The proposed drill will have a similar design to the TRIDENT drill but longer enabling sampling from a 2-meter depth. The lander deck width, which the drill is stowed across, limits the maximum drill length and thus drilling depth.

The MLE sampling system consists of five major subsystems: (1) 2 m drill with instrumented auger, (2) 3-DoF deployment boom, (3) pneumatic transfer system, (4) sample carousel, and (5) biobarrier. These subsystems are shown in their stowed and deployed configurations in Figure D-1. The 3 DoF arm has been scaled up to accommodate larger and heavier drill. The subsystems work together to collect, transfer, and deliver samples to instruments in addition to making in-situ measurements. Each subsystem is described in detail in the following sections (the carousel is described in the main body).

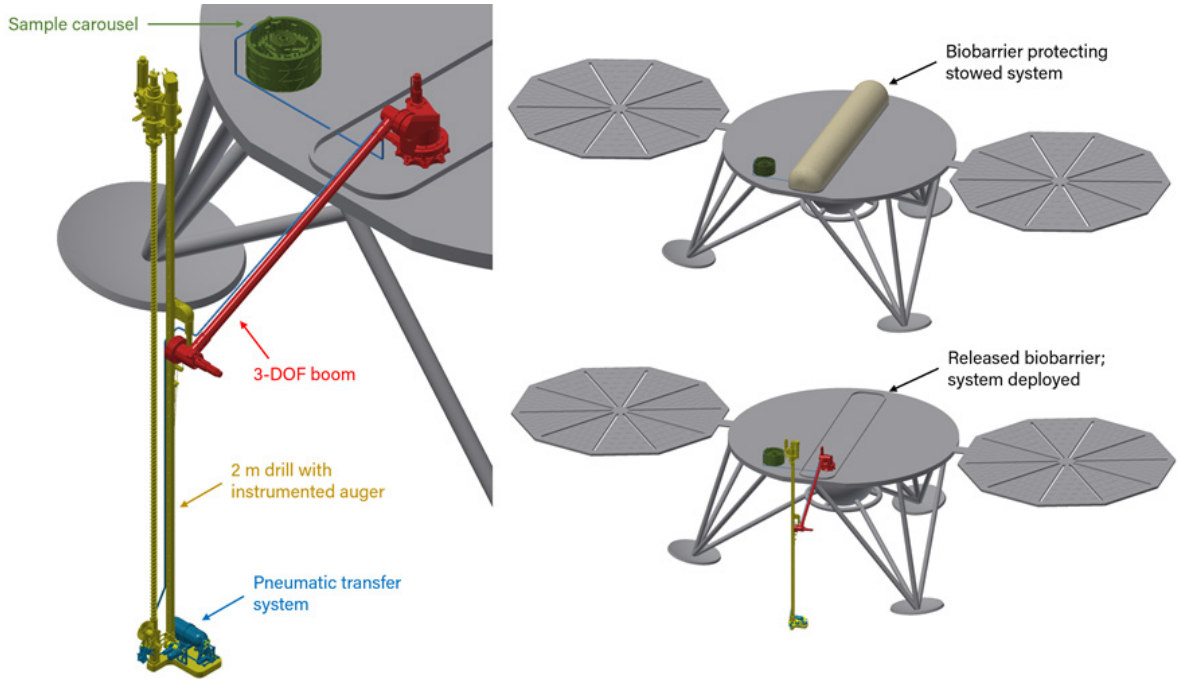

Figure D-1. Sampling system concept. A 2-meter drill is deployed using a 3-DoF robotic arm. Drill cuttings are trapped in auger flutes and selectively diverted into a sample chamber at the surface. A pneumatic transfer system carries samples from the chamber to a sample carousel on the lander. Some instruments are integrated with the sample carousel, others are integrated directly with the drill auger so that measurements can be taken at depth.

During cruise to Mars, the drill is stowed in a biobarrier across the lander deck, similar to the approach used in the Mars Phoenix mission and depicted in Figure D-2. After landing, the biobarrier opens and the drill is deployed to the surface using a 3-DoF deployment arm. The arm allows for deploying the drill across an arc on the surface and with pitch orientation control to improve alignment with the surface normal for drilling.

[1] The drill was deployed using the 3-DoF arm in the laboratory environment as well as in the Mars chamber with limited motion due to size of the chamber.

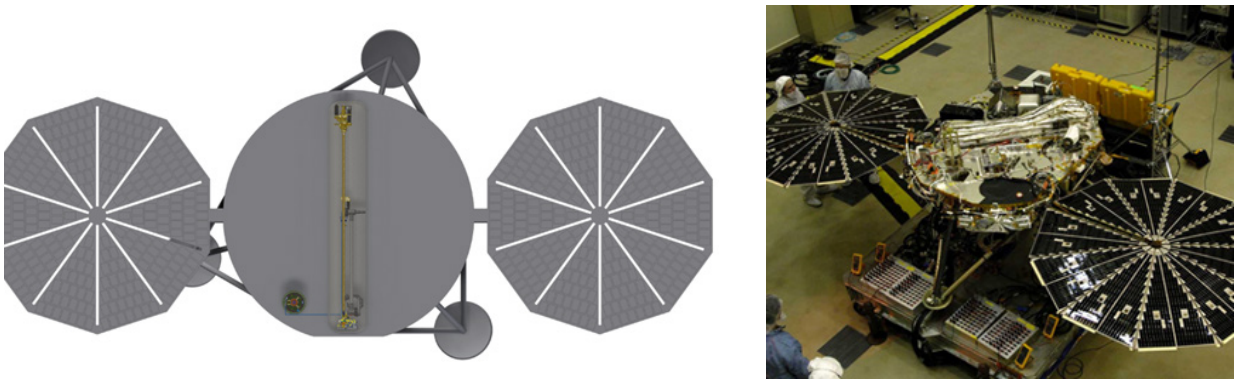

Figure D-2. Biobarrier stowed across a representative lander deck (left), and example of Mars Phoenix robotic arm stowed across lander deck (right).

D.2 THE TWO-METER MLE DRILL AND INSTRUMENTED AUGER

D.2.1 DRILL SUBSYSTEM AND METHOD

The MLE drill is rotary-percussive, which enables it to cut into icy material as hard as rock. This system is shown in Figure D-3, and is comprised of a rotary percussive drill head, a drill feed linear stage along which the drill head travels, a drill string outfitted with sensors for drilling and sampling, and a brushing station for passively delivering material into the pneumatic transfer system. The pneumatic transfer system, located on the drill's footpad, is discussed in detail in Section D.2.4. The drill head provides a percussive energy set to ~2.5 J/blow with a maximum frequency of ~1000 blows per minute. The rotation speed is 120 revolutions per minute and the stall torque is 16 N-m. The mass of the drill system is 43 kg, including 7 kg harness and avionics. The stowed drill packaging dimensions are 271 cm × 21 cm × 31 cm. The biobarrier needs to be designed to fit these dimensions.

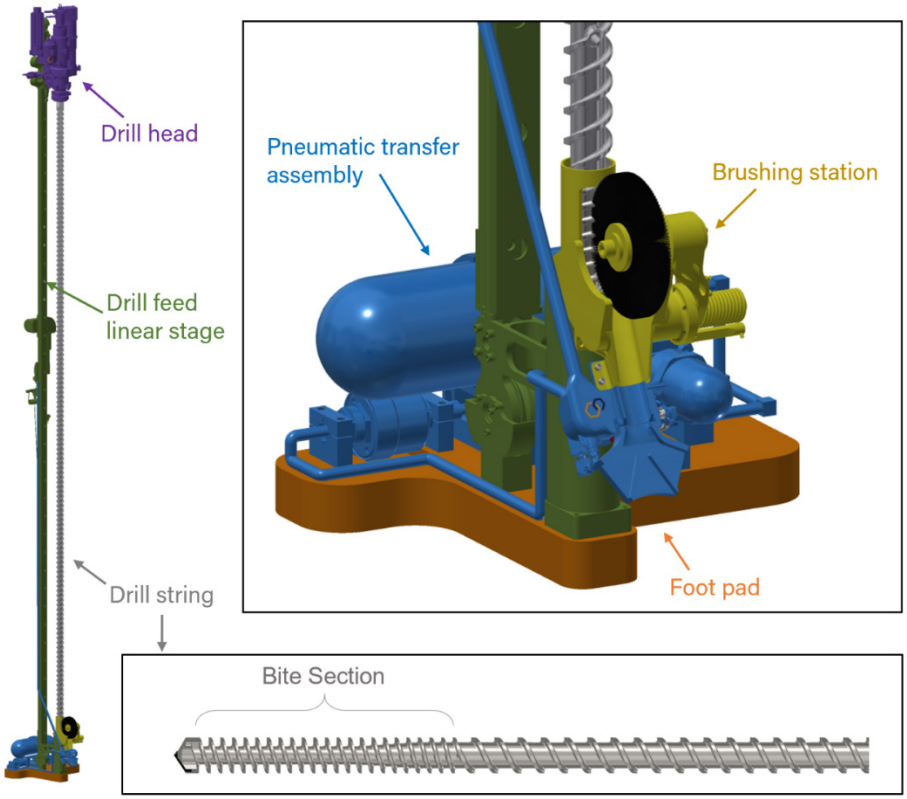

Figure D-3. 2-meter MLE drill subsystems. The sampling auger is pictured at the bottom.

To reduce thermal risks, risk of getting stuck, drilling power, and to provide stratigraphic information, the drill captures samples in so-called 20 cm "bites" (Figure D-4). That is, the system drills a depth of 20 cm at a time, and the drill is retracted after each additional 20 cm bite. The cuttings from each bite are retained in the auger flutes. For this reason, the auger is split into two sections (Figures D-3 and D-4). The lower section has flutes designed for sample retention: the flutes are deep and have low pitch. The upper section is designed for efficient conveyance of material to the surface: the flutes are shallow, and the pitch is steep. This combination allows efficient sampling but inefficient conveyance—the drill should not be used to drill to 2 m depth in a single run as this will lead to increased drilling power and, ultimately, heating of the target material.

Material retained in the flutes is removed using the brushing station. During the ascent of the drill, the auger is turned slowly, which causes the brush to passively rotate such that it directs the captured cuttings down a chute. This chute will nominally allow cuttings to accumulate at the base of the footpad, or it may direct cuttings to the pneumatic transfer system as discussed in Section D.2.4. The auger can be optionally passed through the brushing station multiple times as a method of minimizing cross-contamination. This process is illustrated in Figure D-4.

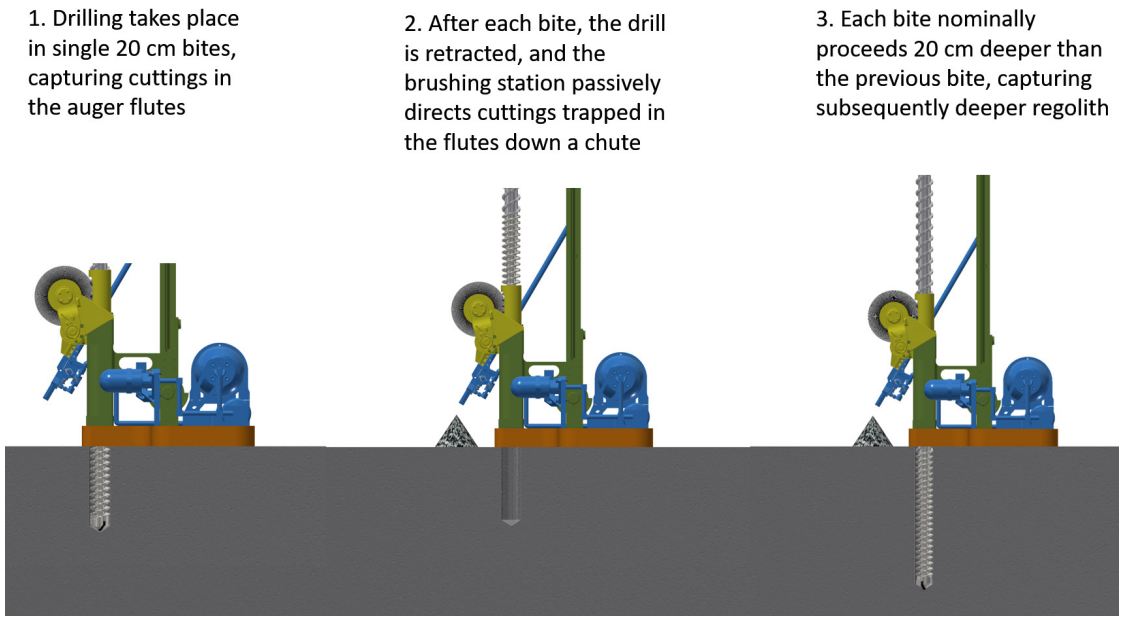

Figure D-4. Illustration of bite sampling approach.

D.2.2 INSTRUMENTED AUGER

In addition to serving as a sampling tool, the MLE drill is also an instrument. It has an internal channel that allows for a variety of instruments to be located inside and wired through the auger. These include two resistance temperature detectors (RTDs): one is located inside the drill bit, and the other is co-located with a 40 W heater approximately 5 cm above the bit. These sensors measure downhole temperature and thermal conductivity, and thus can provide thermal gradient and heat flow measurements.

A sapphire window for in-situ imaging is located 30 cm above the bit and integrated into the auger flutes to avoid interrupting the flow of cuttings. Another sapphire window is located directly in the drill bit, opposite one of the RTDs. This setup can support many types of imagers, including a Laser Induced Breakdown Spectrometer (LIBS), neutron spectrometer, near-infrared spectrometer, or a visible imager (Zacny et al. 2016). A laser or LED component may be co-located with the imager to illuminate sample in-situ. Harnessing for these is accommodated using a fiber optic rotary joint (FORJ), which allows the bulk of the instrumentation to be accommodated outside the auger. Finally, integrated and recessed into the bit itself is a dielectric spectroscopy probe (DSP). It is worth

noting that the auger serves as a flexible platform and could accommodate other or additional in-situ instruments as well. The existing instrumentation is pictured in Figure D-5.

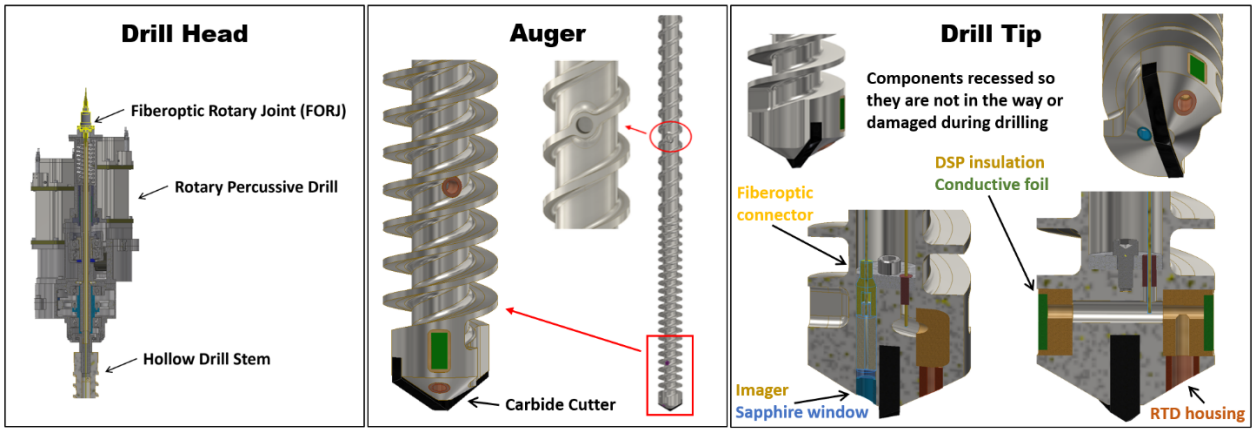

Figure D-5. Auger-integrated instrumentation.

In addition to this active instrumentation, various attributes of the sampling system can provide information about the sample and sampling environment as well. During drilling, the power and penetration rate are used to determine regolith strength. The drill can also provide bearing capacity of the top surface from measuring the sinkage of its footpad into the surface, as well as angle of repose from measuring the angle of the cuttings pile. The 20 cm bite method of drilling also enables more accurate measurement of subsurface temperature and material strength. Every time the drill is lowered into the borehole, it will be pre-loaded onto the bottom of the borehole and cold soaked without drilling (i.e., no heat input). This cold soaking with be used to extrapolate the subsurface temperature. In addition, when the drilling starts, the drilling power will be initially attributed to penetrating/breaking the icy-formation. As the drill continues drilling deeper, the power starts increasing due to the cuttings removal (i.e., auger) contribution to the total power budget (the drill can only measure the total drilling power—contribution of drilling and cuttings removal). As such knowing the initial drilling power and the power once the drill has penetrated 10 cm will allow determination of the auger-contribution to the total power budget.

It should be noted that some fall back material is possible if the borehole is unstable. If indeed there is fallback material being accumulated at the bottom of the hole, the drill can perform several 'cleaning' runs to remove that material until the borehole becomes stable.

D.2.3 3-DOF DEPLOYMENT BOOM

The drill is mounted on a 3-DoF boom that serves to deploy and position the sampling system for surface operations. As compared to a Z-stage deployment, the 3-DoF boom can accommodate a larger variety of terrain angles and is thus well suited to a lander application.

Figure D-6 shows the 1-meter Icebreaker drill being deployed from a TRL 5 3-DoF boom. The system has been tested in a number of configurations, including kinematic positions that are suitable for dropping a sample off with a drill bit. The system has also been tested in a Mars chamber with a limited range of motion due to the small size of the chamber (1 m × 1 m × 3.5 m).

The drill does not need to be vertical for its operation—it can be placed at any angle; this significantly increased the area where the drill can be placed. In addition, ice-rich area at the sites such as Mars Phoenix, is relatively rock free and flat—ideal for drill placement. If surface area variability is of concern, the auger tube can be extended below the footpad; in turn the auger tube would engage with the surface as opposed to the footpad reducing the overall footprint (Figure D-7).

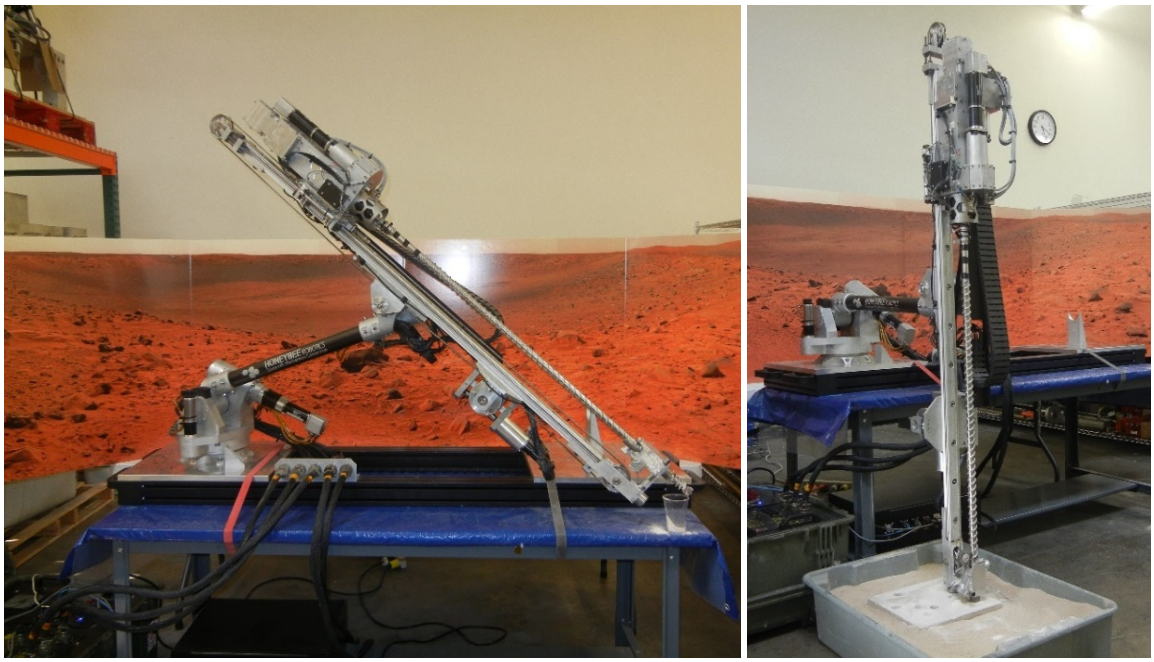

Figure D-6. Icebreaker drill prototype has been deployed using a 3-DoF boom (Zacny et al. 2013).

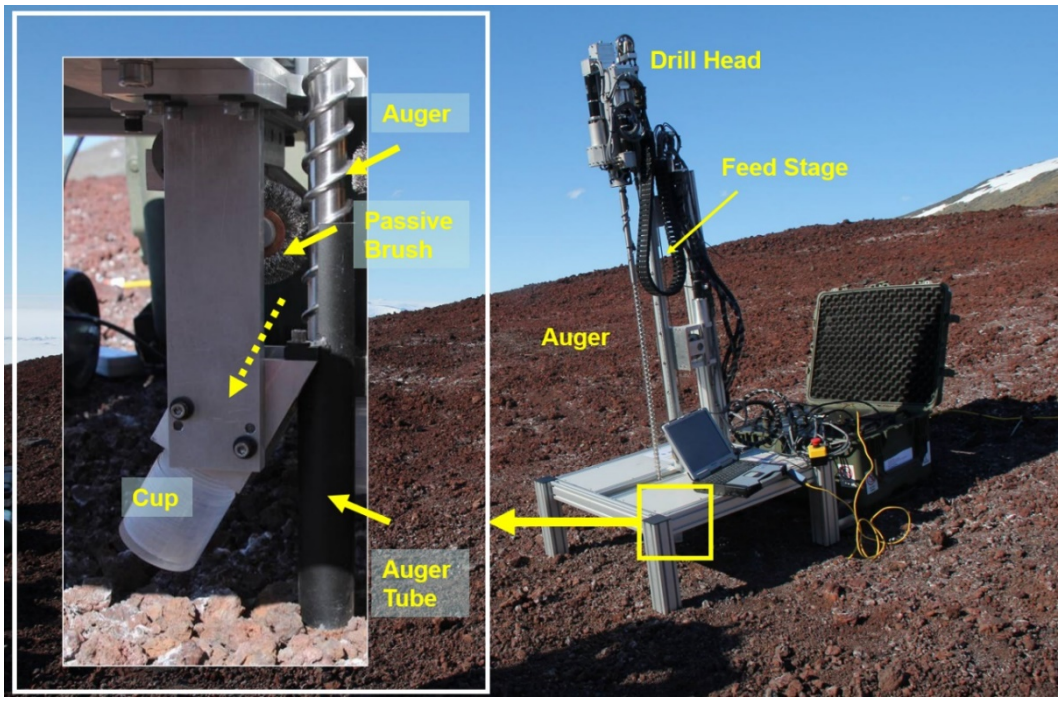

Figure D-7. Icebreaker undergoing tested outside of McMurdo station. Note the drill is preloaded using the auger tube to minimize the footprint.

D.2.4 PNEUMATIC TRANSFER

The pneumatic transfer system is located on the footpad of the drill subsystem. It is comprised of a sample chamber with an actuated trap door, a gas supply assembly, and tubing for sample transfer. The system operates by filling the sample chamber using the trapdoor mechanism and a ~50 psi puff of gas to transport sample through the transfer tubes and to the sample carousel. The major components of the subassembly are shown in Figure D-8.

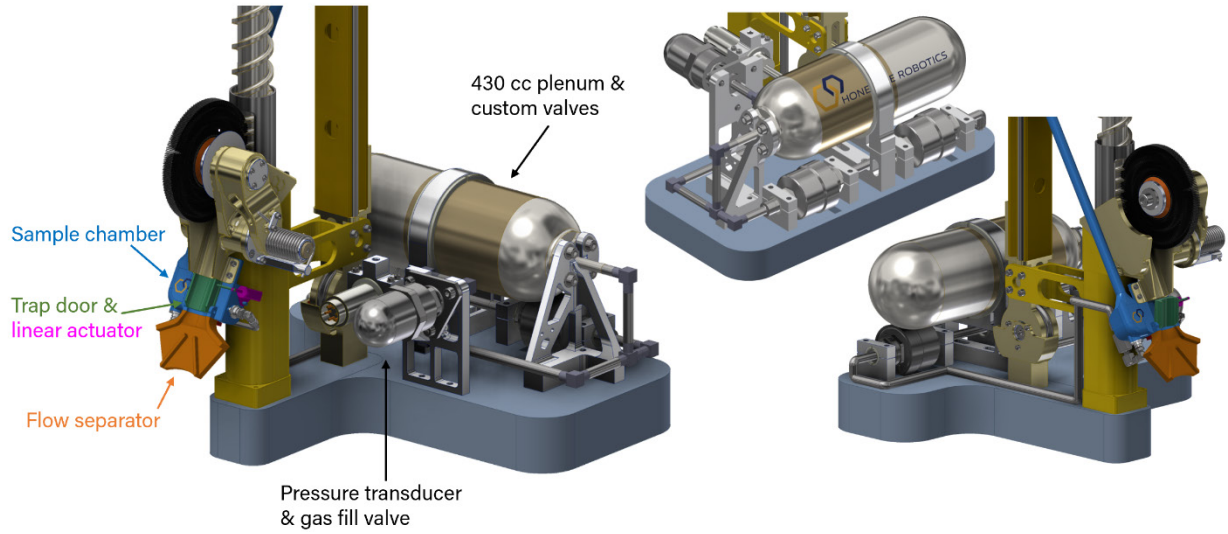

Figure D-8. Left: Labeled major components of pneumatic transfer assembly. Right: Isometric views of the back and other side of assembly.

The sample chamber has a notional internal volume of ~20 cc (this can be adjusted based filling and sample delivery efficiencies) and is mounted directly to the chute on the brushing station. It contains a section of chute that can be opened using a linear actuator (the "trap door") allowing cuttings to enter the sample chamber rather than collecting at the base of the drill. For cuttings that are not selected for sampling, a flow separator divides the stream to ensure that the cuttings pile does not overwhelm the base of the drill. Figure D-9 shows the system with the trapdoor open and closed. Note that this trap door does not need to provide a leak-tight seal when closed in order to have successful pneumatic transfer. Figure D-10 shows the prototype pneumatic system being tested in a lab and Mars chamber.

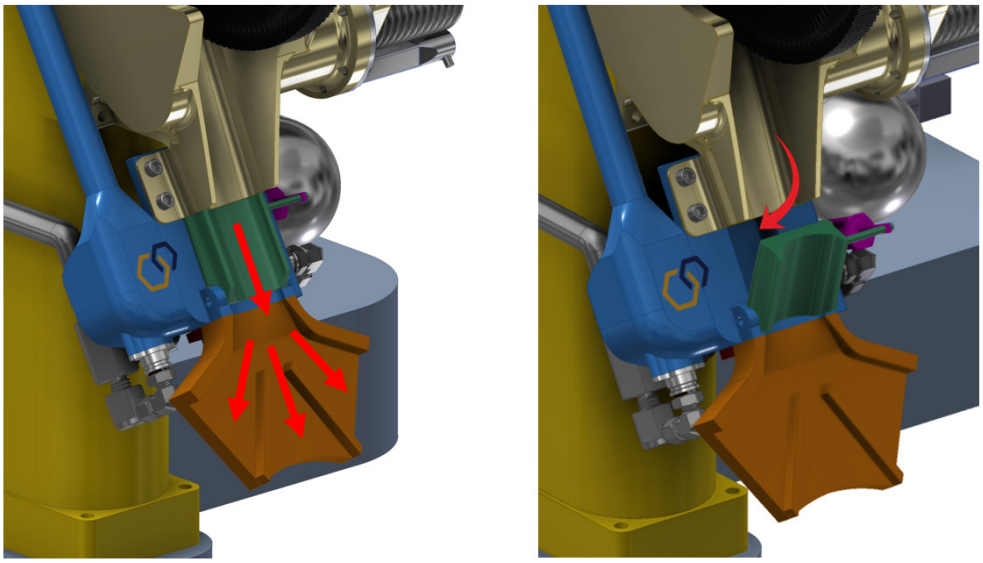

Figure D-9. Left: Trap door closed; cuttings pile will accumulate at the base of the drill with cuttings directed by the flow separator, as shown by red lines. Right: Trap door open; cuttings fall into the sample chamber.

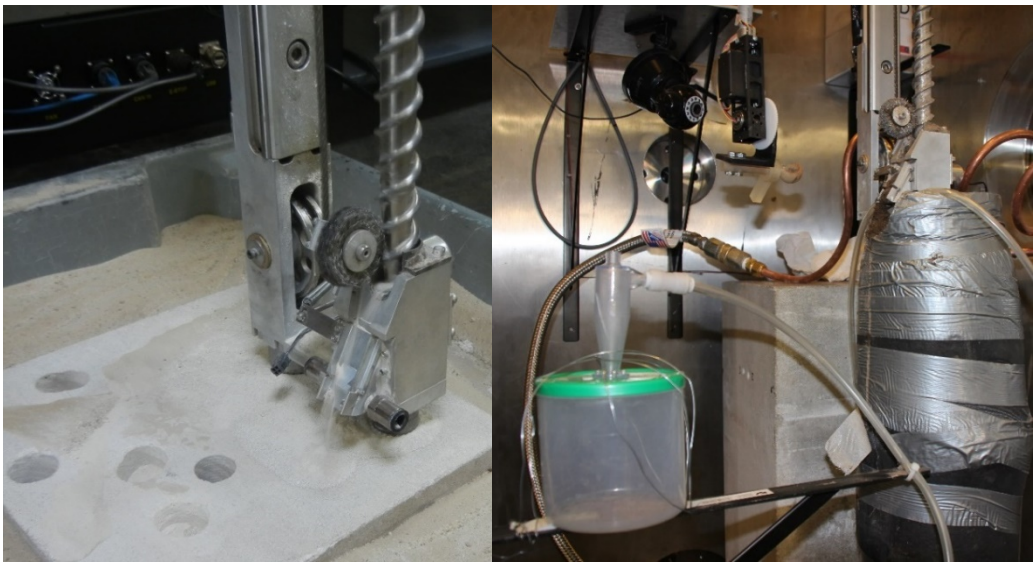

Figure D-10. Pneumatic system undergoing testing at 1 ATM (left) and in March chamber (right).

The gas supply assembly draws from Honeybee Robotics experience with the JAXA Mars Moon eXploration mission. It satisfies stringent planetary protection requirements by utilizing custom valves without greases or contaminant elements such as Molybdenum. In addition to these valves, the assembly contains a 430 cc gas plenum, a pressure transducer, and a gas fill valve. This assembly is kept cold throughout the mission to reduce thermal alteration of the sample during pneumatic transfer. The gas lines from the supply system are connected to strategically directed entrances in the sample chamber. These allow the gas to readily transport the sample through the transfer tubes and to the sample chamber via the path illustrated in Figure D-11.

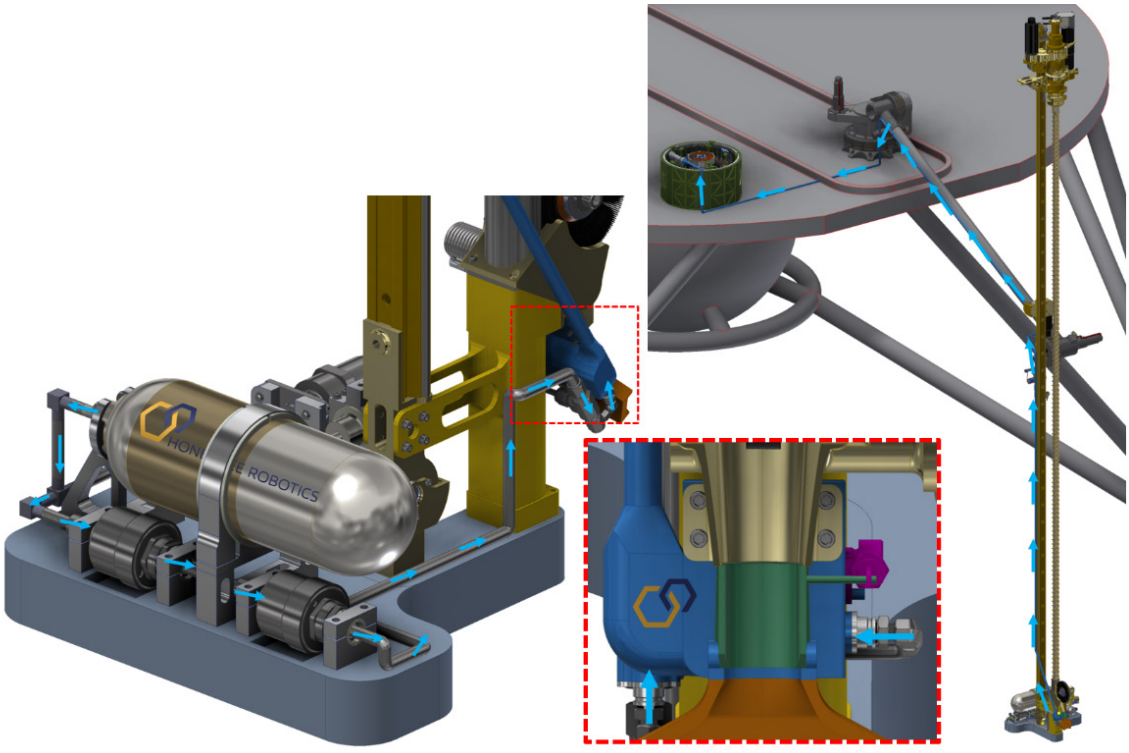

Figure D-11. Left: Path taken for gas to travel from plenum to sample chamber. Center: Strategically directed gas inlets to sample chamber. Right: Path gas and sample take to reach sample carousel.

The gas supply assembly is placed at the drill's footpad to avoid having to implement rotary-joints if such a system was placed on the lander. However, sample transfer tubes will need to cross several rotary-joints in order for the sample to be delivered from the sample chamber to the carousel. There exist several options for a flexible transfer tube such as metallic bellows and swivels. The Dragonfly mission, for example, is implementing Teflon tube for the pneumatic sample transfer system, and PlanetVac is using a rotary elbow for the 19D lunar mission.

D.2.5 BIOBARRIER

A biobarrier similar in style to the one used on the Phoenix lander (Figure D-12) has been selected for planetary protection on this mission. The biobarrier will enclose the 3-DoF arm and entire drilling and pneumatic systems. When the system is ready for use, the biobarrier will release to allow the 3-DoF arm to deploy the MLE sampling system. Figure D-13 shows the sampling system first stowed in a conceptual biobarrier, and then when the biobarrier is released and the sampling system is deployed.

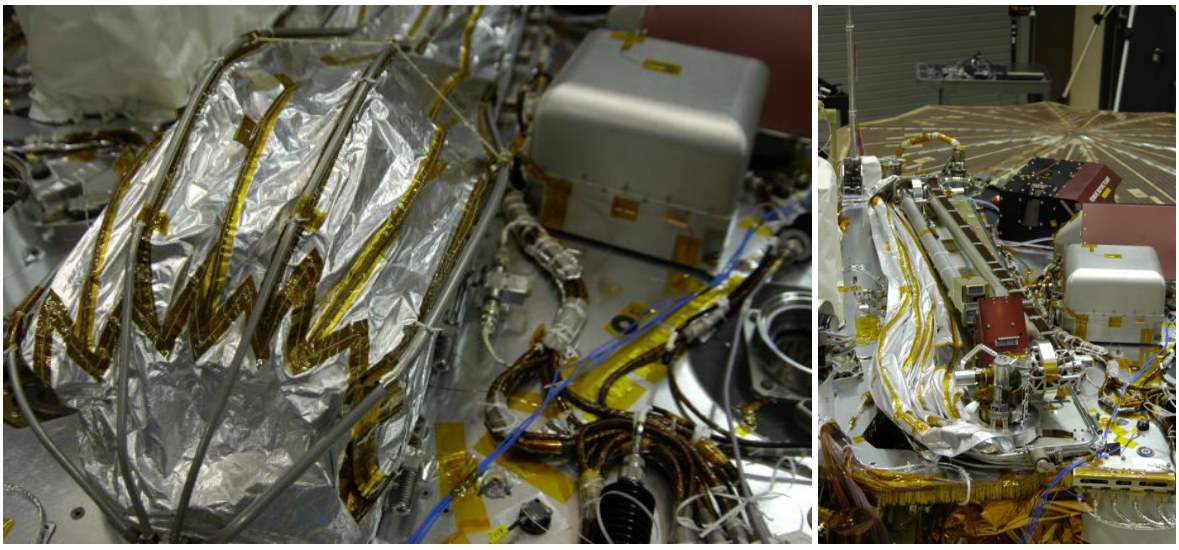

Figure D-12. Left: Mars Phoenix biobarrier in stowed position. Right: Biobarrier released to expose robotic arm.

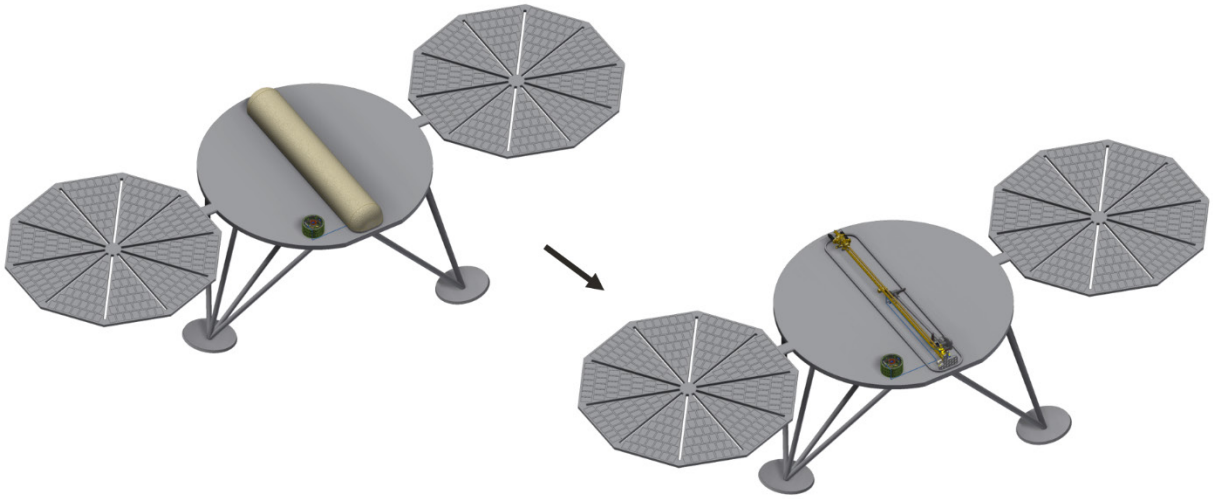

Figure D-13. Left: Biobarrier with sampling system stowed for flight. Right: Biobarrier released immediately prior to sampling system deployment.

D.3 CONCEPT OF OPERATIONS

There are five main steps in the deployment and operation of the MLE sampling system. First, the biobarrier is released. Second, the sampling system is deployed using the 3-DoF boom. During this time, the drill temperature is monitored to better understand the sampling environment. Third, the drilling operations take place. As noted previously, drilling operations take place in ~20 cm bites, which has many advantages including maintaining the integrity of the subsurface strategraphy. The drill is retracted after each bite, and sample is removed from the auger flutes using a passively rotating brush. Fourth, when desired, a trap door on the pneumatic transfer subsystem will open to capture sample inside a sample chamber. When sampling is complete, the trap door is returned to its original position. In preparation for the next and final step, an individual sample cup is raised to the funnel at the base of the diverter. Last is pneumatic transfer, during which strategically directed puffs of gas from a ~50 psi plenum transport the captured sample from the chamber to the carousel on the lander. Gas and sample flow through the diverter, which directs some sample into the raised sample cup, and the overflow is routed outside the lander. This process is summarized in Figure D-14.

The sample delivery system would need to be tested and validated with a range of simulants to identify locations prone to clogging and potential level of cross contamination (this study, for example, is currently being done for Dragonfly, which has a pneumatic sample transfer system). The study should also include determination of how many 'cleaning' puffs would be needed (if any) to clean the sample chamber and sample transfer lines.

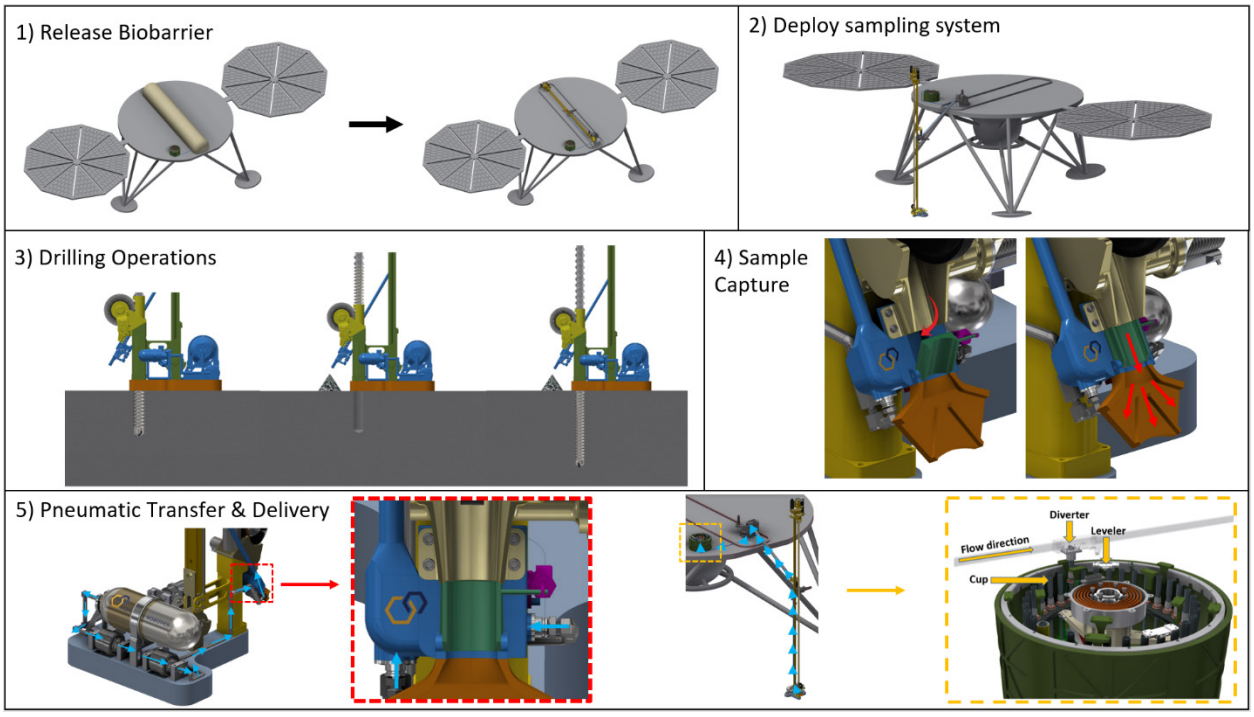

Figure D-14. Visual summary of MLE sampling system concept of operations.

D.4 SAMPLING SYSTEM HERITAGE

The sampling system concept is based on designs for the Honeybee Robotics TRIDENT drill, which is under development for deployment on the VIPER and PRIME1 lunar missions (Zacny et al. 2021) and the drill system from the previously proposed Icebreaker mission as shown in Figure D-15 (Zacny et al. 2013). The TRIDENT drill would be used to cut into cryogenic lunar ice and regolith. The Icebreaker drill was proposed to drill in the Mars northern polar regions. The concept has been validated in various laboratory setting tests and field campaigns.

The Icebreaker, PRIME1, and VIPER missions all have 1-meter drill systems with single rigid drill stems that operate similarly to the proposed drill, but the proposed drill would have a longer single rigid drill stem to enable sample acquisition to a depth of 2 meters. The drills of the PRIME1 and VIPER system would be mounted vertically whereas the Icebreaker drill design was stowed across the lander deck and deployed with a 3-DoF arm as for the proposed sampling system.

TRIDENT has undergone several end-to-end tests at NASA Glenn Research Center and in the Honeybee Robotics Mars chamber (Figure D-16). These tests were done using various simulants with varying water-ice and perchloate concentrations (Mars Mojave Simulant (Peters et al. 2008)) with a large fraction of small pebble-sized rocks, which was saturated with water containing 1–2% perchlorate salt and frozen to −200°C; Mars Mojave Simulant regolith saturated with water and frozen to −20°C; Ice at −20°C; Ice with 1–2% perchlorate at −20°C). In addition, the Icebreaker drill has undergone field tests in the Arctic, Atacama, and Antarctica (Zacny et al. 2011; Zacny et al. 2013).

a) Icebreaker b) PRIME1 2022 c) VIPER 2023

Figure D-15. Mission concepts whose drills the sampling system is based upon: a) previously proposed Mars Icebreaker mission, and TRIDENT drill of the b) 2022 lunar PRIME1 mission and c) 2023 lunar VIPER mission.

Figure D-16. Left: TRIDENT drill undergoing TVAC tests at NASA GRC. Center: Icebreaker drill in Mars chamber. Right: Icebreaker drill undergoing testing in Antarctic Dry Valleys.

E ENTRY, DESCENT, AND LANDING PERFORMANCE ANALYSIS

Six arrival opportunities were considered, comprised of the open and close for three different launch period/solar longitude combinations: 2037 @ Ls = 22 deg, 2039 @ Ls = 75 deg, and 2039 @ Ls = 90 deg. Hypersonic entry, descent, and landing (EDL) metrics are typically driven by entry velocity, so analysis was focused around the state where entry velocity was highest—the close of the launch period for the 2037 launch opportunity, as shown in Figure E-1.

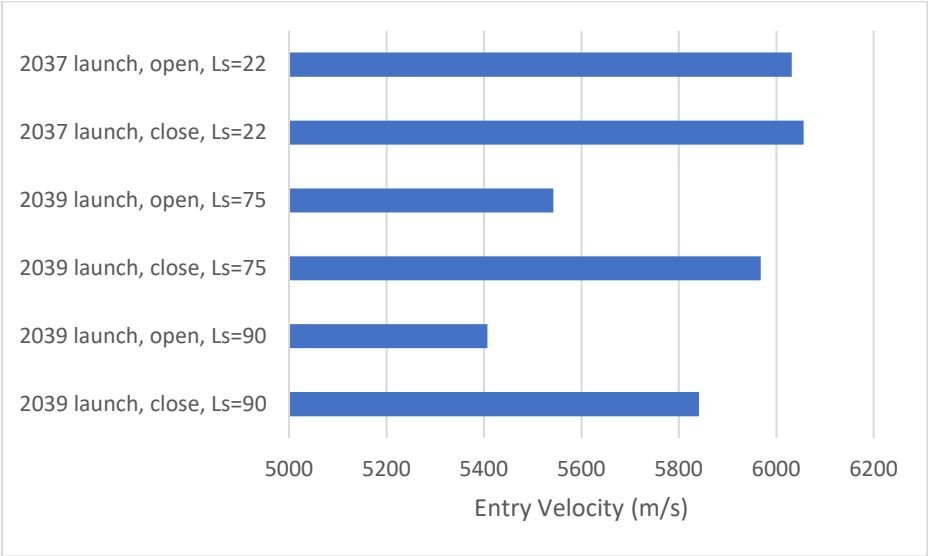

Figure E-1. Variation of arrival conditions.

Entry states corresponding to a sweep of entry flight path angles (EFPAs) were run for each arrival epoch to evaluate EDL performance. Runs were made for both current best estimate (CBE) and maximum possible value (MPV) spacecraft masses, however, only results for the MPV scenario are shown here, since they are more conservative. Through this sweep, we see that at an EFPA of −10.5 deg, the trajectory begins to exhibit signs that skipout is imminent, as shown by the flattening of altitude in Figure E-2.

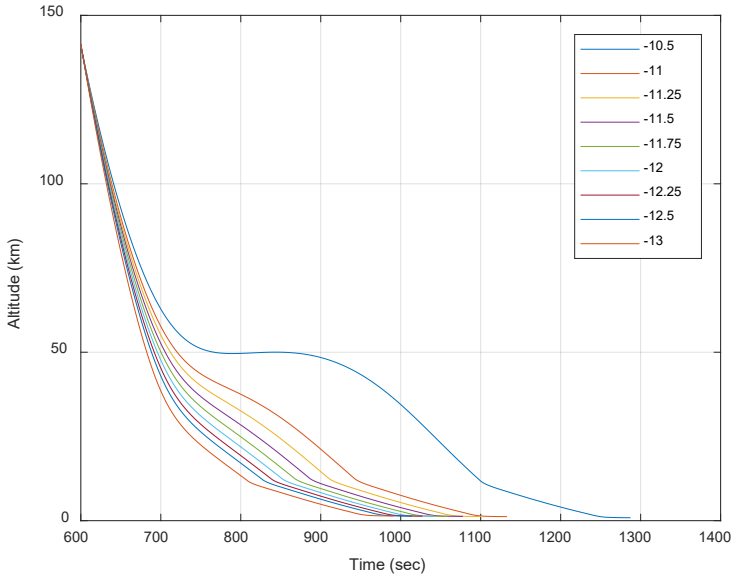

Figure E-2. Entry flight angles.

It is customary to carry at least 1 deg of EFPA margin from the point where altitude inflection is first seen, thus it would be expected to choose an EFPA of no shallower than −11.5 deg. With this constraint, we continue to look at hypersonic and parachute deploy performance to select a nominal design EFPA. All other things being equal, we would attempt to maximize parachute deploy altitude to maintain a healthy parachute descent timeline margin. Across the range of EFPA's considered, the maximum chute deploy altitude is seen at −11.25 deg (Figure E-3); however, since that value violates our skipout constraint, we would select −11.5 deg as our design value, subject to other EDL metrics being acceptable.

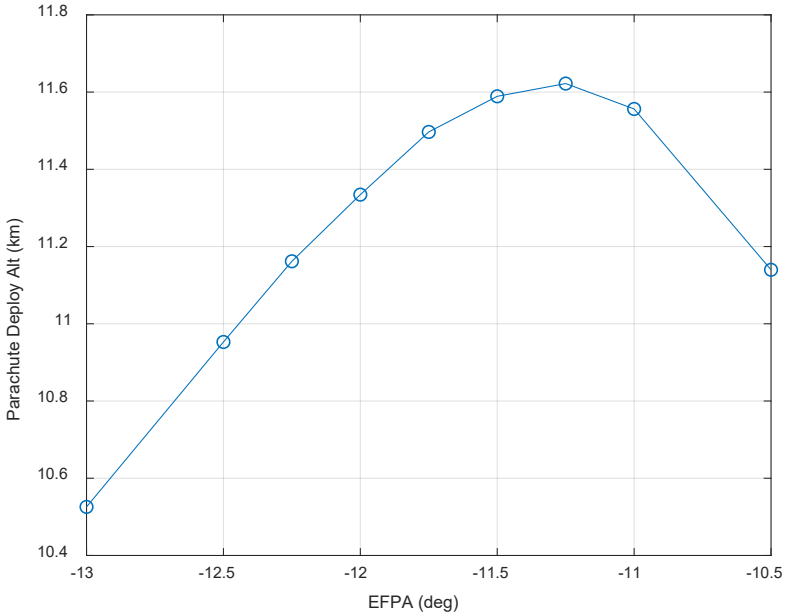

Figure E-3. Entry flight angles vs. parachute deploy altitude.

Although the selection of a 3.65 m diameter aeroshell is required to accommodate the payload, it also allows the entry ballistic coefficient to remain the same, or even lower than what was obtained on NSY. Furthermore, since the radius of the heatshield nose is proportional to the diameter of the heatshield, and convective aeroheating has an inverse relationship with nose radius, peak convective heating rates are actually lower than estimated on NSY, despite entry velocities being as high as seen on NSY.

Parachute deployment is targeted to Mach 1.7 (nominal), which leads to dynamic pressures in-family with those used during NSY design and flight. Deploy altitude is also very comparable to NSY at 11.6 km. By selecting a 1:1 scale of a Viking DGB, we are able to maintain the ballistic coefficient during parachute descent at a level comparable to that on NSY, resulting in similar terminal velocities.

By adding 3× MR-104 engines, we are able to maintain a similar lander thrust-to-weight, keeping terminal descent within a similar range of altitudes and velocities as NSY/PHX. The heavier lander does result in increased terminal descent fuel usage—now ~72 kg. This, plus a conservative assumption for cruise usage is accommodated by the larger propellant capacity provided in the lander design.

A Monte Carlo analysis was not performed, so a statistical landed footprint is not available, but an estimate was made using steep and shallow entries. The steep case, −11.75 deg EFPA, coupled with 1-sigma high density, and 3-sigma high drag, provides the heel, while the shallow case, −11.25 deg EFPA, using 1-sigma low density and 3-sigma low drag, serves as the toe of the range estimate. This results in an estimated footprint length of 207 km. A similar approach of combining EFPA, drag,

and density is used on other landers to develop bounding trajectories for aerothermal analysis, so it was felt that it would apply reasonably to a footprint assessment as well. Taking this approach with NSY resulted in estimates that bounded the 3-sigma ellipse predicted by the Monte Carlo.

A comparison of the key EDL metrics is shown in Table E-1. Note that statistical data is provided for NSY, but only nominal data was generated for MLE. Also note that a landing site elevation of -3.0 km w.r.t MOLA was assumed for all MLE cases.

Table E-1. EDL metrics comparison vs. EFPA.

EFPA	E_Vel	Max-G	Max-Qdot	Int_Ht	Cht_Alt	Cht_Q	Cht_M	Sep_Alt	Sep_Vel	Fuel_Rem
−10.50°	6056.5 m/s	2.77 G	32.4 W/cm^2	4497.9 J/cm^2	11140 m	572 Pa	1.70	1126 m	56.5 m/s	5.88 kg
−11.00°	6056.4 m/s	4.39 G	37.4 W/cm^2	3625.9 J/cm^2	11556 m	534 Pa	1.70	1163 m	57.6 m/s	5.09 kg
−11.25°	6056.4 m/s	5.13 G	39.6 W/cm^2	3416.2 J/cm^2	11622 m	530 Pa	1.71	1162 m	57.8 m/s	4.81 kg
−11.50°	6056.3 m/s	5.82 G	41.5 W/cm^2	3256.8 J/cm^2	11589 m	530 Pa	1.71	1170 m	57.9 m/s	4.96 kg
−11.75°	6056.3 m/s	6.48 G	43.2 W/cm^2	3127.8 J/cm^2	11497 m	534 Pa	1.71	1141 m	57.9 m/s	5.26 kg
−12.00°	6056.2 m/s	7.10 G	44.7 W/cm^2	3019.9 J/cm^2	11334 m	539 Pa	1.70	1148 m	58.0 m/s	5.03 kg
−12.25°	6056.2 m/s	7.67 G	46.2 W/cm^2	2927.2 J/cm^2	11162 m	547 Pa	1.70	1146 m	58.0 m/s	5.25 kg
−12.50°	6056.1 m/s	8.23 G	47.6 W/cm^2	2846.2 J/cm^2	10953 m	555 Pa	1.70	1151 m	58.1 m/s	5.07 kg
−13.00°	6056.1 m/s	9.29 G	50.1 W/cm^2	2709.6 J/cm^2	10526 m	575 Pa	1.70	1152 m	58.2 m/s	4.82 kg

Comparing vehicle characteristics (mass, ballistic coefficient, thrust-to-weight; Table E-2) and EDL metrics (Table E-3) against past Mars landers with similar designs shows that the MLE design compares very favorably.

Table E-2. EDL vehicle characteristics.

	Unit	Values	PHX	InSight	MLE
Max Wet Entry Mass	kg	CBE/MEV/MPV	572.2/(NA)/606	606/(NA)/625	952/(NA)/1209
Entry Ballistic Coefficient		min/max	62/67	67/69	55/70
On-chute Ballistic Coefficient		min/max	7.4/7.9	7.6/8.1	6.6/8.4
Max Wet Lander Mass	kg	CBE/MEV/MPV	362.6/426	366/(NA)/435	645
Lander Thrust/Weight		min/max	2.0/2.4	2.3/2.4	2.0/2.5

Table E-3. EDL metrics.

	Unit	Values	PHX	InSight	MLE
Ventry (125 km alt)	km/s	metric	5.6	6	6.06
EFPA	deg	metric	-13	-12	-11.5
Peak Heating Rate	W/cm^2	nompredict/req	46/80	45.8/84	42/TBD
Integrated Heating	J/cm^2	nompredict/req	2405.8/4150	2693/3497	3257/TBD
Peak Deceleration	g's	nompredict/req	8.2/15	7.6/13	7.3/TBD
Chute Deploy Mach		req/nompredict/req	1.4/1.36/1.68/1.89/2.1	1.1/1.69/ 2.1	1.1/1.7/2.1
Chute Deploy Q	Pa	req/nompredict/req	300/489/540	300/525/650	TBD/530/TBD
Time on Chute	Sec	nompredict	172	135	140
Lander Sep Alt	m	metric	930	1128	1170
Lander Sep Velocity	m/s	metric	57	61	58
Touchdown Vvert	m/s	req/nompredict/req	1.4/2.4/3.4	1.4/2.4/3.4	1.4/2.4/3.4
Touchdown Vhorz	m/s	nompredict/req	0.1/1.4	0.0/1.4	0/1.4
SemiMajor Axis	km	99%	101.6	116.4	207
SemiMinor Axis	km	99%	21.5	25.5	(NA)

F COST MODEL ANALYSES

F.1 STUDY PHASE E POINT ESTIMATE

The InSight mission planned operations cost at launch (reported in the Launch CADRe; Table F-1) was used to derive the MLE study point cost estimate for Phase E–F operations. The costs were first escalated to FY25$ using the NASA Inflation Index. Burn rates were calculated based on the InSight operations schedule.

The InSight FY18 burn rate was chosen to calculate the MLE cruise cost (Table F-2). The InSight mission launched May 2018 (Phase E start was 30 days after launch, June 2018). The InSight FY19 burn rate was chosen to represent the first 4 months of MLE surface operations in which both drilling/analysis and meteorology would occur. The remaining 21 months of MLE operations consist of only meteorology (and 1 month of closeout) and was therefore estimated using the InSight FY20 burn rate.

Table F-1. InSight planned Phase E cost.

InSight Planned Phase E (Source: Launch CADRe)	FY12	FY13	FY14	FY15	FY16	FY17	FY18	FY19	FY20	FY21	Total
RY$K	$0	$0	$0	$0	$0	$0	$17,957	$47,354	$13,558	$2,042	$80,910
NASA Inflation to FY25	1.286	1.267	1.242	1.218	1.201	1.179	1.151	1.128	1.105	1.091	
FY25$K	$0	$0	$0	$0	$0	$0	$20,674	$53,413	$14,987	$2,228	$91,302

Table F-2. InSight-derived Phase E burn rate applied to MLE study estimate.

Insight				MLE		
FY	FY25$M	Months per FY	Burn Rate ($M/month)	Representative Phase	Months per Phase	Estimate FY25$M
FY18	$20.7	4 (June 2018–Sept 2018)	$5.17	Cruise	10	$51.7
FY19	$53.4	12 (Oct 2018–Sept 2019)	$4.45	Drilling/Analysis/Meteorology	4	$17.8
FY20	$15.0	12 (Oct 2019–Sept 2020)	$1.25	Meteorology/Closeout	21	$26.2
					Subtotal	**$95.7**
					25% Reserves	**$23.9**
					Total	**$119.6**

F.2 ANALOGIES

F.2.1 PHOENIX RA/BB

The study team analyzed robotic arm assemblies as seen in Phoenix (Robotic Arm [RA]/ Biobarrier [BB]), InSight (Instrument Deployment System [IDS]), OSIRIS-REx (Touch-And-Go Sample Acquisition Mechanism [TAGSAM] + Sample Acquisition and Return Assembly [SARA]). The costs for each were escalated to FY25$ using NASA Inflation for comparison (Tables F-3 to F-5). The highest cost assembly (Phoenix) was chosen as the cost was the most conservative.

Table F-3. Phoenix RA/BB cost in FY22$K.

Phoenix RA/BB (As Reported in EOM CADRe)	FY03	FY04	FY05	FY06	FY07	FY08	FY09	FY10	FY11	Total
RY$K	$0	$579	$5,482	$8,693	$1,900	$2	$0	$0	$0	$16,656
NASA Inflation to FY25	1.614	1.560	1.514	1.467	1.413	1.364	1.339	1.321	1.300	
FY25$K	$0	$904	$8,297	$12,754	$2,684	$3	$0	$0	$0	$24,642

Table F-4. InSight IDS cost in FY22$K.

InSight IDS (As Reported in Launch CADRe)	FY12	FY13	FY14	FY15	FY16	FY17	FY18	FY19	FY20	FY21	Total
RY$K	$0	$3,544	$9,126	$4,865	$233	$842	$8	$0	$0	$0	$18,618
NASA Inflation to FY25	1.286	1.267	1.242	1.218	1.201	1.179	1.151	1.128	1.105	1.091	
FY25$K	$0	$4,490	$11,338	$5,925	$280	$993	$9	$0	$0	$0	$23,036

Table F-5. OSIRIS-REx TAGSAM + SARA cost FY22$K.

OSIRIS-REx TAGSAM + SARA (As Reported in Launch CADRe)	FY10	FY11	FY12	FY13	FY14	FY15	FY16	FY17	Total
TAGSAM RY$K	$45	$130	$1,216	$3,409	$4,893	$4,759	$1,037	$57	$15,545
SARA RY$K	$0	$0	$0	$46	$629	$2,354	$1,225	$11	$4,266
NASA Inflation to FY25	1.321	1.300	1.286	1.267	1.242	1.218	1.201	1.179	
TAGSAM FY25$K	$60	$168	$1,564	$4,319	$6,079	$5,796	$1,245	$67	$19,298
SARA FY25$K	$0	$0	$0	$58	$782	$2,868	$1,472	$13	$5,193
Total TAGSAM + SARA FY25K	$60	$168	$1,564	$4,377	$6,861	$8,664	$2,717	$80	$24,491

F.2.2 MSL SAM

Table F-6. MSL SAM cost FY22$K.

MSL SAM (As Reported in Launch CADRe)	FY02	FY03	FY04	FY05	FY06	FY07	FY08	FY09	FY10	FY11	FY12	FY13	Total
RY$K	$0	$0	$0	$7,415	$25,702	$31,273	$16,271	$9,774	$10,969	$4,707	$1,039	$0	$107,149
NASA Inflation to FY25	1.649	1.614	1.56	1.514	1.467	1.413	1.364	1.339	1.321	1.3	1.286	1.267	
FY25$K	$0	$0	$0	$11,227	$37,704	$44,188	$22,194	$13,087	$14,489	$6,119	$1,336	$0	$150,345

F.2.3 INSIGHT IDC

Table F-7. InSight IDC cost FY22$K.

InSight IDC (As Reported in Launch CADRe)	FY12	FY13	FY14	FY15	FY16	FY17	FY18	FY19	FY20	FY21	Total
RY$K	$0	$451	$1,430	$1,696	$0	$0	$0	$0	$0	$0	$3,577
NASA Inflation to FY25	1.286	1.267	1.242	1.218	1.201	1.179	1.151	1.128	1.105	1.091	
FY25$K	$0	$571	$1,777	$2,066	$0	$0	$0	$0	$0	$0	$4,414

F.2.4 INSIGHT SPACECRAFT CONTRACT AND AIT&V

Table F-8. InSight spacecraft contract and AIT&V cost FY22$K.

InSight 06.16 S/C Contract and AIT&V (As Reported in Launch CADRe)	FY12	FY13	FY14	FY15	FY16	FY17	FY18	FY19	FY20	FY21	Total
06.16 Spacecraft Contract RY$K	$0	$33,234	$117,697	$66,169	$16,728	$12,945	$13,825	$0	$0	$0	$260,598
10 AIT&V RY$K	$0	$305	$4,405	$14,257	$4,815	$5,042	$9,241	$0	$0	$0	$38,064
NASA Inflation to FY25	1.286	1.267	1.242	1.218	1.201	1.179	1.151	1.128	1.105	1.091	
06.16 Spacecraft Contract FY25$K	$0	$42,104	$146,238	$80,592	$20,095	$15,266	$15,917	$0	$0	$0	$320,213
10 AIT&V FY25$K	$0	$386	$5,473	$17,365	$5,784	$5,946	$10,639	$0	$0	$0	$45,593

F.3 WRAP FACTOR

Work breakdown structure (WBS) elements that are primarily a level of effort, such as project management, systems engineering, and mission assurance, are estimated using a wrap factor based on historical data from missions that are comparable in terms of scope, mission class, and/or partnerships. Wrap rates were calculated using real year $ as reported in CADRe.

Wrap factors were generated for Phase B–D for the following WBS elements:

- 01 Project Management
- 02 Project System Engineering
- 03 Safety and Mission Assurance
- 12 Mission Design and Navigation

Wrap factor is calculated off of the Phase B–D cost of the identified WBS element divided by the total mission Phase B–D cost less launch vehicle (LV). For in-house missions, product assurance costs at the payload and spacecraft levels are included in the WBS 03 Mission Assurance wrap in order to present consistency with competed mission bookkeeping.

- 05.01 Payload Management
- 05.02 Payload Systems Engineering

Wrap factor is calculated off of the Phase B–D cost of the identified WBS element divided by the WBS 05 Payload Phase B–D cost.

- 06.01 Spacecraft Management
- 06.02 Spacecraft Systems Engineering

Wrap factor is calculated off of the Phase B–D cost of the identified WBS element divided by the WBS 06 Spacecraft and WBS 10 Project System integration and test (I&T) Phase B–D cost.

- 04 Science
- 07 Mission Operations System
- 09 Ground Data System

Wrap factor is calculated off of the Phase B–D cost of the identified WBS element divided by the total mission Phase B–D cost less launch vehicle.

Table F-9. Historical wrap factor analysis.

Note	Mission	WBS 01	WBS 02 + 12	WBS 03	WBS 01, 02, 03, 12	WBS 4	WBS7/9	05.01+ 05.02	06.01+ 06.02
Mars	Insight	2.9%	5.0%	5.1%	13.0%	2.4%	8.0%	*20.6%**	8.1%
Mars	MRO	2.0%	2.3%	3.0%	7.3%	0.9%	5.8%	4.6%	*0.0%**
Mars	Phoenix	2.1%	4.5%	1.5%	8.1%	3.9%	7.3%	7.3%	*1.5%**
Mars	MSL	2.1%	4.3%	4.5%	10.9%	1.0%	4.4%	6.4%	3.5%
Competed NF	Juno	2.7%	3.7%	5.7%	12.0%	3.3%	5.5%	7.7%	4.3%
Competed Disc.	Dawn	3.7%	5.0%	4.6%	13.3%	2.2%	8.9%	10.9%	5.1%
Competed Disc.	GRAIL	2.6%	5.4%	4.3%	12.4%	4.4%	6.5%	6.5%	4.9%
	Average	**2.6%**	**4.3%**	**4.1%**	**11.0%**	**2.6%**	**6.7%**	**7.2%**	**5.2%**

**Outlier values excluded from average calculations*

F.4 SEER-H 7.4

The SEER-H 7.4 model was used for the benchmark cost validation. The SEER benchmark estimates six elements of the NASA standard WBS (WBS 01, 02, 03, 05, 06, and 10). WBS 04, 07, and 09 are not estimated by SEER and were therefore validated with wrap factors. Flight software costs was estimated using a rule of thumb of 10% of the hardware cost.

The MLE Master Equipment List (MEL; Appendix G) was used as the main input source with the following logic applied for mass:

- Current best estimate (CBE) unit mass was applied to the "Least" mass input parameter
- CBE until mass plus contingency was applied to "Likely" mass input parameter

- 30% was added to the "Likely" mass input and applied to the "Most" mass input parameter

Flight Units, Spares, and Engineering Model Units followed the following logic:

- Quantity Per Next Higher Element = Flight Unit Count
- Prototype Quantity:
  - If engineering models (EMs) are identified for the component, then each EM = 0.65
  - If no EMs are identified, then Prototype Quantity = 1.5 (Protoflight)
- Production Quantity:
  - If the component has EMs listed, then Production Quantity = Total Flight Unit Count plus Total Spare Count
  - If the component does not have EMs listed, then the first unit is modeled as Protoflight (see Prototype Quantity above) and the Production Quantity = Total Flight Unit Count plus Total Spare Count minus 1 (for the Protoflight unit)

In order to produce a conservative cost estimate, the model acquisition category settings followed the SEER Guidance Rev 3.1, which assumes higher levels of modification (major and make). Examples of this can be seen below in areas like Telecom and Propulsion.

Telecom:

- Modeled hardware using radio frequency (RF) components knowledge base as make consistent with SEER guidance, however, the majority of the components are typically commercial-off-the-shelf (COTS) or build-to-print (BTP) with part numbers identified in the MEL.

Propulsion:

- Modeled hardware using propulsion components knowledge base as make consistent with SEER guidance, however, components are typically either COTS or BTP with part numbers identified in the MEL.

Additionally, SEER Guidance Rev 3.1 was followed for settings for a Class B mission such as Certification Level and Reliability Standard, which apply to all components. Specific recommended settings like Design Complexity and Complexity of Form were followed and adjusted to the applicable components.

F.5 PROJECT COST ESTIMATING CAPABILITY (PCEC)

PCEC was used to estimate WBS 01 Project Management, 02 Project Systems Engineering, WBS 03 Mission Assurance, 04 Science, 05.01 Payload Management, 05.02 Payload Systems Engineering, 06 Spacecraft, 07/09 MOS/GDS, and 10 AIT&V. The Multi Element Robotic Spacecraft PCEC model was chosen for the MLE model run. The mapping of PCEC model outputs to the MLE WBS is noted in Table F-10.

Table F-10. PCEC mapping to MLE WBS.

PCEC Cost Output Mapping		PCEC Output	MLE WBS Mapping
WBS #	Level	WBS Element	
0	1	System Name	
1.0	2	Project Management	WBS 01, 02, 03
2.0	2	Systems Engineering	
3.0	2	Safety and Mission Assurance	
4.0	2	Science/Technology	WBS 04, 07, 09
5.0	2	Payload(s)	
5.01	3	Payload Management	WBS 05.01, 05.02
5.02	3	Payload System Engineering	
5.03	3	Payload Product Assurance	Mapped to WBS 01, 02, 03
5.10	3	Instruments - EMPTY ROLLUP	Pass Through
5.x	3	Payload I&T	Mapped to WBS 10

Table F-10. PCEC mapping to MLE WBS.

PCEC Cost Output Mapping		PCEC Output	MLE WBS Mapping
WBS #	Level	WBS Element	
6.0	2	Flight System \ Spacecraft	
6.01	3	Flight System Project Management	WBS 06.01, 06.02
6.02	3	Flight System Systems Engineering	
6.03	3	Flight System Product Assurance	Mapped to WBS 01, 02, 03
6.10	3	Lander	WBS 06.16
--	4	SC Elt 1 Management	
--	4	SC Elt 1 Systems Engineering	
--	4	SC Elt 1 Product Assurance	
--	4	Structures & Mechanisms	
--	4	Thermal Control	
--	4	Electrical Power & Distribution	
--	4	GN&C	
--	4	Propulsion	
--	4	Communications	
--	4	C&DH	
--	4	SC Elt 1 I&T	
6.20	3	Cruise	
--	4	SC Elt 2 Management	
--	4	SC Elt 2 Systems Engineering	
--	4	SC Elt 2 Product Assurance	
--	4	Structures & Mechanisms	
--	4	Thermal Control	
--	4	Electrical Power & Distribution	
--	4	GN&C	
--	4	Propulsion	
--	4	Communications	
--	4	C&DH	
--	4	SC Elt 2 I&T	
6.30	3	EDL	
--	4	SC Elt 3 Management	
--	4	SC Elt 3 Systems Engineering	
--	4	SC Elt 3 Product Assurance	
--	4	Structures & Mechanisms	
--	4	Thermal Control	
--	4	Electrical Power & Distribution	
--	4	GN&C	
--	4	Propulsion	
--	4	Communications	
--	4	C&DH	
--	4	SC Elt 3 I&T	
6.x	3	Flight System I&T	
7.0	2	Mission Operations System (MOS)	
--	3	MOS/GDS Development (Phase B-D)	WBS 04, 07, 09
--	3	Mission Ops & Data Analysis (Phase E)	Space Operations Cost Model (SOCM)
8.0	2	Launch Vehicle/Services	Not Applicable
9.0	2	Ground Data System (GDS)	Included in WBS 04, 07, 09
10.0	2	System Integration, Assembly, Test & Check Out	WBS 10
11.0	2	Education & Public Outreach	Not Applicable

F.6 NASA INSTRUMENT COST MODEL (NICM)

F.6.1 SCIENCE PAYLOAD NICM SYSTEM

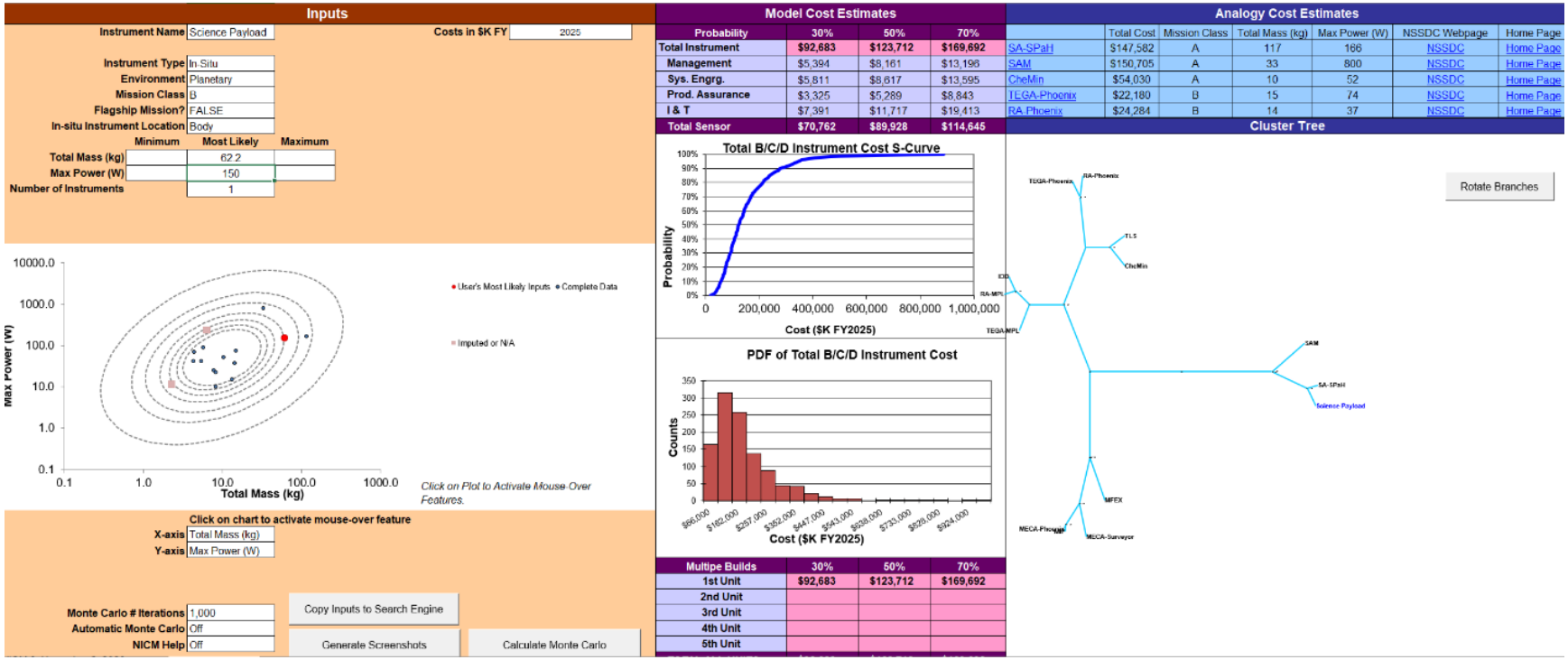

Figure F-1. MLE Science Payload NICM system results.

F.6.2 INSTRUMENT CAMERA NICM SYSTEM

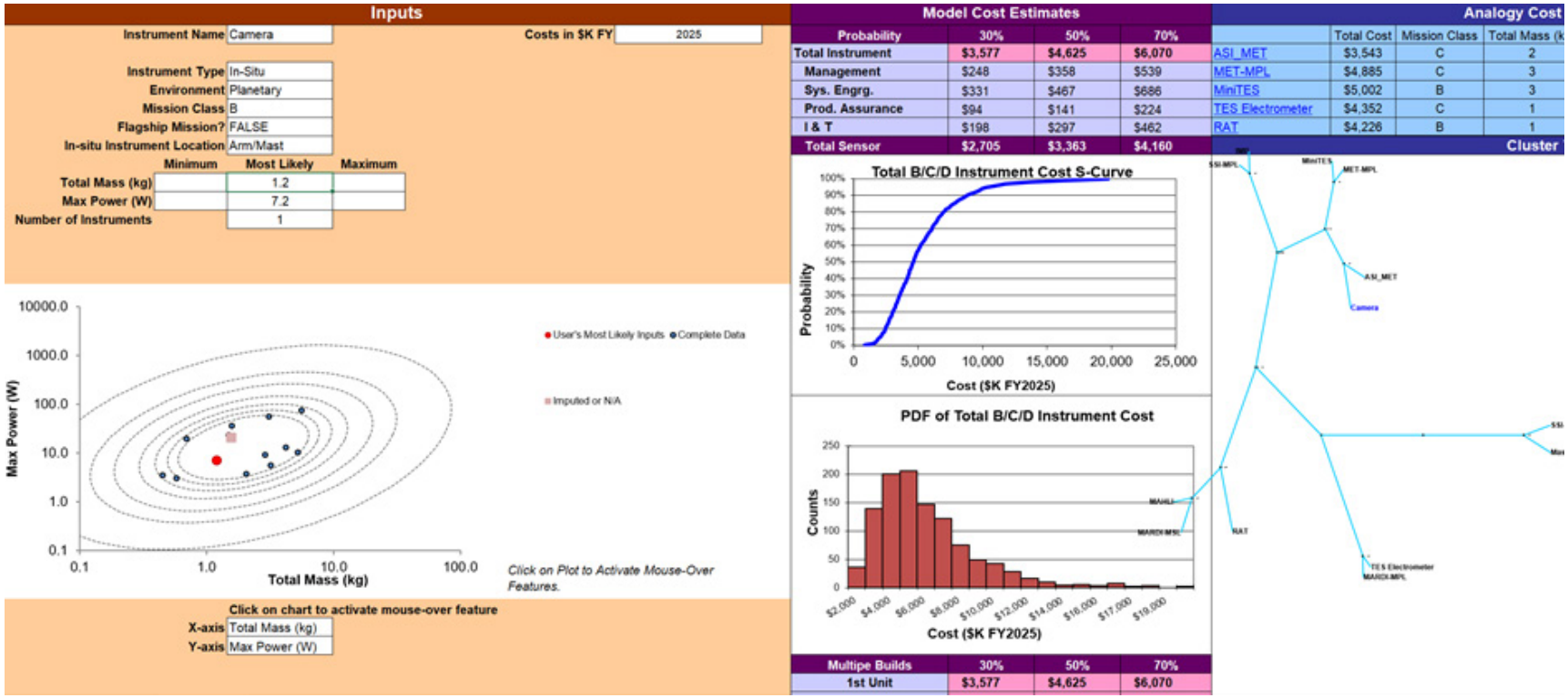

Figure F-2. MLE Instrument Camera NICM system results.

F.7 MARS INSTRUMENT COST TO MASS SCALING

One of the approaches to estimating the cost of the Science Payload was by analyzing the relationship between cost versus mass of flown Mars instruments. The cost and mass from the NICM database of 39 Mars instruments was used to produce the regression analysis to estimate the MLE Science Payload cost.

Table F-11. Historical Mars instruments cost to mass database.

Instrument Name Abbreviated	Mission Name Abbreviated	Destination Type	B/C/D Cost ($K FY2025)	Total Mass (kg)
ASI_MET	Mars Pathfinder	Planetary	$3,543	2.0
CheMin	MSL	Planetary	$54,030	10.4
CRISM	MRO	Planetary	$47,762	33
CTX	MRO	Planetary	$8,871	3.4
GRS_MO	Mars Observer	Planetary	$74,921	26.0
GRS_Odyssey	Mars Odyssey	Planetary	$47,346	31
HiRISE	MRO	Planetary	$80,175	64.2
IDD	MER	Planetary	$15,902	5.4
IMP	Mars Pathfinder	Planetary	$14,300	5.2
MAG MAVEN	MAVEN	Planetary	$6,434	2
MAHLI	MSL	Planetary	$9,610	1.6
MARCI	MRO	Planetary	$5,346	1
MARDI-MSL	MSL	Planetary	$5,027	1.5
MARIE	Mars Odyssey	Planetary	$5,766	3.3
MastCam	MSL	Planetary	$28,912	3.1
MCS	MRO	Planetary	$21,856	9.0
MECA-Phoenix	Phoenix	Planetary	$13,874	7.8
MECA-TECP	Phoenix	Planetary	$5,383	0.5
MER Camera	MER	Planetary	$5,694	0.3
MFEX	Mars Pathfinder	Planetary	$38,134	13.3
MiniTES	MER	Planetary	$5,002	3.2
MOC-MO	Mars Observer	Planetary	$49,987	24
MOLA-MO	Mars Observer	Planetary	$55,727	25
NGIMS_MAVEN	MAVEN	Planetary	$20,923	12.4
ONC	MRO	Planetary	$8,830	2.9
PMIRR	Mars Observer	Planetary	$76,195	44
RAD	MSL	Planetary	$24,330	1.9
RA-Phoenix	Phoenix	Planetary	$24,284	14.4
RAT	MER	Planetary	$4,226	1
SAM	MSL	Planetary	$150,705	33.3
SEP	MAVEN	Planetary	$4,359	3.2
SSI-Phoenix	Phoenix	Planetary	$11,774	6
STATIC	MAVEN	Planetary	$9,461	4.5
SWEA	MAVEN	Planetary	$5,316	2.9
SWIA	MAVEN	Planetary	$3,323	6.2
TEGA-Phoenix	Phoenix	Planetary	$22,180	14.9
TES_MO	Mars Observer	Planetary	$52,562	14.4
THEMIS	Mars Odyssey	Planetary	$26,428	13.0
TLS	MSL	Planetary	$39,500	4.4

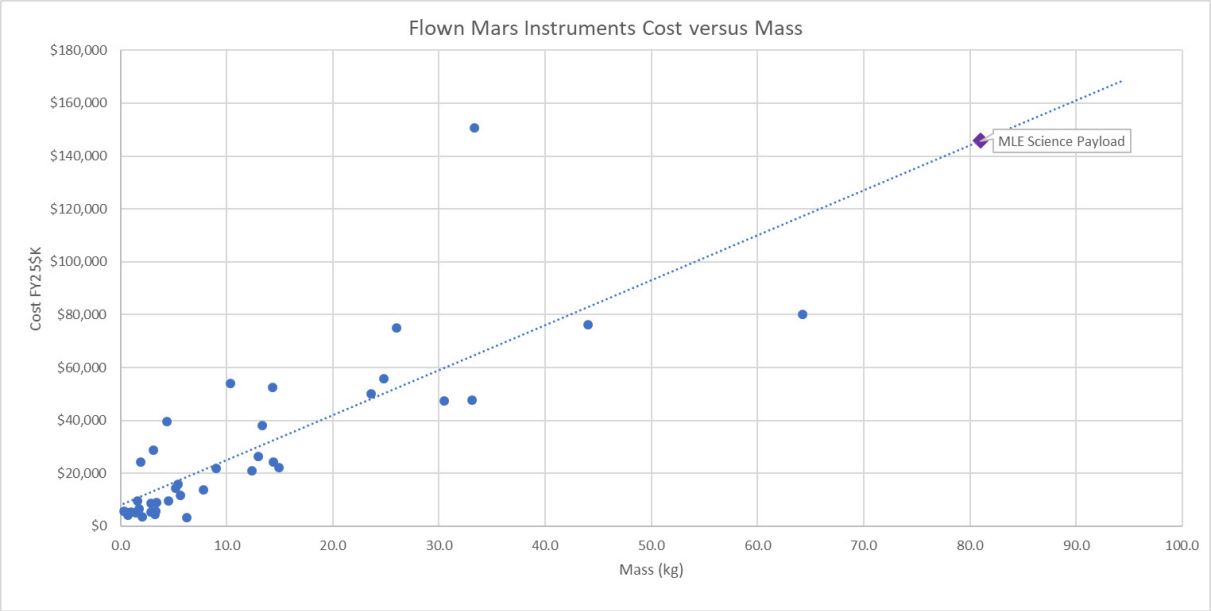

Figure F-3. Flown Mars instruments cost vs. mass regression.

F.8 SPACE OPERATIONS COST MODEL (SOCM)

Table F-12. SOCM inputs.

SOCM Mission Characteristics	Inputs
Mission Type	Lander
Target	Mars
Cruise Mission Duration	10 months
Encounter Mission Duration	24 months
Post Flight Data Analysis Duration	1 months
Mission Risk Class	Medium
Development Schedule	Long > 4 years
Lead Organization Level of Experience	Average
MOS SW Maturity/ Heritage	Average
S/C Design Implementation	Cost-Capped
Design Complexity	Medium

Table F-13. SOCM results.

PLANETARY – LEVEL 1 OUTPUTS					
LEVEL I COST OUTPUT					
	Level 1 Mission Operations Cost Estimate			2025	
TTR			*constant FY $K*		
		Cruise	Encounter	Post-Flight DA	Total
1.0	Mission Planning & Integration	185.4	1,320.8		1,506.2
2.0	Command/Uplink Management	686.0	4,782.1		5,468.0
3.0	Mission Control & Ops	1,424.4	9,917.9		11,342.3
4.0	Data Capture	3,844.0	13,432.6		17,276.7
5.0	POS/Loc Planning & Analysis	2,148.1	10,788.7		12,936.8
6.0	S/C Planning & Analysis	2,388.4	10,291.5		12,679.9
7.0	Sci Planning & Analysis	734.5	7,090.9		7,825.4
8.0	Science Data Processing	314.6	1,531.7	63.8	1,910.2
9.0	Long-term Archives	427.1	1,492.5	62.2	1,981.8
10.0	System Engineering, Integration, & Test	1,560.9	7,406.0		8,966.9
11.0	Computer & Comm Support	733.2	3,800.4	158.4	4,692.0
12.0	Science Investigations	943.8	4,595.2	191.5	5,730.5
13.0	Management	2,154.3	5,624.0		7,778.2
	Project Direct Total	**17,544.7**	**82,074.4**	**475.8**	**100,094.9**

F.9 MISSION OPERATIONS COST ESTIMATION TOOL (MOCET)

NASA Mission Operations Cost Estimation Tool

About MOCET...

Mission Type	Planetary
Mission Name	Mars Life Explorer
Mission Class	Large (New Frontiers, Directed Survey)
Science Theme	

Inflate Costs To: FY2025

Legend:
- Input
- Calculated/Read-Only
- Invalid/Incomplete
- N/A

Apply

Description	Phase Start	Duration (months)	Estimating Phase	Parameter 1	Value 1	Parameter 2	Value 2	Cost/Mo (FY25 $M)	Total Cost (FY25 $M)	Total Cost (RY $M)	Notes
Phase E Start (Launch + 30 Days)	June 2035	0.0	Checkout Cruise	Enhanced Navigation?	No			3.36	0.11	0.14	
Cruise	June 2035	10.0	Nominal/Quiescent Cruise	Is Quiescent?	Yes			1.83	18.24	23.76	
EDL	April 2036	0.0	Approach/EDL	Cruise Avg Cost	Phase E Start (Launch + 30 Days)			3.64	0.00	0.00	
Prime Ops	April 2036	25.0	Prime Landed Ops	Cruise Avg Cost	Phase E Start (Launch + 30 Days)			2.48	62.00	84.34	
Data Analysis	May 2038	1.0	Data/Sample Analysis	Collection Avg Cost	Prime Ops			1.86	1.84	2.55	
End of Mission	05-31-2038							Total	$ 82.19	$ 110.79	

Figure F-4. MOCET results.

G MASTER EQUIPMENT LIST

Representative experienced industry study partner Lockheed Martin provided the EDL analysis and heritage for the basis of this MEL. Detailed values are provided for technical, risk, and cost models and form the basis for this Mars Life Explorer final study report and conclusions. Phoenix and InSight heritage provide the backbone of the heritage for Mars Life Explorer.

Table G-1. Total MLE launch mass with contingency based on heritage and best practices, maximum expected values, maximum possible values, and additional margin above maximum possible value.

Launch Total	CBE	Cont %	MEV	MPV	Margin %
C&DH	13.6	5.0%	14.2	15	5.3%
EPS	82.1	5.0%	86.2	97	12.5%
Harness	39.6	6.6%	42.3	48	13.6%
Telecom	26.9	5.3%	28.3	32	13.1%
GN&C	27.4	5.0%	28.7	32	11.3%
Structures	500.2	9.2%	546.1	602	10.2%
Mechanisms	57.2	8.7%	62.2	70	12.6%
Propulsion	78.3	5.8%	82.8	92	11.1%
Thermal	26.7	6.7%	28.5	33	15.7%
Ballast	15.0	6.7%	16.0	18	12.5%
Flight System Subtotal	867.0	7.9%	935.5	1039.0	11.1%
Payload	98.0	18.4%	116.0	150	29.3%
Dry	965.0	9.0%	1051.5	1189.0	13.1%
Lander Fuel	115	0.0%	115	115	0.0%
Lander Helium	1	0.0%	1	1	0.0%
Launch Total	**1081.0**	**8.0%**	**1167.5**	**1305.0**	**11.8%**

Table G-6. Comparison of MLE, Phoenix, and InSight in detail for Launch, Entry, and Landed Mass. Note Phoenix and InSight are actual as-flown values.

	MLE			Phoenix			InSight		
	Launch	Entry	Landed	Launch	Entry	Landed	Launch	Entry	Landed
Allocation	1189.0	1087.0	565.0	641	552	364	743	575	392
CBE	965.0	875.3	449.6	584	503	330.7	577	497	325
BTP/OTS CBE	250.8	198.1	183.7	424.6	373.8	224.6	442	371	204
Contingency	12.5	9.9	9.2	7.7	6.4	4.8	13	9	7
Non-BTP Allocation	925.7	879.0	372.1	208.7	171.8	134.6	288	195	181
CBE Modified	714.3	677.2	265.8	159.3	129.2	106	135	126	121
Contingency	73.9	71.3	30.3	15.2	12.9	11.1	16	18	15
Contingency %	10.3%	10.5%	11.4%	9.5%	10.0%	10.5%	11.9%	14.3%	12.4%
Margin Above Contingency	137.5	130.5	76.0	34.2	29.7	17.5	137	51	45
Margin Above Contingency	17.4%	17.4%	25.7%	19.6%	20.9%	14.9%	90.7%	35.4%	33.1%
As Launched Mass				596.9	514.9	342.9	623.6	544.2	354.1
% Growth (Liftoff/CSR CBE)	23.2%	24.2%	25.7%	2.2%	2.4%	3.7%	8.1%	9.5%	9.0%
Available kg for growth	224.0	211.7	115.4	57	49	33.3	166	78	67
Actual Growth in kg	N/A	N/A	N/A	12.9	11.9	12.2	46.6	47.2	29.1
Payload Growth in kg	N/A	N/A	N/A	13.1	13.1	13.1	23.0	23.0	23.0

Table G-2. Allocation, CBE, and MEV for the MLE lander backshell, heatshield, cruise stage, and total. Allocation means designed for max launch vehicle and subsequent EDL.

Allocation	Lander	Backshell	Heatshield	Cruise Stage	Total
C&DH	15				15
EPS	75			22	97
Harness	38	5		5	48
Telecom	16	5		11	32
GN&C	23			9	32
Structures	122	299	145	36	602
Mechanisms	18	35	14	3	70
Propulsion	92				92
Thermal	16	8	4	5	33
Ballast			7	11	18
FS Margin					0
FS Subtotal	415	352	170	102	1039
Payload	150				150
Subtotal	565	352	170	102	1189
Project Margin					0
Dry Subtotal	565	352	170	102	1189
Helium	1				1
Fuel	115				115
Oxidizer					0
Fuel/Ox Subtotal					0
Total	681	352	170	102	1305

CBE	Lander	Backshell	Heatshield	Cruise Stage	Total
C&DH	13.6				13.6
EPS	63.9			18.3	82.1
Harness	31.7	4.3		3.7	39.6
Telecom	13.0	4.5		9.4	26.9
GN&C	19.9			7.5	27.4
Structures	102.6	239.4	123.0	35.2	500.2
Mechanisms	15.0	31.3	9.0	1.9	57.2
Propulsion	78.3				78.3
Thermal	13.7	7.4	1.8	3.9	26.7
Ballast			5.0	10.0	15.0
FS Margin					0.0
FS Subtotal	351.6	287.0	138.8	89.7	867.0
Payload	98.0				98.0
Subtotal	449.6	287.0	138.8	89.7	965.0
Project Margin					0.0
Dry Subtotal	449.6	287.0	138.8	89.7	965.0
Helium					0.0
Fuel					0.0
Oxidizer					0.0
Wet Subtotal					0.0
Total	**44955.3%**	**28695.7%**	**13880.0%**	**89.7231268**	**96503.3%**

MEV	Lander	Backshell	Heatshield	Cruise Stage	Total
C&DH	14.2				14.2
EPS	67.1			19.2	86.2
Harness	33.9	4.5		3.9	42.3
Telecom	13.7	4.8		9.9	28.3
GN&C	20.8			7.9	28.7
Structures	109.8	263.4	135.3	37.6	546.1
Mechanisms	16.2	34.1	9.9	2.0	62.2
Propulsion	82.8				82.8
Thermal	14.4	8.1	2.0	4.0	28.5
Ballast			5.5	10.5	16.0
FS Margin					0.0
FS Subtotal	373.0	314.8	152.7	95.0	935.5
Payload	116.0				116.0
Subtotal	489.0	314.8	152.7	95.0	1051.5
Project Margin					0.0
Dry Subtotal	489.0	314.8	152.7	95.0	1051.5
Helium					0.0
Fuel					0.0
Oxidizer					0.0
Wet Subtotal					0.0
Total	**48900.0%**	**31483.7%**	**15268.0%**	**94.9502171**	**105146.7%**

Table G-3. Accounts for all landed mass with contingency and margin.

Landed	CBE	Cont %	MEV	MPV	Margin %
C&DH	13.6	5.0%	14.2	15	5.3%
EPS	63.9	5.0%	67.1	75	11.8%
Harness	31.7	7.0%	33.9	38	12.0%
Telecom	13.0	5.6%	13.7	16	16.8%
GN&C	19.9	5.0%	20.8	23	10.3%
Structures	102.6	7.0%	109.8	122	11.1%
Mechanisms	15.0	8.0%	16.2	18	11.0%
Propulsion	78.3	5.8%	82.8	92	11.1%
Thermal	13.7	5.0%	14.4	16	11.4%
Ballast	0.0	0.0%	0.0	0	0.0%
Flight System Subtotal	351.6	6.1%	373.0	415.0	11.3%
Payload	98.0	18.4%	116.0	150	29.3%
Dry Lander	449.6	8.8%	489.0	565.0	15.5%

Table G-4. Accounts for all entry mass with contingency and margin.

Entry	CBE	Cont %	MEV	MPV	Margin %
C&DH	13.6	5.0%	14.2	15	5.3%
EPS	63.9	5.0%	67.1	75	11.8%
Harness	36.0	6.8%	38.4	43	12.0%
Telecom	17.5	5.5%	18.5	21	13.8%
GN&C	19.9	5.0%	20.8	23	10.3%
Structures	465.1	9.3%	508.5	566	11.3%
Mechanisms	55.3	8.8%	60.2	67	11.3%
Propulsion	78.3	5.8%	82.8	92	11.1%
Thermal	22.9	7.0%	24.5	28	14.4%
Ballast	5.0	10.0%	5.5	7	27.3%
Flight System Subtotal	777.3	8.1%	840.5	937.0	11.5%
Payload	98.0	18.4%	116.0	150	29.3%
Dry Entry	875.3	9.3%	956.5	1087.0	13.6%

Table G-5. Accounts for all baseline payload mass with contingency.

MLE Baseline Payload	CBE (kg)	Cont %	Max Exp Val
Engineering			
Single Segment 2 m Rotary Percussive Drill	20.0	15%	23.0
3DOF Drill Boom	7.0	15%	8.1
Drill Avionics Box	7.0	20%	8.4
Biobarrier	3.0	15%	3.5
Gas Sample Transfer System	8.0	30%	10.4
InSight Context Camera (ICC)	0.9	5%	0.9
Downhole Engineering Sensors and Imager	2.0	15%	2.3
Science			
Biosignature Detection Suite	35.0	15%	40.3
Chemistry, Mineral, Conductivity Suite	14.0	15%	16.1
Wind, Water, and Radiative Flux Suite	3.0	15%	3.5
Total	**99.9**	**16%**	**116.3**

Table G-7. MLE mass details for the entire flight system down to the subsystem at a component level. The contingency values are based on best practice of heritage, design, and analysis with additional info on past program inheritance.

Hardware Elements	# EM's	# Spares	FLIGHT	Unit Mass (kg)	CBE (kg)	Basis of Contingency	Contingency %	Max Expected Value, kg	Program Inheritance
LANDER									
C&DH Subsystem Box			1		13.6		5%	14.2	
Spaceflight Computer (SFC)	2	1	2	0.54	1.1	OTS	5%	1.1	InSight/JUNO/MAVEN/GRAIL/MRO
C&DH Power Supply - High Efficiency (CPS-HE)	4	1	2	0.64	1.3	OTS	5%	1.3	InSight
Analog Acquisition Card (AAC)	2	1	2	0.34	0.7	BTP	5%	0.7	InSight/JUNO/MAVEN/GRAIL/MRO
Uplink Downlink Card (ULDL)	2	1	2	0.30	0.6	BTP	5%	0.6	InSight/JUNO/MAVEN/GRAIL/MRO
GN&C Interface Card (GIF)	2	1	2	0.32	0.6	BTP	5%	0.7	InSight/JUNO/MAVEN/GRAIL/MRO
InSight Payload Interface Card (IPIC)	2	1	2	0.55	1.1	BTP	5%	1.2	InSight/GRAIL
C&DH Module Interface Card (CMIC)	4	1	2	0.31	0.6	BTP	5%	0.6	InSight/JUNO/MAVEN/GRAIL/MRO
Backplane	2	1	1	1.00	1.0	BTP	5%	1.1	InSight
Chassis + Hardware	2	0	1	6.57	6.6	BTP	5%	6.9	InSight
Lander Power			1	Total	63.9		5%	67.1	
Li Ion Battery (NCA + LTE Chemistries)	2	1	2	10.5	21.0	OTS	5%	22.0	InSight/Phoenix
T-0 Diode Assemblies + Connectors			3	0.2	0.5	BTP	5%	0.5	InSight/Phoenix
Landed Solar Arrays (Larger Ultra-Flex)	0	0	2	9.7	19.5	OTS	5%	20.4	InSight/Phoenix
Power Distribution & Drive Unit (PDDU)			**1**		**16.1**		**5%**	**16.9**	
High-Efficiency Power Supply Card (HEPS)	0	1	1	0.9	0.9	BTP	5%	0.9	InSight/PHX/MRO/MAVEN/JUNO/ODY
Analog Acquisition Card (AAC)	0		2	0.3	0.7	BTP	5%	0.7	InSight/JUNO/MAVEN/GRAIL/MRO
Universal Switch Module Card (USM)	0	1	4	1.3	5.4	BTP	5%	5.6	InSight/JUNO/MAVEN/GRAIL/MRO
Solar Array & Battery Control Card (SABC)	0	1	2	0.9	1.8	BTP	5%	1.9	InSight/GRAIL
Backplane	0	1	1	1.6	1.6	BTP	5%	1.6	InSight
Chassis + Hardware			1	5.8	5.8	BTP	5%	6.1	InSight
Pyro & Propulsion Unit (PAPU)			**1**		**6.9**		**5%**	**7.2**	
POP-Prop Card	0	1	1	1.0	1.0	BTP	5%	1.0	InSight/MAVEN/GRAIL
POP-Pyro Card	0	1	2	1.0	1.9	BTP	5%	2.0	InSight/MAVEN/GRAIL
Backplane	0	1	1	1.7	1.7	BTP	5%	1.7	InSight/MAVEN
Chassis + Hardware	0		1	2.3	2.3	BTP	5%	2.5	InSight/MAVEN
Lander Harness			1		31.7		7%	33.9	
Main & Payload Harnesses + Enable Plugs			1	28.3	28.3	MM-E	7%	30.2	InSight/Phoenix
Prop Harness			1	1.2	1.2	MM-E	7%	1.3	InSight/Phoenix
Pyro Harness			1	2.3	2.3	MM-E	7%	2.5	InSight/Phoenix

Table G-7. MLE mass details (cont.)

Hardware Elements	# EM's	# Spares	FLIGHT	Unit Mass (kg)	CBE (kg)	Basis of Contingency	Contingency %	Max Expected Value, kg	Program Inheritance
LANDER									
Lander Telecom			1	Total	13.0		6%	13.7	
UHF Transceiver	0	1	2	1.8	3.7	OTS	5%	3.8	InSight/Phoenix/ODY
UHF Antenna System (Helix)	0	0	1	0.6	0.6	N(E)	20%	0.7	Phoenix/ODY/MRO
UHF Diplexer		0	2	0.4	0.7	OTS	5%	0.8	InSight/Phoenix/ODY
Coax Transfer Switch			2	0.1	0.2	OTS	5%	0.2	InSight/Phoenix/MAVEN
Coax Cables			1	1.9	1.9	OTS	5%	2.0	InSight/Phoenix
Solid State Power Amplifier (SSPA)		1	1	1.4	1.4	OTS	5%	1.4	InSight/Phoenix/MSL
Small Deep Space Transponder (SDST)		1	1	3.1	3.1	OTS	5%	3.3	InSight/MAVEN/MSL/JUNO/MRO/Phoenix/ODY
X-Band Diplexer	0	0	1	0.5	0.5	OTS	5%	0.6	InSight/MAVEN
Medium Gain Antenna (MGA)			1	0.7	0.7	MM-E	5%	0.7	InSight/Phoenix/ODY/MRO
Hybrid Coupler, Attenuators, Loads & Adapters			1	0.2	0.2	OTS	5%	0.2	InSight/MAVEN
Lander Mechanisms			1	Total	15.0		8%	16.2	
Lander/BS R&R Details			3	1.1	3.3	BTP	5%	3.4	InSight/Phoenix
Lander/BS Sep Nuts 3/8"	15		3	0.27	0.8	BTP	5%	0.9	InSight/Phoenix
SA Gimbals			2	4.56	9.1	M-E	10%	10.0	MAVEN
Leg Sep Nuts	15		3	0.15	0.5	BTP	5%	0.5	InSight/Phoenix
Misc Mechanism Details			1	1.4	1.4	BTP	5%	1.4	InSight/Phoenix
Lander Structure			1	Total	102.6		7%	109.8	
Primary Structure (w/o Sci Deck)			1	25.2	25.2	MM-E	7%	26.9	InSight/Phoenix
Science Deck			1	26.6	26.6	MM-E	7%	28.5	InSight/Phoenix
Lander Legs			3	9.2	27.7	MM-E	7%	29.7	InSight/Phoenix
Secondary Structure; Misc HW			1	23.2	23.2	MM-E	7%	24.8	InSight/Phoenix
Lander Thermal Control			1	Total	13.7		5%	14.4	
TE Batt Insulation			10	0.40	4.0	BTP	5%	4.2	InSight/Phoenix
MLI Insulation			1	3.60	3.6	BTP	5%	3.8	InSight/Phoenix
Heat Pipes		0	3	0.37	1.1	OTS	5%	1.2	InSight/Phoenix
Heaters, Sensors, Thermostats			1	4.95	4.9	OTS	5%	5.2	InSight/Phoenix
Heaters	0	0	138	0.0	2.8		5.0%	3.0	InSight/Phoenix
Sensors	0	0	49	0.0	1.0		5.0%	1.0	InSight/Phoenix
Thermostats	0	0	56	0.0	1.1		5.0%	1.2	InSight/Phoenix

Table G-7. MLE mass details (cont.)

Hardware Elements	# EM's	# Spares	FLIGHT	Unit Mass (kg)	CBE (kg)	Basis of Contingency	Contingency %	Max Expected Value, kg	Program Inheritance
LANDER									
Lander Propulsion			1	Total	78.3		6%	82.8	
Helium Tank			2	3.65	7.3	OTS	5%	7.7	InSight
Fuel Tank w/ Diaphragm			3	5.49	16.5	OTS	5%	17.3	XSS-11
Descent REA's 68lbf		1	12	0.88	10.6	OTS	5%	11.1	InSight/Phoenix
Descent REA's 150 lbf		1	3	1.90	5.7	OTS	5%	6.0	Magellan
Descent REA brackets			3	2.00	6.0	M-E	10%	6.6	
Cruise REMs [1.0 lbf REA+5.0 lbf REA]		1	4	1.20	4.8	OTS	5%	5.0	InSight/Phoenix
GHe/Hydrazine Filter			1	0.25	0.3	OTS	5%	0.3	InSight/JUNO/MAVEN
3/4" Hydrazine Filter			2	0.89	1.8	OTS	5%	1.9	InSight/Phoenix
1/2" Normally Closed Pyrovalve w/NSI		0	2	0.21	0.4	OTS	5%	0.4	InSight/Phoenix
3/8" Normally Closed Pyrovalve w/NSI			2	0.24	0.5	OTS	5%	0.5	InSight/Phoenix
Pressure Transducer - Low Pressure			2	0.22	0.4	OTS	5%	0.5	InSight/Phoenix
Service Valve - Low Pressure			5	0.19	1.0	OTS	5%	1.0	InSight/JUNO
Latch Valve			3	0.55	1.7	OTS	5%	1.7	InSight/Phoenix
GHe/Hydrazine Filter			2	0.25	0.5	OTS	5%	0.5	InSight/JUNO/MAVEN
3/8" Normally Open Pyrovalve w/NSI			3	0.24	0.7	OTS	5%	0.7	InSight/Phoenix
3/8" Normally Closed Pyrovalve w/NSI			1	0.18	0.2	OTS	5%	0.2	InSight/Phoenix
Pressure Transducer - High Pressure			1	0.22	0.2	OTS	5%	0.2	InSight/Phoenix
Pressure Regulator		0	1	2.27	2.3	OTS	5%	2.4	InSight/Phoenix
Service Valve - 1/8"		0	1	0.06	0.1	OTS	5%	0.1	InSight/Phoenix
Service Valve - High Pressure		0	2	0.19	0.4	OTS	5%	0.4	InSight/JUNO
Other Prop Hardware			1	17.13	17.1	MM-E	7%	18.3	InSight/Phoenix
Lander AAC			1	Total	19.854		5%	20.847	
MIMU		1	2	4.65	9.3	OTS	5%	9.8	InSight/Phoenix
Landing Radar Electronics	1.00	1.00	2	4.17	8.3	OTS	5%	8.8	InSight/Phoenix
Landing Radar Cables			11	0.05	0.6	OTS	5%	0.6	InSight/Phoenix
Landing Radar Switches			2	0.16	0.3	OTS	5%	0.3	InSight/Phoenix
Landing Radar Canted Antennas	1.00		2	0.11	0.2	OTS	5%	0.2	InSight/Phoenix
Landing Radar Nadir Antennas	1.00		6	0.18	1.1	OTS	5%	1.1	InSight/Phoenix
Lander Dry Mass without Payload			**1**	**Total**	**351.6**		**6%**	**373.0**	
Payload			1	Total	98.0		18%	116.0	
Payload			1	98.0	98.0	Pay	18.4%	116.0	
Lander Dry Mass with Payload			**1**	**Total**	**449.6**		**9%**	**489.0**	

Table G-7. MLE mass details (cont.)

Hardware Elements	# EM's	# Spares	FLIGHT	Unit Mass (kg)	CBE (kg)	Basis of Contingency	Contingency %	Max Expected Value, kg	Program Inheritance
Cruise Stage									
Cruise Stage Power			1	Total	18.3		5%	19.2	
CS Solar Array Assembly (inclds structure)	0.10		2	9.1	18.3	BTP	5%	19.2	InSight/Phoenix/MAVEN
Cruise Stage Harness			1	Total	3.7		5%	3.9	
Cruise Stage Harness (inclds T0)			1	3.7	3.7	BTP	5.0%	3.9	InSight/Phoenix
Cruise Stage Telecom			1	Total	9.38		5%	9.9	
Cruise Solid State Power Amp			2	1.4	2.7	OTS	5.0%	2.9	InSight/Phoenix/MSL
SDST			1	3.0	3.0	OTS	5.0%	3.2	InSight/MAVEN/MSL/JUNO/MRO/Phoenix/ODY
Cruise Diplexer			1	0.5	0.5	OTS	5.0%	0.6	InSight/MAVEN
Cruise Xmit MGA/RX	0		1	0.4	0.4	OTS	5.0%	0.4	InSight/Phoenix/ODY/MRO
Cruise Rcv & Xmt LGA Patch	0	0	2	0.05	0.1	OTS	5%	0.1	InSight/Phoenix/ODY/MRO
Coax Switch			2	0.1	0.2	OTS	5.0%	0.2	InSight/Phoenix/ODY/MRO
Bandpass Filter			1	0.4	0.4	OTS	5.0%	0.4	InSight/MAVEN
Notch Filter			1	0.1	0.1	OTS	5.0%	0.1	InSight/MAVEN
Coax			1	1.4	1.4	OTS	5%	1.5	InSight/Phoenix
Mics RF HW			1	0.4	0.4	OTS	5%	0.4	InSight/Phoenix
Cruise Stage Mechanisms			1	Total	1.9		7%	2.0	
Misc Cruise Stage Mechanisms			1	1.9	1.9	MM-E	7.0%	2.0	InSight/Phoenix
Cruise Stage Structure			1	Total	35.2		7%	37.6	
CS Primary Structure			1	21.1	21.1	MM-E	7.0%	22.5	InSight/Phoenix
CS Secondary Structure			1	14.1	14.1	MM-E	7.0%	15.1	InSight/Phoenix
Cruise Stage Thermal Control			1	Total	3.9		5%	4.0	
CS Heat Pipes		0.00	1	0.5	0.5	OTS	5.0%	0.6	InSight/Phoenix
CS Heaters	0.00	0.00	16	0.1	1.1	OTS	5.0%	1.1	InSight/Phoenix
Temp Sensors	0.00	0.00	6	0.0	0.0	OTS	5.0%	0.0	InSight/Phoenix
Thermostats	0.00	0.00	8	0.0	0.1	OTS	5.0%	0.1	InSight/Phoenix
CS MLI			1	2.0	2.0	OTS	5.0%	2.1	InSight/Phoenix
CS Misc paint, etc.			1	0.1	0.1	OTS	5.0%	0.1	InSight/Phoenix
Cruise Stage Ballast			1	Total	10.0		5%	10.5	
Cruise Ballast			1	10.0	10.0	BTP	5%	10.5	InSight/Phoenix
Cruise Stage AAC			1	Total	7.5		5%	7.9	
Star Tracker Optical heads			2	1.3	2.7	OTS	5%	2.8	GOES/Lucy
Star Tracker Electronics			1	3.7	3.7	OTS	5%	3.9	GOES/Lucy
Star Tracker Harness			2	0.4	0.9	OTS	5%	0.9	GOES/Lucy
Sun Sensor Assembly			2	0.1	0.2	OTS	5%	0.3	InSight/Phoenix/MAVEN/MRO
Cruise Stage Dry Mass			**1**	**Total**	**89.7**		**6%**	**95.0**	

Table G-7. MLE mass details (cont.)

Hardware Elements	# EM's	# Spares	FLIGHT	Unit Mass (kg)	CBE (kg)	Basis of Contingency	Contingency %	Max Expected Value, kg	Program Inheritance
BACKSHELL									
Backshell Harness			1	Total	4.3		5%	4.5	
Backshell Harness			1	4.3	4.3	BTP	5%	4.5	InSight/Phoenix
Backshell Telecom			1	Total	4.5		5%	4.8	
EDL Antenna, UHF			1	4.2	4.2	OTS	5%	4.4	InSight/Phoenix
Coax to Cruise Stage			3	0.1	0.3	OTS	5.0%	0.3	InSight/Phoenix
Backshell Mechanisms			1	Total	31.3		9%	34.1	
BS/Lander Sep components			3	2.9	8.7	M-E	10.0%	9.6	InSight/Phoenix
BS/HS Sep components			9	1.7	15.1	M-E	10.0%	16.6	InSight/Phoenix
BS/CS Sep assembly			2	1.4	2.7	BTP	5.0%	2.9	
HS/BS 1/4" Sep Nuts	21		9	0.13	1.1	BTP	5.0%	1.2	InSight/Phoenix
BS/CS 3/8" Sep Nuts	12		9	0.19	1.7	BTP	5.0%	1.7	InSight/Phoenix
BS/CS Sep components			6	0.3	2.0	M-E	5.0%	2.1	InSight/Phoenix
Backshell Structure			1	Total	239.4		10%	263.4	
BS Primary Structure			1	140.8	140.8	M-E	10.0%	154.9	InSight/Phoenix/Viking
BS Secondary Structure			1	17.5	17.5	M-E	10.0%	19.3	InSight/Phoenix/Viking
Backshell TPS			1	26.7	26.7	M-E	10.0%	29.4	InSight/Phoenix/Viking
Parachute			1	54.4	54.4	M-E	10.0%	59.9	Viking
Backshell Thermal Control			1	Total	7.4		10%	8.1	
BS Blankets			1	4.40	4.4	M-E	10%	4.8	InSight/Phoenix
Coatings			1	3.00	3.0	M-E	10%	3.3	
Backshell Ballast			1	Total	0.0		0%	0.0	
Backshell Dry Mass			**1**	**Total**	**286.96**		**10%**	**314.8**	

Table G-7. MLE mass details (cont.)

Hardware Elements	# EM's	# Spares	FLIGHT	Unit Mass (kg)	CBE (kg)	Basis of Contingency	Contingency %	Max Expected Value, kg	Program Inheritance
HEATSHIELD									
Heatshield Mechanisms			**1**	**Total**	**9.0**		10%	**9.9**	
HS/BS Sep R&R details			9	1.0	9.0	M-E	10.0%	9.9	InSight/Phoenix/Viking
Heatshield Structures			**1**	**Total**	**123.0**		10%	**135.3**	
Primary Structure (3.65m dia)			1	65.9	65.9	M-E	10.0%	72.5	InSight/Phoenix/Viking
Secondary Structure			1	9.4	9.4	M-E	10.0%	10.3	InSight/Phoenix/Viking
HS-TPS Film Adhesive			1	5.1	5.1	M-E	10.0%	5.6	InSight/Phoenix/Viking
Heatshield TPS (0.59 inches)			1	42.6	42.6	M-E	10.0%	46.9	InSight/Phoenix/Viking
Heatshield Ballast			**1**	**Total**	**5.0**		10%	**5.5**	
Heat Shield Ballast			1	5.0	5.0	M-E	10.0%	5.5	InSight/Phoenix/Viking
Heatshield Thermal			**1**	**Total**	**1.8**		10%	**2.0**	
HS Blankets, including tape			1	1.8	1.8	M-E	10%	2.0	InSight/Phoenix/Viking
Heatshield Dry Mass			**1**	**Total**	**133.80**		**10%**	**147.2**	

H REFERENCES

Section 1 References

Bandfield, Joshua L. 2007. "High-Resolution Subsurface Water-Ice Distributions on Mars." *Nature* 447 (7140): 64-67. https://doi.org/10.1038/nature05781. https://doi.org/10.1038/nature05781.

Bandfield, Joshua L., and William C. Feldman. 2008. "Martian High Latitude Permafrost Depth and Surface Cover Thermal Inertia Distributions." *Journal of Geophysical Research: Planets* 113 (E8). https://doi.org/https://doi.org/10.1029/2007JE003007. https://agupubs.onlinelibrary.wiley.com/doi/abs/10.1029/2007JE003007.

Bramson, A. M., S. Byrne, and J. Bapst. 2017. "Preservation of Midlatitude Ice Sheets on Mars." *Journal of Geophysical Research: Planets* 122 (11): 2250-2266. https://doi.org/https://doi.org/10.1002/2017JE005357. https://agupubs.onlinelibrary.wiley.com/doi/abs/10.1002/2017JE005357.

Bramson, Ali M., Shane Byrne, Nathaniel E. Putzig, Sarah Sutton, Jeffrey J. Plaut, T. Charles Brothers, and John W. Holt. 2015. "Widespread Excess Ice in Arcadia Planitia, Mars." *Geophysical Research Letters* 42 (16): 6566-6574. https://doi.org/https://doi.org/10.1002/2015GL064844. https://agupubs.onlinelibrary.wiley.com/doi/abs/10.1002/2015GL064844.

Butcher, Frances E. G., M. R. Balme, C. Gallagher, N. S. Arnold, S. J. Conway, A. Hagermann, and S. R. Lewis. 2017. "Recent Basal Melting of a Mid-Latitude Glacier on Mars." *Journal of Geophysical Research: Planets* 122 (12): 2445-2468. https://doi.org/https://doi.org/10.1002/2017JE005434. https://agupubs.onlinelibrary.wiley.com/doi/abs/10.1002/2017JE005434.

Cabrol, Nathalie A. 2021. "Tracing a Modern Biosphere on Mars." *Nature Astronomy* 5 (3): 210-212. https://doi.org/10.1038/s41550-021-01327-x. https://doi.org/10.1038/s41550-021-01327-x.

Callahan, Michael P., Aaron S. Burton, Jamie E. Elsila, Eleni M. Baker, Karen E. Smith, Daniel P. Glavin, and Jason P. Dworkin. 2013. "A Search for Amino Acids and Nucleobases in the Martian Meteorite Roberts Massif 04262 Using Liquid Chromatography-Mass Spectrometry." *Meteoritics & Planetary Science* 48 (5): 786-795. https://doi.org/https://doi.org/10.1111/maps.12103. https://onlinelibrary.wiley.com/doi/abs/10.1111/maps.12103.

Conley, Catharine A., and John D. Rummel. 2010. "Planetary Protection for Human Exploration of Mars." *Acta Astronautica* 66 (5): 792-797. https://doi.org/https://doi.org/10.1016/j.actaastro.2009.08.015. https://www.sciencedirect.com/science/article/pii/S0094576509004317.

Dundas, Colin M., Ali M. Bramson, Lujendra Ojha, James J. Wray, Michael T. Mellon, Shane Byrne, Alfred S. McEwen, Nathaniel E. Putzig, Donna Viola, Sarah Sutton, Erin Clark, and John W. Holt. 2018. "Exposed Subsurface Ice Sheets in the Martian Mid-Latitudes." *Science* 359 (6372): 199-201. https://doi.org/10.1126/science.aao1619. https://science.sciencemag.org/content/sci/359/6372/199.full.pdf.

Fairén, Alberto G., Victor Parro, Dirk Schulze-Makuch, and Lyle Whyte. 2017. "Searching for Life on Mars before It Is Too Late." *Astrobiology* 17 (10): 962-970. https://doi.org/10.1089/ast.2017.1703. https://www.liebertpub.com/doi/abs/10.1089/ast.2017.1703.

Fornaro, Teresa, Andrew Steele, and John Robert Brucato. 2018. "Catalytic/Protective Properties of Martian Minerals and Implications for Possible Origin of Life on Mars." *Life* 8 (4): 56.

Golombek, M, N Williams, P Wooster, A McEwen, N Putzig, A Bramson, J Head, J Heldmann, M Marinova, and D Beaty. 2021. "Spacex Starship Landing Sites on Mars." Lunar and Planetary Science Conference.

Good, A., Johnson A., and G. Hautaluoma. 2021. Nasa Insight's 'Mole' Ends Its Journey on Mars. https://www.nasa.gov/feature/jpl/nasa-insight-s-mole-ends-its-journey-on-mars.

Hallsworth, John E. 2021. "Mars' Surface Is Not Universally Biocidal." *Environmental Microbiology* n/a (n/a). https://doi.org/https://doi.org/10.1111/1462-2920.15494. https://sfamjournals.onlinelibrary.wiley.com/doi/abs/10.1111/1462-2920.15494.

Hays, Lindsay E, Heather V Graham, David J Des Marais, Elisabeth M Hausrath, Briony Horgan, Thomas M McCollom, M Niki Parenteau, Sally L Potter-McIntyre, Amy J Williams, and Kennda L Lynch. 2017. "Biosignature Preservation and Detection in Mars Analog Environments." *Astrobiology* 17 (4): 363-400.

Holt, John W., Ali Safaeinili, Jeffrey J. Plaut, James W. Head, Roger J. Phillips, Roberto Seu, Scott D. Kempf, Prateek Choudhary, Duncan A. Young, Nathaniel E. Putzig, Daniela Biccari, and Yonggyu Gim. 2008. "Radar Sounding Evidence for Buried Glaciers in the Southern Mid-Latitudes of Mars." *Science* 322 (5905): 1235-1238. https://doi.org/10.1126/science.1164246. https://science.sciencemag.org/content/sci/322/5905/1235.full.pdf.

MEPAG. 2020. *Mars Scientific Goals, Objectives, Investigations, and Priorities: 2020.* (D. Banfield). https://mepag.jpl.nasa.gov/reports.cfm.

MEPAG NEX-SAG. 2015. *Report from the Next Orbiter Science Analysis Group (Nex-Sag).* Chaired by B. Campbell and R. Zurek. http://mepag.nasa.gov/reports.cfm.

Morgan, G. A., N. E. Putzig, M. R. Perry, H. G. Sizemore, A. M. Bramson, E. I. Petersen, Z. M. Bain, D. M. H. Baker, M. Mastrogiuseppe, R. H. Hoover, I. B. Smith, A. Pathare, C. M. Dundas, and B. A. Campbell. 2021. "Availability of Subsurface Water-Ice Resources in the Northern Mid-Latitudes of Mars." *Nature Astronomy* 5: 230. https://doi.org/10.1038/s41550-020-01290-z. https://ui.adsabs.harvard.edu/abs/2021NatAs...5..230M.

Muirhead, Brian K., Austin K. Nicholas, Jeffrey Umland, Orson Sutherland, and Sanjay Vijendran. 2020. "Mars Sample Return Campaign Concept Status." *Acta Astronautica* 176: 131. https://doi.org/10.1016/j.actaastro.2020.06.026. https://ui.adsabs.harvard.edu/abs/2020AcAau.176..131M.

P-SAG. 2012. "Analysis of Strategic Knowledge Gaps Associated with Potential Human Missions to the Martian System: Final Report of the Precursor Strategy Analysis Group (P-Sag)." D.W. Beaty and M.H. Carr (co-chairs) + 25 co-authors, sponsored by MEPAG/SBAG.

Pavlov, A. A., G. Vasilyev, V. M. Ostryakov, A. K. Pavlov, and P. Mahaffy. 2012. "Degradation of the Organic Molecules in the Shallow Subsurface of Mars Due to Irradiation by Cosmic Rays." *Geophysical Research Letters* 39 (13). https://doi.org/https://doi.org/10.1029/2012GL052166. https://agupubs.onlinelibrary.wiley.com/doi/abs/10.1029/2012GL052166.

Persson, Erik. 2019. "Ethics for an Uninhabited Planet." In *The Human Factor in a Mission to Mars: An Interdisciplinary Approach*, edited by Konrad Szocik, 201-216. Cham: Springer International Publishing.

Piqueux, Sylvain, Jennifer Buz, Christopher S. Edwards, Joshua L. Bandfield, Armin Kleinböhl, David M. Kass, Paul O. Hayne, The MCS, and THEMIS Teams. 2019. "Widespread Shallow Water Ice on Mars at High Latitudesand Midlatitudes." *Geophysical Research Letters* 46 (24): 14290-14298. https://doi.org/https://doi.org/10.1029/2019GL083947. https://agupubs.onlinelibrary.wiley.com/doi/abs/10.1029/2019GL083947.

Williams, Amy, Jennifer Eigenbrode, Melissa Floyd, Mary Beth Wilhelm, Shane O'Reilly, Sarah Stewart Johnson, Kathleen Craft, Christine Knudson, Slavka Andrejkovičová, and James MT Lewis. 2019. "Recovery of Fatty Acids from Mineralogic Mars Analogs by Tmah Thermochemolysis for the Sample Analysis at Mars Wet Chemistry Experiment on the Curiosity Rover." *Astrobiology* 19 (4): 522-546.

Zacny, K, P Chu, V Vendiola, E Seto, J Quinn, B Eichenbaum, J Kleinhenz, A Colaprete, and R Elphic. 2021. "Trident Drill for Viper and Prime1 Missions to the Moon." Lunar and Planetary Science Conference.

Section 3 References

Arvidson, R. E., R. G. Bonitz, M. L. Robinson, J. L. Carsten, R. A. Volpe, A. Trebi-Ollennu, M. T. Mellon, P. C. Chu, K. R. Davis, J. J. Wilson, A. S. Shaw, R. N. Greenberger, K. L. Siebach, T. C. Stein, S. C. Cull, W. Goetz, R. V. Morris, D. W. Ming, H. U. Keller, M. T. Lemmon, H. G. Sizemore, and M. Mehta. 2009. "Results from the Mars Phoenix Lander Robotic Arm Experiment." *Journal of Geophysical Research: Planets* 114 (E1). https://doi.org/https://doi.org/10.1029/2009JE003408. https://agupubs.onlinelibrary.wiley.com/doi/abs/10.1029/2009JE003408.

Danko, David C., Maria A. Sierra, James N. Benardini, Lisa Guan, Jason M. Wood, Nitin Singh, Arman Seuylemezian, Daniel J. Butler, Krista Ryon, Katerina Kuchin, Dmitry Meleshko, Chandrima Bhattacharya, Kasthuri J. Venkateswaran, and Christopher E. Mason. 2021. "A Comprehensive Metagenomics Framework to Characterize Organisms Relevant for Planetary Protection." *Microbiome* 9 (1): 82. https://doi.org/10.1186/s40168-021-01020-1. https://doi.org/10.1186/s40168-021-01020-1.

ESA. 2012. The Exomars Drill Unit. https://exploration.esa.int/web/mars/-/43611-rover-drill.

Golombek, M, N Williams, P Wooster, A McEwen, N Putzig, A Bramson, J Head, J Heldmann, M Marinova, and D Beaty. 2021. "Spacex Starship Landing Sites on Mars." Lunar and Planetary Science Conference.

Mank, Z. D., K. A. Zacny, D. Sabahi, M. J. Buchbinder, B. C. Bradley, L. A. Stolov, J. Sparta, L. D. Sanasarian, J. T. Costa, P. J. van Susante, N. Putzig, B. H. Wilcox, and J. Kleinhenz. 2021. "Redwater: A Rodwell System to Extract Water from Martian Ice Deposits." In *Earth and Space 2021*, 471-480.

Van Winnendael, M, P Baglioni, and J Vago. 2005. "Development of the Esa Exomars Rover." 8th International Symposium on Artificial Intelligence, Robotics and Automation in Space - iSAIRAS, Munich, Germany, 5-8 September.

Zacny, K., G. Paulsen, C. P. McKay, B. Glass, A. Davé, A. F. Davila, M. Marinova, B. Mellerowicz, J. Heldmann, and C. Stoker. 2013. "Reaching 1 M Deep on Mars: The Icebreaker Drill." *Astrobiology* 13 (12): 1166-1198.

Zacny, K., P. van Susante, T. Putzig, M. Hecht, and D. Sabahi. 2018. "Redwater: Extraction of Water from Mars Ice Deposits." Space Resources Roundtable, Colorado School of Mines, Golden, CO, June 12-14.

Zacny, Kris, Gale Paulsen, and Brian Glass. 2010. "Field Testing of Planetary Drill in the Arctic." AIAA Space 2010 Conference & Exposition.

Zacny, Kris, Gale Paulsen, Chris Mckay, Brian Glass, Mateusz Szczesiak, Jack Craft, Chris Santoro, Jeff Shasho, Alfonso Davila, Margarita Marinova, Wayne Pollard, and William Jackson. 2011. "Testing of a 1 Meter Mars Icebreaker Drill in a 3.5 Meter Vacuum Chamber and in an Antarctic Mars Analog Site." In *Aiaa Space 2011 Conference &Amp; Exposition*.

Appendix B References

Arvidson, R. E., R. G. Bonitz, M. L. Robinson, J. L. Carsten, R. A. Volpe, A. Trebi-Ollennu, M. T. Mellon, P. C. Chu, K. R. Davis, J. J. Wilson, A. S. Shaw, R. N. Greenberger, K. L. Siebach, T. C. Stein, S. C. Cull, W. Goetz, R. V. Morris, D. W. Ming, H. U. Keller, M. T. Lemmon, H. G. Sizemore, and M. Mehta. 2009. "Results from the Mars Phoenix Lander Robotic Arm Experiment." *Journal of Geophysical Research: Planets* 114 (E1). https://doi.org/https://doi.org/10.1029/2009JE003408. https://agupubs.onlinelibrary.wiley.com/doi/abs/10.1029/2009JE003408.

Banfield, D., and R. Dissly. 2005. "A Martian Sonic Anemometer." 2005 IEEE Aerospace Conference, 5-12 March 2005.

Blake, David, David Vaniman, Cherie Achilles, Robert Anderson, David Bish, Tom Bristow, Curtis Chen, Steve Chipera, Joy Crisp, David Des Marais, Robert T. Downs, Jack Farmer, Sabrina Feldman, Mark Fonda, Marc Gailhanou, Hongwei Ma, Doug W. Ming, Richard V. Morris, Philippe Sarrazin, Ed Stolper, Allan Treiman, and Albert Yen. 2012. "Characterization and Calibration of the Chemin Mineralogical Instrument on Mars Science Laboratory." *Space Science Reviews* 170 (1): 341-399. https://doi.org/10.1007/s11214-012-9905-1. https://doi.org/10.1007/s11214-012-9905-1.

Bonitz, Robert G., Lori Shiraishi, Matthew Robinson, Raymond E. Arvidson, P. C. Chu, J. J. Wilson, K. R. Davis, G. Paulsen, A. G. Kusack, Doug Archer, and Peter Smith. 2008. "Nasa Mars 2007 Phoenix Lander Robotic Arm and Icy Soil Acquisition Device." *Journal of Geophysical Research: Planets* 113 (E3). https://doi.org/https://doi.org/10.1029/2007JE003030. https://agupubs.onlinelibrary.wiley.com/doi/abs/10.1029/2007JE003030.

Brinckerhoff, W. B., A. Grubisic, S. A. Getty, R. M. Danell, R. D. Arevalo, X. Li, F. van Amerom, M. Castillo, J. Eigenbrode, P. Chu, K. Zacny, J. Spring, M. Casey, E. Lalime, and T. Hoehler. 2018. "Emili: Europan Molecular Indicators of Life Investigation." In *Earth and Space 2018*, 524-532.

Chong, Y. G., P. Willis, C. Lindensmith, and A. Noell. 2019. Owls Project: Looking for Life on Ocean Worlds. https://microdevices.jpl.nasa.gov/capabilities/in-situ-instruments-chemical-analysis/owls-project/.

De Sanctis, Maria Cristina, Francesca Altieri, E. Ammannito, David Biondi, Simone De Angelis, Marco Meini, Giuseppe Mondello, Samuele Novi, Riccardo Paolinetti, Massimo Soldani, R. Mugnuolo, s Pirrotta, Jorge Vago, and the team. 2017. "Ma_Miss on Exomars: Mineralogical Characterization of the Martian Subsurface." *Astrobiology* 17: 612-620. https://doi.org/10.1089/ast.2016.1541.

Ehlmann, BL, J Blacksberg, X Chen, W Johnson, M Kenyon, and C Raymond. 2019. "A 2u Swir-Mir Point Spectrometer for Smallsat and Landed Missions: Enabling Characterization of Solar System Volatiles." Lunar and Planetary Science Conference.

Goesmann, Fred, William B Brinckerhoff, François Raulin, Walter Goetz, Ryan M Danell, Stephanie A Getty, Sandra Siljeström, Helge Mißbach, Harald Steininger, and Ricardo D Arevalo Jr. 2017. "The Mars Organic Molecule Analyzer (Moma) Instrument: Characterization of Organic Material in Martian Sediments." *Astrobiology* 17 (6-7): 655-685.

Hoffman, John H., Roy C. Chaney, and Hilton Hammack. 2008. "Phoenix Mars Mission—the Thermal Evolved Gas Analyzer." *Journal of the American Society for Mass Spectrometry* 19 (10): 1377-1383. https://doi.org/10.1016/j.jasms.2008.07.015.

Kounaves, Samuel P., Michael H. Hecht, Steven J. West, John-Michael Morookian, Suzanne M. M. Young, Richard Quinn, Paula Grunthaner, Xiaowen Wen, Mark Weilert, Casey A. Cable, Anita Fisher, Kalina Gospodinova, Jason Kapit, Shannon Stroble, Po-Chang Hsu, Benton C. Clark, Douglas W. Ming, and Peter H. Smith. 2009. "The Meca Wet Chemistry Laboratory on the 2007 Phoenix Mars Scout Lander." *Journal of Geophysical Research: Planets* 114 (E3).

https://doi.org/https://doi.org/10.1029/2008JE003084. https://agupubs.onlinelibrary.wiley.com/doi/abs/10.1029/2008JE003084.

Lin, Y., F. Zhong, B. L. Henderson, V. Abrahamsson, I. Kanik, J. Gross, L. Newlin, W. W. Schubert, L. Matthies, C. Edwards, J. Bapst, J. Balaram, and T. Tzanetos. 2021. "Masex — a Dedicated Life Detection Mission on Mars." *Bulletin of the AAS* 53 (4). https://doi.org/https://doi.org/10.3847/25c2cfeb.33226b42.

Mahaffy, Paul R., Christopher R. Webster, Michel Cabane, Pamela G. Conrad, Patrice Coll, Sushil K. Atreya, Robert Arvey, Michael Barciniak, Mehdi Benna, Lora Bleacher, William B. Brinckerhoff, Jennifer L. Eigenbrode, Daniel Carignan, Mark Cascia, Robert A. Chalmers, Jason P. Dworkin, Therese Errigo, Paula Everson, Heather Franz, Rodger Farley, Steven Feng, Gregory Frazier, Caroline Freissinet, Daniel P. Glavin, Daniel N. Harpold, Douglas Hawk, Vincent Holmes, Christopher S. Johnson, Andrea Jones, Patrick Jordan, James Kellogg, Jesse Lewis, Eric Lyness, Charles A. Malespin, David K. Martin, John Maurer, Amy C. McAdam, Douglas McLennan, Thomas J. Nolan, Marvin Noriega, Alexander A. Pavlov, Benito Prats, Eric Raaen, Oren Sheinman, David Sheppard, James Smith, Jennifer C. Stern, Florence Tan, Melissa Trainer, Douglas W. Ming, Richard V. Morris, John Jones, Cindy Gundersen, Andrew Steele, James Wray, Oliver Botta, Laurie A. Leshin, Tobias Owen, Steve Battel, Bruce M. Jakosky, Heidi Manning, Steven Squyres, Rafael Navarro-González, Christopher P. McKay, Francois Raulin, Robert Sternberg, Arnaud Buch, Paul Sorensen, Robert Kline-Schoder, David Coscia, Cyril Szopa, Samuel Teinturier, Curt Baffes, Jason Feldman, Greg Flesch, Siamak Forouhar, Ray Garcia, Didier Keymeulen, Steve Woodward, Bruce P. Block, Ken Arnett, Ryan Miller, Charles Edmonson, Stephen Gorevan, and Erik Mumm. 2012. "The Sample Analysis at Mars Investigation and Instrument Suite." *Space Science Reviews* 170 (1): 401-478. https://doi.org/10.1007/s11214-012-9879-z. https://doi.org/10.1007/s11214-012-9879-z.

Naz, N., and S. P. Kounaves. 2021. "Analysis of Synthetic Terrestrial and Modeled Enceladian Seawater Using the Microfluidic Wet Chemistry Laboratory (Mwcl)." March 01, 2021. https://ui.adsabs.harvard.edu/abs/2021LPI....52.2233N.

Noell, Aaron Craig, Elizabeth A Jaramilllo, Samuel P Kounaves, Michael H Hecht, Daniel Jed Harrison, Richard C Quinn, Joshua Forgione, Jessica Koehne, and Antonio J Ricco. 2019. "Mica: Microfluidic Icy-World Chemistry Analyzer." *Proceedings of the AbSciCon, Bellevue, WA, USA*: 24-28.

Pérez-Izquierdo, Joel, Eduardo Sebastián, Germán M. Martínez, Andrés Bravo, Miguel Ramos, and Jose A. Rodríguez Manfredi. 2018. "The Thermal Infrared Sensor (Tirs) of the Mars Environmental Dynamics Analyzer (Meda) Instrument Onboard Mars 2020, a General Description and Performance Analysis." *Measurements* 122: 432. https://doi.org/10.1016/j.measurement.2017.12.004. https://ui.adsabs.harvard.edu/abs/2018Meas..122..432P.

Rafkin, S. 2015. "A Multi-Channel Tunable Laser Spectrometer for in Situ Measurement of Planetary Atmospheres." 2015 IEEE Aerospace Conference, 7-14 March 2015.

Rampe, Elizabeth, David Blake, Philippe Sarrazin, Thomas Bristow, Marc Gailhanou, Barbara Lafuente, Valerie Tu, Kris Zacny, and Robert Downs. 2020. "Cheminx: A Next Generation Xrd/Xrf for Quantitative Mineralogy and Geochemistry on Mars." *Decadal Survey White Paper*.

Rieder, R., R. Gellert, J. Brückner, G. Klingelhöfer, G. Dreibus, A. Yen, and S. W. Squyres. 2003. "The New Athena Alpha Particle X-Ray Spectrometer for the Mars Exploration Rovers." *Journal of Geophysical Research: Planets* 108 (E12). https://doi.org/https://doi.org/10.1029/2003JE002150. https://agupubs.onlinelibrary.wiley.com/doi/abs/10.1029/2003JE002150.

Rodriguez-Manfredi, J. A., M. de la Torre Juárez, A. Alonso, V. Apéstigue, I. Arruego, T. Atienza, D. Banfield, J. Boland, M. A. Carrera, L. Castañer, J. Ceballos, H. Chen-Chen, A. Cobos, P. G. Conrad, E. Cordoba, T. del Río-Gaztelurrutia, A. de Vicente-Retortillo, M. Domínguez-Pumar, S. Espejo, A. G. Fairen, A. Fernández-Palma, R. Ferrándiz, F. Ferri, E. Fischer, A. García-

Manchado, M. García-Villadangos, M. Genzer, S. Giménez, J. Gómez-Elvira, F. Gómez, S. D. Guzewich, A. M. Harri, C. D. Hernández, M. Hieta, R. Hueso, I. Jaakonaho, J. J. Jiménez, V. Jiménez, A. Larman, R. Leiter, A. Lepinette, M. T. Lemmon, G. López, S. N. Madsen, T. Mäkinen, M. Marín, J. Martín-Soler, G. Martínez, A. Molina, L. Mora-Sotomayor, J. F. Moreno-Álvarez, S. Navarro, C. E. Newman, C. Ortega, M. C. Parrondo, V. Peinado, A. Peña, I. Pérez-Grande, S. Pérez-Hoyos, J. Pla-García, J. Polkko, M. Postigo, O. Prieto-Ballesteros, S. C. R. Rafkin, M. Ramos, M. I. Richardson, J. Romeral, C. Romero, K. D. Runyon, A. Saiz-Lopez, A. Sánchez-Lavega, I. Sard, J. T. Schofield, E. Sebastian, M. D. Smith, R. J. Sullivan, L. K. Tamppari, A. D. Thompson, D. Toledo, F. Torrero, J. Torres, R. Urquí, T. Velasco, D. Viúdez-Moreiras, S. Zurita, and Meda team The. 2021. "The Mars Environmental Dynamics Analyzer, Meda. A Suite of Environmental Sensors for the Mars 2020 Mission." *Space Science Reviews* 217 (3): 48. https://doi.org/10.1007/s11214-021-00816-9. https://doi.org/10.1007/s11214-021-00816-9.

Smith, P. H., L. Tamppari, R. E. Arvidson, D. Bass, D. Blaney, W. Boynton, A. Carswell, D. Catling, B. Clark, T. Duck, E. DeJong, D. Fisher, W. Goetz, P. Gunnlaugsson, M. Hecht, V. Hipkin, J. Hoffman, S. Hviid, H. Keller, S. Kounaves, C. F. Lange, M. Lemmon, M. Madsen, M. Malin, W. Markiewicz, J. Marshall, C. McKay, M. Mellon, D. Michelangeli, D. Ming, R. Morris, N. Renno, W. T. Pike, U. Staufer, C. Stoker, P. Taylor, J. Whiteway, S. Young, and A. Zent. 2008. "Introduction to Special Section on the Phoenix Mission: Landing Site Characterization Experiments, Mission Overviews, and Expected Science." *Journal of Geophysical Research: Planets* 113 (E3). https://doi.org/https://doi.org/10.1029/2008JE003083. https://agupubs.onlinelibrary.wiley.com/doi/abs/10.1029/2008JE003083.

Taylor, Peter A., David C. Catling, Mike Daly, Cameron S. Dickinson, Haraldur P. Gunnlaugsson, Ari-Matti Harri, and Carlos F. Lange. 2008. "Temperature, Pressure, and Wind Instrumentation in the Phoenix Meteorological Package." *Journal of Geophysical Research: Planets* 113 (E3). https://doi.org/https://doi.org/10.1029/2007JE003015. https://agupubs.onlinelibrary.wiley.com/doi/abs/10.1029/2007JE003015.

Trainer, M. G., W. B. Brinckerhoff, A. Grubisic, R. M. Danell, D. Kaplan, F. H. W. van Amerom, X. Li, C. Freissinet, C. Szopa, A. Buch, J. C. Stern, S. Teinturier, C. A. Malespin, P. W. Barfknecht, P. R. Stysley, D. B. Coyle, M. W. Mullin, B. L. James, E. I. Lyness, R. S. Wilkinson, J. W. Kellogg, K. Zacny, D. C. Wegel, E. P. Turtle, and Dragonfly Team. 2021. "Development of the Dragonfly Mass Spectrometer (Drams) for Titan." March 01, 2021. https://ui.adsabs.harvard.edu/abs/2021LPI....52.1532T.

Webster, C. R., G. J. Flesch, L. Christensen, D. Keymeulen, and S. Forouhar. 2012. "Miniature Tunable Laser Spectrometers for Quantifying Atmospheric Trace Gases, Water Resources, Earth Back-Contamination, and in Situ Resource Utilization." June 01, 2012.

Webster, Chris R, Paul R Mahaffy, Sushil K Atreya, Greg J Flesch, and Ken A Farley. 2013. "Measurements of Mars Methane at Gale Crater by the Sam Tunable Laser Spectrometer on the Curiosity Rover." *LPSC XXXXIV, abstract* 1366.

Wilhelm, MB, AJ Ricco, M Chin, JL Eigenbrode, L Jahnke, PM Furlong, DK Buckner, T Chinn, K Sridhar, and T McClure. 2020. "Excalibr: An Instrument for Uncovering the Origin of the Moon's Organics." *LPI Contributions* 2241: 5116.

Willis, Peter A, M Fernanda Mora, Jessica S Creamer, Aaron Noell, Florian Kehl, Konstantin Zamuruyev, Mauro Sergio Ferreira Santos, Tony Ricco, Richard Quinn, and Jennifer Stern. 2019. "Organic Capillary Electrophoresis Analysis System (Oceans) Subsystem of the Europan Molecular Indicators of Life Investigation (Emili)."

Zent, Aaron P., Michael H. Hecht, Doug R. Cobos, Gaylon S. Campbell, Colin S. Campbell, Greg Cardell, Marc C. Foote, Stephen E. Wood, and Manish Mehta. 2009. "Thermal and Electrical Conductivity Probe (Tecp) for Phoenix." *Journal of Geophysical Research: Planets* 114 (E3). https://doi.org/https://doi.org/10.1029/2007JE003052. https://agupubs.onlinelibrary.wiley.com/doi/abs/10.1029/2007JE003052.

Appendix D References

Peters, Gregory H., William Abbey, Gregory H. Bearman, Gregory S. Mungas, J. Anthony Smith, Robert C. Anderson, Susanne Douglas, and Luther W. Beegle. 2008. "Mojave Mars Simulant—Characterization of a New Geologic Mars Analog." *Icarus* 197 (2): 470-479. https://doi.org/https://doi.org/10.1016/j.icarus.2008.05.004. https://www.sciencedirect.com/science/article/pii/S0019103508002017.

Zacny, K, P Chu, V Vendiola, E Seto, J Quinn, B Eichenbaum, J Kleinhenz, A Colaprete, and R Elphic. 2021. "Trident Drill for Viper and Prime1 Missions to the Moon." Lunar and Planetary Science Conference.

Zacny, K, M Shara, G Paulsen, B Mellerowicz, J Spring, A Ridilla, H Nguyen, K Ridilla, M Hedlund, and R Sharpe. 2016. "Development of a Planetary Deep Drill." In *Earth and Space 2016: Engineering for Extreme Environments*, 256-266. American Society of Civil Engineers Reston, VA.

Zacny, K., G. Paulsen, C. P. McKay, B. Glass, A. Davé, A. F. Davila, M. Marinova, B. Mellerowicz, J. Heldmann, and C. Stoker. 2013. "Reaching 1 M Deep on Mars: The Icebreaker Drill." *Astrobiology* 13 (12): 1166-1198.

Zacny, Kris, Gale Paulsen, Chris Mckay, Brian Glass, Mateusz Szczesiak, Jack Craft, Chris Santoro, Jeff Shasho, Alfonso Davila, Margarita Marinova, Wayne Pollard, and William Jackson. 2011. "Testing of a 1 Meter Mars Icebreaker Drill in a 3.5 Meter Vacuum Chamber and in an Antarctic Mars Analog Site." In *Aiaa Space 2011 Conference &Amp; Exposition*.